The Pennsylvania State University

The Graduate School

College of Engineering

ROLE OF HEMODYNAMIC FORCES IN SMOOTH MUSCLE CELL CONTRACTION AND TRANSVASCULAR FILTRATION IN VIVO

A Thesis in

Bioengineering

by

Min-ho Kim

Submitted in Partial Fulfillment
of the Requirements
for the Degree of

Doctor of Philosophy

December 2004

The thesis of Min-ho Kim was reviewed and approved* by the following:

Norman R. Harris
Associate Professor of Bioengineering
Thesis Advisor
Chair of Committee

Herbert H. Lipowsky
Professor of Bioengineering

Peter J. Butler
Assistant Professor of Bioengineering

Donna H. Korzick
Assistant Professor of Physiology and Kinesiology

John M. Tarbell
Distinguished Professor of Biomedical Engineering
City College of New York / CUNY
Special Member

Herbert H. Lipowsky
Professor of Bioengineering
Head of the Department of Bioengineering

*Signatures are on file in the Graduate School

ABSTRACT

The vascular wall is continuously exposed to two hemodynamic forces imparted by blood flow: pressure and shear stress. Significant changes in hemodynamic forces can occur in many physiological and pathophysiological circumstances. Changes in vascular pressure and blood flow-induced shear stress can affect vascular endothelium and smooth muscle cells (SMCs) mechanically. When vascular pressure is increased, an increase in transvascular filtration is driven by a classical Starling mechanism. This increased transvascular filtration is expected to induce increases in shear stresses through the inter-endothelial cleft surfaces and SMCs.

A main hypothesis of the current study is that transvascular filtration-induced shear stress might play important roles in endothelial barrier function and SMC contractions. To address this hypothesis, we investigated the effect of pressure-induced transvascular fluid flux on SMC contraction in vivo. We also investigated the effects of pressure and shear on endothelial barrier functions for water transport.

In the current study performed *in vivo* and in excised arterioles, interstitial flow-induced shear stress through the vascular wall driven by transvascular filtration was hypothesized to be a mechanical factor that can play a role in the myogenic response in addition to the role of vascular stretch and wall tension. To address this hypothesis, we investigated the relationship between filtration rate (J_v) and the myogenic response by modifying plasma osmotic pressure to attenuate J_v during a step increase in hydrostatic pressure. The myogenic response was attenuated significantly when an osmotic solution of albumin, or albumin plus Ficoll, was infused into the bloodstream to decrease fluid filtration. Moreover, the same inhibition of myogenic tone was found in isolated,

cannulated rat soleus muscle arterioles when filtration was osmotically attenuated by intravascular dextran. Taken together, these results are consistent with the hypothesis that shear stress on arteriolar smooth muscle, induced by transvascular fluid filtration, is a contributing factor that helps control myogenic tone.

To understand the role of hemodynamic forces in regulating microvascular permeability, we have investigated effects of acute changes in shear and pressure on endothelial barrier function for water transport. In the study performed in the microvessels of the mesentery, we have obtained evidence that hydraulic conductivity might be regulated via a NO-dependent mechanism in response to acute change in shear rate. Additionally, the effect of sustained changes in pressure on hydraulic conductivity was also investigated using micro-perfusion technique. The substantial increase in hydraulic conductivity was observed following a pressure increase in both small arterioles and venules. It is likely that pressure-induced mechanical stimulus activates a biochemical response that can lead to increase in hydraulic conductivity in response to pressure change. Furthermore, our results suggested that an adaptive sealing effect induced by a step change in pressure also partially contributes to regulate endothelial barrier function. These findings support the idea that endothelial transport barrier responds actively to changes in hemodynamic forces in the microcirculation and regulate transport pathways for water through biological as well as mechanical mechanisms.

TABLE OF CONTENTS

LIST OF FIGURES ……. x

LIST OF TABLES……... xiv

ACKNOWLEDGEMENTS……. xv

CHAPTER 1 INTRODUCTION AND BACKGROUND ……. 1

1.1 Introduction …… 1

1.2 Background and Literature Review…… 3

1.2.1 Role of hemodynamics in microvascular permeability ……. 3

1.2.1.1 Microvascular permeability …….. 3

1.2.1.2 Effects of hemodynamic forces on microvascular permeability: role of shear stress …… 4

1.2.1.3 Effects of hemodynamic forces on microvascular permeability: role of pressure ……. 5

1.2.1.4 Role of nitric oxide in hydraulic conductivity in microcirculation ……..... 6

1.2.2 Fluid flux through inter-endothelial cleft ……... 8

1.2.3 Role of hemodynamics in local regulation of microvascular tone …. 9

1.2.3.1 Local regulation of vascular tone ……. 9

1.2.3.2 Shear-dependent vasoregulation ……... 10

1.2.3.3 Pressure-induced vascular SMC contraction: myogenic response 11

1.2.3.3.1 General overview of myogenic response…….. 11

1.2.3.3.2 Mechanical factors regulating the myogenic response: role of stretch …… 13

1.2.3.3.3 Mechanical factors regulating the myogenic response: role of wall tension ……... 14

1.2.4 Fluid flux through vascular SMCs ……..….... 14

1.3 Specific Objectives…… 16

1.4 Issues Addressed in the Current study …….. 16

1.5 Collaborative Work Included in the Thesis ……. 18

CHAPTER 2 GENERAL METHODS ……... 19

2.1 Animal Preparations ……... 19

2.2 Video Microscopy …….…. 19

2.3 Measurement of Transvascular Filtration ……..…. 20

2.4 Starling Forces Regulating Fluid Filtration…… 21

2.5 Statistics ……. 22

CHAPTER 3 CONTROL OF THE ARTERIOLAR MYOGENIC RESPONSE BY TRANSVASCULAR FILTRATION ..…… 25

3.1 Introduction …… 25

3.2 Materials and Methods .....…. 27

3.2.1 Animal preparation…….…... 27

3.2.2 Video microscopy …….. 27

3.2.3 Velocity measurement ……... 27

3.2.4 Vascular occlusion ……... 28

3.2.5 Measurement of transvascular filtration…….…... 28

3.2.6 In vivo experimental protocols…….. 29

3.2.7 Starling forces regulating fluid filtration ……... 30

3.2.8 Evaluation of vasoreactivity in isolated soleus feed arterioles…….. 30

3.2.9 Statistics……. 32

3.3 Results .....…. 32

3.4 Discussion ….....…. 35

CHAPTER 4 REGULATION OF HYDRAULIC CONDUCTIVITY IN RESPONSE TO ACUTE CHANGES IN SHEAR RATE AND PRESSURE …….. 54

4.1 Introduction .....…. 54

4.2 Materials and Methods .....…. 56

4.2.1 Animal preparation.....…... 56

4.2.2 Video microscopy .....…... 56

4.2.3 Measurement of transvascular filtration .....…... 57

4.2.4 Measurement of shear rate (SR) .....…... 57

4.2.5 Starling forces regulating fluid filtration .....…... 58

4.2.6 Method of increasing shear rate and hydraulic conductivity measurements in capillary ……. 58

4.2.7 Experimental protocols 59

4.2.8 Statistics 60

4.3 Results 60

4.4 Discussion 63

CHAPTER 5 REGULATION OF HYDRAULIC CONDUCTIVITY IN RESPONSE TO SUSTAINED CHANGE IN PRESSURE 83

5.1 Introduction 83

5.2 Materials and Methods 84

5.2.1 Animal preparation 84

5.2.2 Video microscopy 84

5.2.3 Microperfusion technique and measurement of transvascular filtration 84

5.2.4 Measurement of hydraulic conductivity for cannulated vessels 85

5.2.5 Experimental protocols 86

5.2.6 Statistics 88

5.3 Results 88

5.4 Discussion 90

CHAPTER 6 SUMMARY AND FUTURE STUDY 105

6.1 Summary 105

6.2 Recommendations for Future Study 106

6.2.1 Role of transvascular filtration in regulating myogenic response ……. 106

6.2.2 Role of hemodynamic forces in regulating hydraulic permeability ….. 108

REFERENCES …… 110

APPENDIX …….. 121

LIST OF FIGURES

Figure 2.1. A diagram of experimental setup for intravital microscopy of the rat mesentery ……..24

Figure 3.1. A schematic of micro-occlusion technique for measurements of J_v/S and hydrostatic pressure in small arterioles …….46

Figure 3.2. A diagram of experimental setup for myogenic reactivity of isolated soleus feed arterioles ……47

Figure 3.3. Percent baseline tone, $100\times(D_{max} - D_I)/D_{max}$, as a function of J_v/S.....48

Figure 3.4. Filtration rate vs time following arteriolar occlusion. (A) BSA/Ficoll injection (B) BSA injection……...…49

Figure 3.5. Diameter (% of baseline diameter) vs time following arteriolar occlusion. (A) BSA/Ficoll injection (B) BSA injection…….50

Figure 3.6. Filtration rate vs time (panel A) and diameter (% of baseline diameter) vs time (panel B) following arteriolar occlusions under baseline conditions and subsequent adenosine exposure……51

Figure 3.7. Effect of intravascular dextran on the pressure-myogenic tone relationship of isolated arterioles……...52

Figure 3.8 Myogenic reactivity of excised arterioles in response to a step increase in pressure from 66 to 96 mmHg (A) Diameters normalized to basal conditions, and (B) Myogenic constriction (%)……53

Figure 4.1 Method for increasing capillary shear rate. (A) Baseline capillary shear rate ($SR_{baseline}$) and pressure (P_c) before capillary occlusion. (B) Baseline capillary occlusion for J_v/S measurements. (C) Increased shear rate (SR_{shear}) through capillary by arteriolar occlusion that also increases arteriolar pressure (ΔP_a). (D) J_v/S measurement at increased shear rate and pressure ($P_a+\Delta P_a$)……76

Figure 4.2. Effects of acute change in shear rate on capillary J_v/S and $L_{p.}$ (A) Baseline measurements of J_v/S. (B) % change in J_v/S in response to acute increase in shear rate at time = 5 and 50 s following capillary occlusion. (C) Time course of normalized L_p ($=L_{p\ shear} / L_{p\ baseline}$) in response to the increase in shear rate……77

Figure 4.3. Response of L_p in true capillaries. (A) Normalized L_p as a function of percentage change in shear rate. (B) Slope of the linear regression relation between normalized L_p and percentage change in shear rate at different times following capillary occlusion……78

Figure 4.4. Response of L_p in true capillaries. (A) Time course of normalized L_p with and without L-NAME (50 μM) in response to increase in shear rate. (B) % increase in L_p at time=5 and 50 sec……..79

Figure 4.5. Response of L_p to increase in shear rate for small arteriole. (A) Time course of normalized L_p for small arterioles. (B) % increase in L_p at time=5 and 50 sec for arterioles and true capillaries…….80

Figure 4.6. Effect of step change in pressure on the time course of J_v/S in capillaries…81

Figure 4.7. Sensitivity of the normalized L_p (t=5s) with respect to uncertainties in the baseline arteriolar pressure (P_a), magnitude of pressure increase (ΔP_a), and osmotic reflection coefficients (N=15) ……...82

Figure 5.1 Micro-perfusion techniques used in small arterioles and venules. (A) Schematic illustration showing microperfusion technique for pressure change and J_v/S measurements. (B) Microscopic image showing cannulation site. (C) Microscopic image showing microspheres used for flow markers downstream of cannulation site ……...99

Figure 5.2 Time course of J_v/S for small arterioles (N=5). (A) J_v/S (μm/s) vs time (min) with step change in pressure. Pressure was increased from 50 to 100 mmHg at 30 min. Each value was obtained by taking an average for the values between 10 and 20 s following vascular occlusion. (B) Transient response of J_v/S at each time point ……...100

Figure 5.3 J_v/S and percentage change in L_p as a function of time for small arterioles. (A) Percentage change in J_v/S normalized to baseline at 30 min. (B) Percentage change in Lp normalized to baseline at 30 min……...…….101

Figure 5.4 J_v/S and percentage change in L_p as a function of time for small venules. (A) Percentage change in J_v/S normalized to baseline at 30 min with step change in pressure from 20 to 40 mmHg. (B) Percentage change in L_p normalized to baseline at 30 min……...102

Figure 5.5 Effects of L-NAME (100 μM) on J_v/S and percentage change in L_p for small arterioles. (A) Percentage change in Jv/S normalized to baseline at 30 min with step change in pressure from 50 to 100 mmHg without L-NAME and with L-NAME. (B) Comparison of percentage change in L_p normalized to baseline at 30 min between results without L-NAME and with L-NAME…….103

Figure 5.6 Effects of L-NAME (100 μM) on J_v/S and percentage change in Lp for small venules. (A) Percentage change in J_v/S normalized to baseline at 30 min with step change in pressure from 20 to 100 mmHg. (B) Percentage change in L_p normalized to baseline at 30 min between results without L-NAME and with L-NAME……..104

LIST OF TABLES

Table 3.1 Systemic blood pressure, red blood cell velocity and arteriolar pressure…….41

Table 3.2 Illustrative raw data of diameter in response to changes in intraluminal pressure in soleus feed arterioles ……..42

Table 3.3 Illustrative raw data of diameter in response to step increases in pressure from 66 to 96 mmHg in soleus feed arterioles ……..43

Table 4.1 Illustrative raw data of shear rate for capillaries and small arterioles ……..71

Table 4.2 Dependency of the relationship between increase in shear rate (%) and normalized L_p (t=5s) on the uncertainty in the magnitude of pressure increase (ΔP_a) ….72

Table 5.1 Illustrative raw data of J_v/S for small arteriole and venules in response to increases in pressure …….96

ACKNOWLEDGEMENTS

I would like to express my deep gratitude to my advisor, Dr. Norman R. Harris, for his patience and support during my studies toward Ph.D degree. I also want to thank to my committee members, Dr. Tarbell, Dr. Lipowsky, Dr. Butler, and Dr. Korzick, for their critiques and suggestions. In particular, I would like to thank Dr. Tarbell for his valuable recommendations and guidance in conducting my research.

I also thank to Marlena Tickerhoof. Her help in isolated arteriole protocol made a great contribution in justifying our in vivo results. I would like to acknowledge all the members in our former Penn State and current LSU Health Science Center lab. Sharing most of the time with them made me happy and forget difficulties and frustrations encountered during my experiment.

Personally, I would like to thank to my parents, they have been always supporting me in every aspect of life. Furthermost, I am greatly indebted to my family, my wife Jinhee, my son Yuhan and my daughter Yeji, during my study. Their presence, endless patience and love gave me a great energy to achieve this small outcom.

This work was funded by the National Aeronautics and Space Administration Grants NAG3-2746.

Chapter 1

INTRODUCTION AND BACKGROUND

1.1 Introduction

The vascular wall is continuously exposed to two hemodynamic forces imparted by blood flow. One is transmural pressure that imposes circumferential stresses on endothelium and smooth muscle cells (SMCs), and the other is shear stress that imposes a tangential frictional force on luminal endothelium. Significant changes in hemodynamic forces can occur in many physiological and pathophysiological circumstances. During exercise, shear stress changes occur abruptly. Additionally, a postural change or venous occlusion can give rise to an increase in microvascular pressure. When the body is exposed to microgravity, blood pressure is reduced below the heart and elevated above the heart due to removal of the gravitational pressure gradient.

Changes in vascular pressure and blood flow-induced shear stress can affect vascular endothelium and SMCs mechanically. It is widely accepted that endothelial cells can sense and transduce hemodynamic stimuli into changes in cell structure and function (Davis, 1995;Chien *et al.*, 1998;Butler *et al.*, 2002). A change in blood flow is one of the main mechanisms controlling microvascular tone (Davis, 1995). A change in transmural pressure or stretch in vascular SMC also triggers intracellular signal transduction and leads to subsequent cell contraction (myogenic response), synthesis and secretion of molecules (growth factors or collagen) or cell growth and death (Osol, 1995;Rivers, 1995). Recent in vitro findings suggested that vascular

SMC also could be responsive to flow-induced shear stress (Alshihabi *et al.*, 1996;Civelek *et al.*, 2002). When vascular pressure is increased, an increase in transvascular filtration is driven by a classical Starling mechanism. This increased transvascular filtration is expected to induce increases in shear stresses through the inter-endothelial cleft surfaces and SMCs (Tarbell *et al.*, 1999;Tada & Tarbell, 2002). With this evidence, it could be hypothesized that transvascular filtration-induced shear stress may play an important role in endothelial barrier and SMC physiological functions. However, relatively little attention has been devoted to those issues. Much is known about the mechanism of regulating endothelial barrier function by various inflammatory mediators (Michel & Curry, 1999). However, a specific role for hemodynamic stimuli in regulating hydraulic conductivity is not well understood, especially for a sustained change in microvascular pressure gradient in vivo. In addition, in contrast to extensive studies of flow-mediated endothelial mechano-transduction, the effects of flow-induced shear stress on vascular SMC have been ignored based on the reasoning that SMC is distant from the site at which shear is experienced. However, recent study indicate that SMC can be exposed to significant magnitude of shear stress by interstitial flow - comparable to levels imposed by fluid flow on the surface of endothelial cells, even though filtration rates are a small fraction of the blood flow through a vessel (Tada & Tarbell, 2001;Wang & Tarbell, 1995).

Therefore, the main objectives of the present study are to 1) investigate the effects of pressure and shear on endothelial barrier function for water transport and 2) investigate the effects of pressure-induced transvascular fluid flux on SMC

contraction in vivo. The proposed studies will provide an understanding of the biofluid mechanical and biotransport mechanisms that control microvascular perfusion and transvascular exchange in response to changes in hemodynamic forces.

1.2 Background and Literature Review

This section address brief background and previous works in relation with microvascular permeability and local regulation of microvascular tone in response to hemodynamic stimuli.

1.2.1 Role of hemodynamics in microvascular transport

1.2.1.1 Microvascular permeability

Blood vessel walls are lined by a monolayer of endothelial cells which, in addition to providing a blood contacting surface resistance to clotting, forms the principal barrier to transport of water and solutes across the wall. Regulation of water and solute transport is critical for controlling the chemical milieu of tissues serviced by individual vessels (Taylor, 1984). Variations in endothelial resistance to transport of macromolecules such as low density lipoprotein are believed by many to play a role in the localization of atherosclerotic plaques in the arterial system (Barakat *et al.*, 1992;Okano & Yoshida, 1994;White *et al.*, 1991). Changes in the transvascular pressure gradient associated with exposure to microgravity conditions in space travel lead to major fluid shifts between vascular and tissue compartments separated by endothelial barriers (White *et al.*, 1991). These fluid shifts affect physiological adaptation to space in profound ways.

According to Starling's hypothesis, transvascular fluid flux through the endothelial transport barrier is regulated either by changes in the pressure gradient (hydrostatic or oncotic) or by permeability (oncotic reflection coefficient or hydraulic conductivity). The membrane transport property that describes the passage of water across the vascular barrier can be expressed by hydraulic conductivity (L_p). This permeability coefficient relates the net flux of fluid (J_v) to the differences in pressure gradient that drives the fluid through the microvascular wall (Michel & Curry, 1999). Any alteration of L_p may indicate conformational changes in endothelium or formation of intercellular gaps.

Various stimuli can affect microvascular permeability under different pathological and physiological conditions. Acute alteration of the endothelial transport barrier in response to the release of chemical agents (e.g. histamine, thrombin) increases L_p and fluid filtration rate (J_v/S) (Michel & Curry, 1999;Yuan, 2000). Mechanical factors also may affect hydraulic conductivity: endothelial cells may sense and trigger mechanotransduction in response to blood flow shear stress and changes in hydrostatic pressure (Davis, 1995).

1.2.1.2 Effects of hemodynamic forces on microvascular permeability: role of shear stress

Several recent studies have shown that molecular transport through the walls of microvessels can be affected by the change in perfusion rate (Head *et al.*, 1996;Kajimura *et al.*, 1998;Neal & Bates, 2002;Montermini *et al.*, 2002;Yuan *et al.*, 1992;Karmakar, 2001). This phenomenon of flow-dependent changes in

microvascular permeability is now becoming an important physiological mechanism that can explain solute exchanges between blood and tissue in response to a change in blood flow. A small pore model has been proposed as a possible mechanism to account for flow-dependent transport of small solutes (Montermini *et al.*, 2002). This model explains the mechanism for the transport of small solutes in response to a change in perfusion rate by introducing a small pore pathway that is highly permeable to small molecules but less permeable to water and large molecules. However, this finding can be challenged by the observation that the permeability of large solute was also dependent on perfusion rate (Yuan *et al.*, 1992), in addition to several recent studies of shear-induced fluid filtration performed in vitro (Sill *et al.*, 1995;Chang *et al.*, 2000;Demaio *et al.*, 2001) and in vivo (Lever *et al.*, 1992;Williams, 1999;Williams, 2003). The mechanisms responsible for these different observations in fluid filtration in contrast to consistent observation in molecular transport to changes in perfusion rate are not yet clearly understood and this issue remains controversial and under continued study. Therefore, it needs further investigation under different experimental conditions and animal models.

1.2.1.3 Effects of hemodynamic forces on microvascular permeability: role of pressure

Transvascular filtration is expected to increase in proportion to an increased transvascular pressure gradient according to a classic Starling mechanism in which hydraulic conductivity is assumed to be a constant property of the transport barrier. It is generally believed that L_p does not change with an acute change in pressure and

this principle has been used in measuring L_p in micropipette-perfused capillary beds, where the slope of the linear regression plot between filtration rate and pressure is considered to be L_p. This linear relationship was confirmed from various vessel preparations (He *et al.*, 1997;Neal & Bates, 2001;Neal & Bates, 2002;Rumbaut *et al.*, 1995;Rumbaut *et al.*, 2000b;Williams, 1999). However, most of those results were obtained for time periods typically less than 1 min. Despite extensive studies regarding this issue, relatively little attention has been drawn for the issue of a change in pressure over an extended time period. Recently, from in vitro studies of cultured endothelial cell models, a time-dependent change in L_p was observed with step increases in pressure over extended periods of time (5 hours) (Tarbell *et al.*, 1999). It was hypothesized that the increase in L_p resulted from activation of a biochemical response possibly due to elevated endothelial cleft shear stress induced by elevated transmural flow.

Another important mechanism in relation to a pressure effect is a characteristic time-dependent decrease in L_p occurring over 20-40 min following pressure application. This phenomenon, termed a “sealing effect”, might appear to be due to passive compression of pathways for water transport on pressure application. However, recent in vitro findings revealed that biological as well as mechanical mechanisms might play important roles in this adaptive response (Demaio *et al.*, 2004).

1.2.1.4 Role of nitric oxide in hydraulic conductivity in microcirculation

Inflammatory mediators can change microvascular permeability by activating various signaling pathways, which leads to loose or opened intercellular junctions by dissociation of junctional proteins and their connection to the cytoskeleton (Yuan, 2000). It is well established that NO plays an important role in the regulation of microvascular permeability. Nitric oxide synthase (NOS) inhibitors can attenuate the acute increase in microvascular permeability due to various inflammatory mediators such as histamine, ATP, bradykinin, and platelet-activating factor (PAF) [reviewed in (Michel & Curry, 1999)]. In acute inflammation, a calcium-activated, NO-cGMP-dependent pathway is believed to be a common pathway to increase microvascular permeability (He *et al.*, 2000). However, it also should be noted that the application of NOS inhibitors can induce an increase in leukocyte adhesion to endothelial cells and a subsequent increase in hydraulic conductivity in autoperfused vessels (Harris, 1997) as opposed to the observation of individually buffer-perfused vessels in which NOS inhibitors decrease L_p. These findings have suggested that the effect of NOS inhibition on hydraulic conductivity is dependent on the presence of neutrophils, with the effect reversed with anti-neutrophil serum or an antibody against the CD18 leukocyte adhesion molecule (Harris, 1997).

Regarding the role of shear stress and pressure in microvascular permeability, NO release by endothelial cells has been suggested to be an important mechanism. Chang et al. (Chang *et al.*, 2000) have reported that shear stress mediates hydraulic conductivity in a NO-dependent mechanism in cultured endothelial cell models. Investigations performed on individually perfused microvessels indicated that

hydraulic conductivity is decreased by nitric oxide synthase (NOS) inhibition (Rumbaut *et al.*, 1995;Rumbaut *et al.*, 2000b;He *et al.*, 1997).

1.2.2 Fluid flux through inter-endothelial cleft

The inter-endothelial cleft between endothelial cells is believed to be a principal pathway for water and solutes. Even though there is a suggestion of transcellular exchange pathways, it appears that fluid exchange through transcellular pathway is 10% or less of total L_p [reviewed in (Michel & Curry, 1999)]. The effective area for fluid exchange is determined by spacing between the walls of adjacent endothelial cells in the inter-endothelial cleft. The average spacing between adjacent cells is close to 20 nm and the length of the line of contact per unit area per cell is estimated to lie in the range 1,200~2,000 cm/cm^2 in skeletal muscle, heart muscle, and mesenteric capillaries (Adamson, 1993). The maximum area for exchange between cells can be considered being 0.4% of total capillary surface area. However, the tight junction region between the cells is composed of junctional strands that have regions of break or discontinuities. In the region of the tight junction between adjacent cells, in which opposing membrane branches are close to each other, the outer leaflets of the cell membranes are not fused but separated by a mean width of 2.3 nm. In the region of the break or discontinuity, the adjacent cell membrane is separated by 20 nm (Michel & Curry, 1999). The principal pathway through the intercellular cleft lies through the breaks or discontinuities in the junctional strands. In a lanthanum tracer experiment, Adamson et al. (Adamson *et al.*, 1993) found that the fraction of open junctions ranged from 3.4 to 10% of the total length of the junction in frog mesenteric

capillaries. Therefore, assuming one-dimensional flow through the endothelial cleft, the effective area for water exchange can be expected to be in the range of 0.012 to 0.04% of total microvessel surface area. This narrowed pathway for fluid transport is expected to induce an increased inter-endothelial cleft shear stress. The magnitude of cleft shear stress imposed on the walls of the endothelial junctions was estimated to be comparable to the value induced by blood flow acting on the luminal surface (Tarbell *et al.*, 1999).

1.2.3 Role of hemodynamics in local regulation of microvascular tone

1.2.3.1 Local regulation of vascular tone

Vascular tone is the contractile activity of vascular smooth muscle cells in the walls of small arteries and arterioles, and this is a major determinant of the resistance to blood flow. Microvascular tone can be influenced by various vasoactive substances and by hemodynamic factors (shear stress and pressure). In relation to local regulation of blood flow, three main mechanisms have been proposed: metabolic, shear-dependent, and myogenic mechanisms. The metabolic mechanism suggests that arteriolar diameter is controlled by endogenously released vasoactive substances that depend on the metabolic state of the tissue. The pressure-induced myogenic constriction of arterioles is endothelial-independent and intrinsic to SMCs (Meininger & Davis, 1992;Osol, 1995;Schubert & Mulvany, 1999), whereas shear-dependent vasoregulation is endothelium-dependent (Butler *et al.*, 2000;Koller & Kaley, 1991) and mediated by substances released from the endothelium (Davis, 1995). In general,

basal vascular tone is determined by the complex interaction of these mechanisms (Kuo *et al.*, 1991).

1.2.3.2 Shear-dependent vasoregulation

The mechanisms by which flow-induced shear stress plays a crucial role in local regulation of vascular tone have been investigated extensively. Alterations in wall shear stress during changes in blood flow mediate release of NO (Figueroa *et al.*, 2001), prostaglandins (Taba *et al.*, 2000) and endothelium-derived hyperpolarizing factors (EDHF) (Tomioka *et al.*, 1999), and lead to SMC relaxation. In contrast to the activation of NO synthesis via a Ca^{2+}-dependent pathway by vasoactive agents such as histamine or acetylcholine (ACh), an increase in shear stress is known to trigger NO release without a substantial increase in Ca^{2+}, most likely by activation of tyrosine kinase pathways (Ungvari *et al.*, 2001). The reduced release of endothelial NO in response to shear stress can lead to impaired flow-dependent dilation and may be involved in the pathogenesis of cardiovascular disorders such as hypertension and atherosclerosis (Nitenberg *et al.*, 1995) whereas long-term exercise is known to enhance NO-mediated flow-induced dilation (Sun *et al.*, 2002).

A flow-induced vascular response can interact competitively with a pressure-induced myogenic response (de Wit *et al.*, 1998;Kuo *et al.*, 1991). However, in vivo, a shear-dependent increase in endothelial NO release opposing myogenic response has been reported to play a more important role in small arteries or large arterioles than in small arterioles (de Wit *et al.*, 1998). A substantial myogenic response was observed in large arterioles after inhibition of NOS, indicating that NO might provide

an important feedback control mechanism. In this mechanism, myogenic constriction would increase shear rate due to faster velocity through a smaller diameter, thereby, shear simultaneously would increase the NO production and promote an opposing dilation. In smaller arterioles, metabolic signals or EDHF appears to regulate flow-induced vasodilation to greater extents than depending on NO (Tomioka *et al.*, 1999).

1.2.3.3 Pressure-induced vascular SMC contraction: myogenic response

1.2.3.3.1 General overview of myogenic response

The myogenic response is a contraction of smooth muscle in the arteriolar wall in response to an increase in transmural pressure and a relaxation in response to a decrease in pressure. The physiological significance of the myogenic response is local blood flow regulation, determination of basal peripheral vascular resistance, and regulation of capillary hydrostatic pressure (Davis & Hill, 1999).

It is generally accepted that phosphorylation of the 20-kDa regulatory myosin light chain (MLC_{20}) leads to an interaction of actin and myosin and corresponding initiation of SMC contraction via calcium-dependent or calcium-independent pathways (Meininger & Davis, 1992). The rise and fall in intracellular free calcium is the important mechanism that initiates contraction and relaxation of SMC, respectively (Davis & Hill, 1999). The signaling mechanism underlying initiation of the myogenic response is similar to the SMC contraction response in general and it involves Ca^{2+}/calmodulin-myosin light chain kinase-mediated phosphorylation of the regulatory light chains of myosin. It has been well known that pressure application onto the vascular wall initiates membrane depolarization of SMC. The membrane

depolarization results in Ca^{2+} influx from the extracellular space via L-type voltage-gated calcium channels (VGCCs). In several vessel preparations, the blockers of VGCCs inhibited not only the myogenic response but also increases in intracellular Ca^{2+} concentration (Schubert & Mulvany, 1999). Unlike striated muscle, where Ca^{2+} binds to the thin-filament-associated protein troponin, in smooth muscle Ca^{2+} binds to calmodulin. This calcium-calmodulin complex activates myosin light chain kinase (MLCK), which phosphorylates the serine at position 19 on the 20-kDa regulatory myosin light chain (MLC_{20}) (Somlyo & Somlyo, 1994). It was shown that increasing intraluminal pressure resulted in significant constriction with increased $[Ca^{2+}]_i$ and MLC phosphorylation in isolated arterioles of rat cremaster muscle (Zou *et al.*, 1995). Phosphorylation of MLC20 facilitates the activation of myosin ATPase by actin and leads to cross-bridge cycling and subsequent smooth muscle contraction. Several studies, however, indicate that steady state myogenic tone does not accompany a significant increase in $[Ca^{2+}]_i$. In hamster cheek pouch arterioles, increasing the magnitude of the step size in pressure resulted in greater myogenic responses compared to small pressure steps, yet there was no difference in the steady state $[Ca^{2+}]_i$ change (D'Angelo *et al.*, 1997). According to the study of Hill et al. (Hill *et al.*, 2000), in the case of a ramp increase in pressure from 50 to 120 mmHg where there was no passive stretch of the arteriolar smooth muscle layer nor a transient increase in $[Ca^{2+}]_i$, almost the same amount of steady state myogenic constriction was attained compared to the case of an acute step change in pressure. These findings suggest that a calcium-independent regulatory mechanism may be involved in the regulation of smooth muscle contraction. Even though the intracellular signaling

mechanisms involved in the myogenic response are not fully understood, two putative pathways have been proposed regarding a calcium-independent mechanism: protein kinase C (PKC) (Jarajapu & Knot, 2002) and Rho kinase pathways (Schubert *et al.*, 2002).

1.2.3.3.2 Mechanical factors regulating the myogenic response: role of stretch

It seems clear that membrane depolarization of SMC and subsequent influx of extracellular calcium are important mechanisms that link a pressure increase to myogenic constriction. However, a question that remains unanswered concerns the membrane signals that initiate this response. To date, two mechanical factors regulating the myogenic response have been investigated quite extensively: stretch and tension. A widely held view is that the initial circumferential stretch of SMCs driven by a step increase in pressure activates stretch-sensitive ion channels that induce an increased level of intracellular calcium and activation of the contractile process. When there is an increase in pressure, the vascular wall stretches and results in stretch of SMC also. The stretch of SMC activates membrane depolarization by increasing inward current through stretch-activated nonselective cation channels passing Na^+, K^+ and Ca^{2+} ions (Meininger & Davis, 1992). However, this hypothesis can be argued by the observation that SMC stretch did not sustain the same length, in which SMC stretch initially increases in response to pressure application, but then decreased, often below the initial baseline value during the myogenic constriction even though the vessel maintained sustained membrane depolarization after pressure elevation. Furthermore, it is also suggested that a stretch-induced Ca^{2+} transient is not

an absolute requirement for the development of a steady-state level of myogenic tone based on the observation that the myogenic response was generated without stretch, and without the characteristic initial calcium transient, when pressure was increased in ramp rather than step fashion (Hill *et al.*, 2000).

1.2.3.3.3 Mechanical factors regulating the myogenic response: role of wall tension

In addition to the role of stretch in the myogenic response, an alteration of wall tension (pressure × radius) has been proposed as a possible membrane signal that initiates myogenic constriction. If there is an increase in pressure, there is a rise in wall tension that tends to reach a steady state value that is elevated above the initial state of tone (Hill *et al.*, 2000). This increase in tension may drive the sustained contraction. It has been suggested that an increase in wall tension, not pressure, induces a constriction that leads to a reduction in wall tension, and thereby also inhibits further constriction. A positive correlation was also found between wall tension and both intracellular calcium concentration and MLC phosphorylation (Zou *et al.*, 1995).

1.2.4 Fluid flux through vascular SMCs

The water transported from the endothelial cleft spreads into the intima and flows toward fenestral pores in the internal elastic lamina (IEL). Generally, the intima layer is very thin and largely comprised of proteoglycan and collagen fibers, whereas the media contains alternating SMCs and elastic connective tissue. The proteoglycan

and collagen structure of the intima and fenestral pore differs greatly from that of the media (Lark, 1988). The intima layer is known to have an unexpectedly sparse matrix with an average spacing between matrix elements of 30-40 nm (Frank, 1989), whereas the media layer has a more densely packed matrix possibly due to synthesis of large amounts of chondroitin sulfate proteoglycan from SMCs (Wight, 1983) Darcy permeability and diffusivity of media is estimated to be two orders of magnitude smaller than that of sub-endothelial intima (Huang *et al.*, 1997).

The IEL has leaky fenestral pores and the flow distribution beneath the IEL can be greatly affected by area fraction and diameter of fenestral pores (Tada & Tarbell, 2000). The area fraction occupied by fenestral pores over the IEL is known to be about 7% for rabbit carotid artery (Masuda *et al.*, 1999) and 5% for rat thoracic aorta (Huang *et al.*, 1998). Interestingly flow-induced arterial dilation resulted in remodeling of the IEL where the area fraction of fenestral pores was increased in response to high blood flow (Masuda *et al.*, 1999). The pore size ranged from 2 μm for control to 15 μm when there was an increase in blood flow. Recently, it has been found that the area fraction and diameter of fenestral pores are important factors that affect flow distribution beneath the IEL (Tada & Tarbell, 2001;Tada & Tarbell, 2000). They also showed that the most superficial layer of SMC (closest to the intima) could be exposed to elevated shear stresses as high as 10-50 dyne/cm^2, associated with the distribution of flow through a series of small fenestral pores in the IEL. This amount of shear stress can affect SMC physiological function (Alshihabi *et al.*, 1996;Wang & Tarbell, 2000;Papadaki *et al.*, 1998a;Papadaki *et al.*, 1998b).

Small arterioles play an important role in maintaining vascular tone in response to changes in pressure and blood flow. The competitive response of shear-dependent vasodilation and myogenic constriction may alter arteriolar wall structure and can affect flow and pressure distribution through the vessel wall. Structural changes in the vascular wall in response to an increase in transmural pressure is known to affect intima thickness, and area fraction and average diameter of the fenestral pores as well as transvascular filtration velocity (Huang *et al.*, 1998). These changes in the geometry lead to change in the filtration coefficient.

1.3 Specific Objectives

The primary objectives of the present study are to determine the effects of changes in hemodynamic forces on the transport of water and arteriolar SMC contraction in vivo.

The specific objectives are: 1) to investigate the relationship between transvascular filtration and the myogenic response, 2) to determine whether acute changes in blood flow shear and pressure influence measurement of hydraulic conductivity in autoperfused microvessels, 3) to investigate a role for nitric oxide in shear-mediated changes in hydraulic conductivity, 4) to determine the effects of sustained changes in transvascular pressure on the transport of water, 5) to investigate the role of nitric oxide in pressure-induced changes in hydraulic conductivity.

1.4 Issues Addressed in the Current Study

The main issues included in the current study are composed of two parts. One is to investigate the role of hemodynamics in vascular SMC contraction, which is described in chapter 3. The other is to investigate the role of hemodynamics in microvascular endothelial barrier function assessed by transvascular filtration measurements, which is described in chapter 4 and chapter 5.

Chapter 2 describes general methods used in this study such as animal preparations, intravital video microscopy, and the modified Landis technique for transvascular filtration measurements.

Chapter 3 is devoted to the study of vascular smooth muscle contraction in response to pressure-induced transvascular filtration. Experiments were performed in vivo and in excised arterioles and the relationship between transvascular filtration and myogenic response was investigated.

Chapter 4 presents results concerning the effect of mechanical perturbations (shear and pressure) on hydraulic conductivity measurement in capillaries. Acute increase in shear and pressure were induced and their effects on hydraulic conductivity were assessed from autoperfused microvessels of the rat mesentery.

Chapter 5 addresses the effect of sustained increases in pressure on microvascular hydraulic permeability. Sustained increases in pressure were induced using a micro-perfusion technique in small arterioles and venules. Time-dependent changes in hydraulic conductivity were observed and the role of nitric oxide in this response was also assessed.

Chapter 6 summarizes findings drawn from the current study and discusses future study.

1.5 Collaborative Work Included in the Thesis

Part of the results investigating the role of transvascular filtration in the myogenic response (chapter 3) was obtained in collaboration with Dr.Korzick's lab (Noll Physiological Lab, Pennsylvania State University). Soleus muscle arterioles were prepared from young Wistar rats and myogenic reactivity was assessed in isolated, pressurized arterioles.

Chapter 2

GENERAL METHODS

2.1 Animal Preparation

The following procedures were performed according to institutional guidelines for animal care and use. Rats were initially anesthetized with 1% v/v Halothane (Halocarbon Laboratories, River Edge, NJ) followed by an intraperitoneal injection of 135 mg/kg thiobutabarbital (Inactin, Sigma-Research Biochemicals Inc., St. Louis, MO). The small intestine was exteriorized through a midline abdominal incision, and the rat was placed on its right side on a Plexiglas board so that a selected section of the mesentery could be draped over a glass cover slip glued on a hole centered in the board. The exposed intestine, except for the selected mesenteric section under study, was covered with gauze soaked in bicarbonate-buffered saline (BBS) consisting of 132 mM NaCl, 4.7 mM KCl, 1.2 mM $MgSO_4$, 20 mM $NaHCO_3$ and 2 mM $CaCl_2$. After the board was mounted onto the stage of an inverted microscope, the mesentery and intestine were kept moist with a 2 ml /min superfusion of BBS bubbled with a 95% N_2 and 5% CO_2 gas mixture and warmed to 37˚C. Rectal temperature was monitored with a thermocouple thermometer and maintained near 37˚C by positioning an infrared heat lamp over the rat.

2.2 Video Microscopy

The mesentery was observed through a x10 or x40 (Nikon Plan Apo, 0.95 NA) objective using a 100-W halogen light source, and bright field images were captured

with a color camera (Imagestar IS209, Optical Apparatus Co., Ardmore, PA). The images were then directed through a time-date generator (Panasonic WJ-810, Panasonic, Secaucus, NJ) into a videocassette recorder (Sony SVO-9500, Japan). The taped image was used for playback analysis with an image grabber (Flashpoint 1284M, Integral Technologies, Indianapolis, IN) and image processor (Optimas, Media Cybernetics, Silver Springs, MD). A diagram of experimental setup for intravital microscopy is shown in Figure 2.1.

2.3 Measurement of Transvascular Filtration

Microvascular filtration rate (J_v) was measured using a modification of the original Landis technique (Landis, 1927) during micropipette occlusion. The filtration rate was calculated from the decreasing volume (V) between the micropipette and flow markers (red blood cells or blue-dyed microspheres) that were ~300-600 μm upstream of the occluder. During occlusion, flow markers within the vessel gradually move closer together and toward the occlusion site as the intravascular fluid separating the markers filters across the endothelial barrier into the surrounding tissue. There is also a concomitant change in vessel diameter associated with the myogenic response for arterioles. We assume uniform circular tube geometry of diameter D and length x, where x is the distance of a flow marker from the occlusion site. The calculation of J_v can then be obtained from a volume balance, where the rate of change in V between a marker cell and the occluder is equal to the rate at which plasma volume is filtered out,

$$J_v = -dV/dt \tag{2.1}$$

However, since both the position of the marker cell and the diameter can change, we employ the chain rule:

$$dV/dt = (\partial V/\partial D)\times(dD/dt) + (\partial V/\partial x)\times(dx/dt) \quad (2.2)$$

With $V = \pi D^2 x/4$, the partial derivatives can be computed as $\partial V/\partial D = \pi Dx/2$ and $\partial V/\partial x = \pi D^2/4$. Substituting for these partial derivatives, and then dividing dV/dt by surface area S ($= \pi Dx$), we obtain

$$J_v/S = -(dV/dt)/S = -(1/2) \times (dD/dt) - (D/4x) \times (dx/dt) \quad (2.3)$$

The second term on the right-hand side of this equation is the form used in experimental protocols (Lee *et al.*, 1971) where vascular diameter is at steady state (that is, when dD/dt = 0 in the first term on the right-hand side).

2.4 Starling Forces Regulating Fluid Filtration

Starling's law describes the effects of hydrostatic and osmotic pressures on fluid filtration,

$$J_v/S = L_p[(P_p-P_t)-\sigma(\pi_p-\pi_t)] \quad (2.4)$$

where L_p is the hydraulic conductivity, P is the hydrostatic pressure, π is the osmotic pressure, σ is the osmotic reflection coefficient and the pressure subscripts p and t denote plasma and tissue, respectively. Because the mesentery was exteriorized and superfused with protein-free buffer, tissue hydrostatic and osmotic pressures were negligible.

$$J_v/S = L_p(P_p-\sigma\pi_p) \quad (2.5)$$

2.5 Statistics

Each test was performed using a 95% confidence level to determine significant differences. Minitab software (Minitab Inc., State College, PA) was used for paired-t test, unpaired t-test, and regression analyses. Data among groups were compared with the Bonferroni test. Error bars are presented as ± standard error (SE). Statistical significance was set at $P<0.05$.

Figure Legends

Figure 2.1. A diagram of experimental setup for intravital microscopy of the rat mesentery.

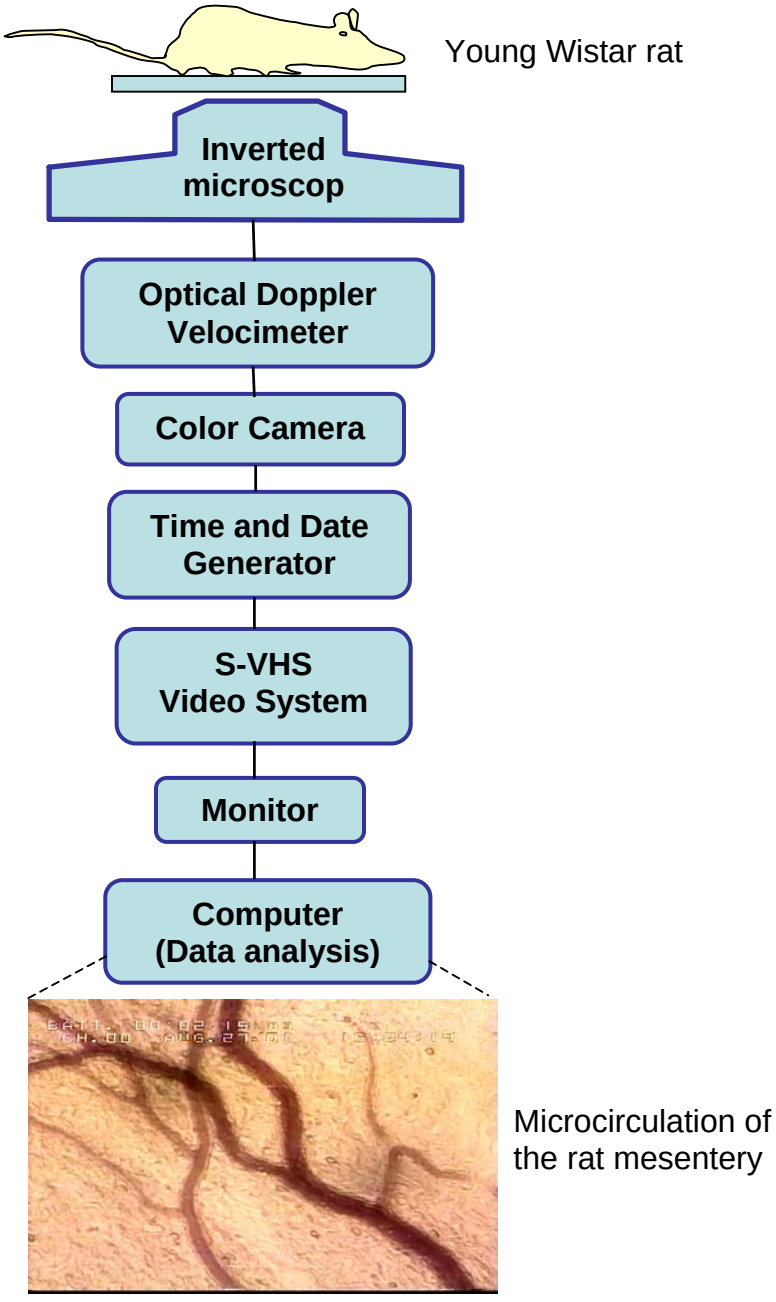
Young Wistar rat
Inverted microscop
Optical Doppler Velocimeter
Color Camera
Time and Date Generator
S-VHS Video System
Monitor
Computer (Data analysis)
Microcirculation of the rat mesentery

Figure 2.1

Chapter 3

CONTROL OF THE ARTERIOLAR MYOGENIC RESPONSE BY TRANSVASCULAR FILTRATION

3.1 Introduction

The cardiovascular system relies on the "myogenic response" to help control excessive filtration of fluid induced by an increase in blood pressure, or to enhance filtration when there is a drop in pressure (Meininger & Davis, 1992). The mechanical forces that mediate the myogenic response are not well established in the literature. To date, two mechanical factors have been investigated quite extensively: stretch and tension. A widely held view is that the initial circumferential stretch of smooth muscle cells (SMC) driven by a step increase in pressure activates stretch-sensitive ion channels that induces an increased level of intracellular calcium and activation of the contractile process (Davis & Hill, 1999). It is also possible to generate a myogenic response without stretch, and without the characteristic initial calcium transient, if the pressure increases in ramp rather than step fashion (Hill *et al.*, 2000). In addition to stretch, there is a rise in wall tension that tends to reach a steady state value that is elevated above the initial state of tone. This increase in tension may drive the sustained contraction (Hill *et al.*, 2000).

A third mechanical factor, which we believe plays a role in the myogenic response, is fluid shear stress through the vascular wall driven by transvascular filtration. Wang and Tarbell (Wang & Tarbell, 1995) estimated the magnitude of interstitial flow shear stress on SMC using a model in which the cells were treated as

an array of cylinders imbedded in a uniform fiber matrix with a uniform superficial velocity as the entrance condition. Peak wall shear stresses were predicted to be ~3 dyne/cm^2 – comparable to levels imposed by fluid flow on the surface of endothelial cells. More recently, Tada and Tarbell (Tada & Tarbell, 2002) showed that the most superficial layer of SMC (closest to the intima) could be exposed to elevated shear stresses as high as 10-50 dyne/cm^2, associated with the distribution of flow through a series of small (1.4 μm) fenestral pores in the internal elastic lamina that separates the SMC-laden media from the intima. When vascular pressure is increased, an increase in transvascular filtration is driven by a classical Starling mechanism, which in turn increases fluid shear stress through the vascular wall. When the SMC layer is exposed to this filtration, we hypothesize subsequent constriction based on the in vitro work by Civelek et al. (Civelek *et al.*, 2002), who have demonstrated shear-induced contraction by SMC monolayers.

In the current study performed *in vivo* and in excised arterioles, we investigated the relationship between filtration rate (J_v) and the myogenic response by modifying plasma osmotic pressure to attenuate J_v during a step increase in hydrostatic pressure. Consistent with our hypothesis, we observed that the myogenic response is significantly inhibited when J_v is reduced. Moreover, we found a statistically significant correlation *in vivo* between basal myogenic tone and J_v.

3.2 Materials and Methods

3.2.1 Animal preparation

Animal procedures were performed in accordance with institutional guidelines. Male Wistar rats were initially anesthetized with Halothane followed by an intraperitoneal injection of 135 mg/kg thiobutabarbital (Inactin, Sigma T-133, St. Louis). For the *in vivo* experiments, the right carotid artery was cannulated for a blood pressure monitor (BP-1, World Precision Instruments, Sarasota, FL), and for systemic injection of the nonionic synthetic polymer of sucrose, Ficoll (70 kD; Sigma F-2878) and/or bovine serum albumin (BSA, Sigma A-4378) in selected experiments. More details about surgery and BBS preparations are given in chapter 2, section 1.

3.2.2 Video microscopy

A description of the video microscopy techniques used are described in chapter 2, section 2.

3.2.3 Velocity measurement

Arteriolar red blood cell centerline velocity (V_{RBC}) was measured with live images using an optical Doppler velocimeter (Microcirculation Research Institute, Texas A&M University, College Station, TX), which uses a grating to produce a periodic signal, and is calibrated with a 1-kHz signal generator. The signal frequency (converted to velocity in mm/s) was evaluated with an oscilloscope and averaged over five trials.

3.2.4 Vascular occlusion

To alter pressure that determines transvascular fluid filtration and myogenic tone, we occluded an autoperfused vessel with a glass micropipette whose tip was pulled and rounded to ~30 μm. The occluder was positioned over a selected arteriole (20-30 μm in diameter) and carefully lowered onto the vessel by micromanipulator to compress the lumen.

Occlusion of the mesenteric arteriole was performed as a step that took one second or less. This technique has been previously published for the hamster cheek pouch (Lombard, 1977), where arteriolar pressure upstream of the occluder increased by 22.5%. A micropressure technique was used in four of our experiments to monitor arteriolar hydrostatic pressure upstream of the occlusion (Figure 3.1). In this method, pressure was measured with a servo-null apparatus (Micropressure System 900A, World Precision Instruments, Sarasota, FL) using pipettes filled with 2M NaCl and a tip resistance of 4-6 MΩ (11-10-S, Frederick Haer & Co, Bowdoinham, ME). Micropipette puncture of the arteriole was facilitated by micromanipulator.

3.2.5 Measurement of transvascular filtration

Arteriolar filtration rate (J_v) was measured using a modification of the original Landis technique during micropipette occlusion and calculated using equation 2.3 as described in chapter 2 (Figure 3.1). More details about measurements of transvasular filtration are described in chapter 2, section 3.

3.2.6 In vivo experimental protocols

Arterioles were occluded for four minutes with a glass micropipette to provide a myogenic response. Fifteen minutes following the release of the baseline occlusion, a mixture of either dialyzed BSA (0.18 g) or BSA plus Ficoll (0.12 g each) was injected to decrease the Starling forces promoting J_v, then a second occlusion was performed. (Preliminary time control experiments were performed to verify that two consecutive myogenic responses, fifteen minutes apart, were equivalent in the absence of osmotic injection.) The amount of BSA plus Ficoll injected (0.24 grams) is approximately the same as the amount of protein present naturally in the rat, giving roughly a two-fold increase in macromolecular solute in the circulation. (In a few preliminary experiments, we found that the same amount of BSA alone, 0.24 grams, caused a drop in systemic pressure without increasing plasma protein concentration equivalent to the amount injected.)

During each experiment, arteriolar diameter was measured before and during the occlusion. After release of the second occlusion, maximal dilation of the arteriole (D_{max}) was obtained by superfusion exposure to 1 mg/ml papaverine to estimate % tone of the baseline diameter. Percent tone was calculated by the following equation.

$$\% \text{ tone} = 100 \times (D_{max} - D_I)/D_{max} \qquad (3.1)$$

where D_I is the initial arteriolar diameter before the first occlusion and D_{max} is the diameter following superfusion of the mesentery with papaverine. Experiments designed to attenuate the myogenic response were performed in the same manner: following a baseline occlusion, 100 μM of endothelium-independent adenosine was

superfused in calcium-free BBS for 20 minutes, as described by Falcone et al. (Falcone *et al.*, 1991) to obtain passive behavior, prior to a second occlusion.

3.2.7 Starling forces regulating fluid filtration

Using equation 2.5 and assuming a very low permeability of the arteriolar wall to albumin ($\sigma = 1$), the equation reduces to

$$J_v/S = L_p(P_p-\pi_p) \tag{3.2}$$

By increasing the protein concentration in plasma and the associated π_p, we were able to reduce J_v/S.

3.2.8 Evaluation of vasoreactivity in isolated soleus feed arterioles

To determine the validity of our hypothesis in a vessel preparation free from confounding flow, neural, and hormonal influences, myogenic reactivity was assessed in isolated, pressurized arterioles. Soleus muscle arterioles were selected for study in the present investigation due to robust myogenic responses known to occur in this vascular bed (Jasperse *et al.*, 1999). Rats were initially anesthetized with Halothane followed by an intraperitoneal injection of 135 mg/kg thiobutabarbital (Inactin, Sigma T-133, St. Louis). The right soleus muscle was excised and moved to a dissecting chamber containing cold physiological saline solution (PSS) (4°C). The PSS used in all experiments contained (in mM) 145 NaCl, 4.7 KCl, 2.0 $CaCl_2$, 1.17 $MgSO_4$, 1.2 NaH_2PO_4, 5.0 glucose, 2.0 pyruvate, 0.02 EDTA, and 3.0 MOPS and was adjusted to a pH of 7.4 and filtered through 0.22-μm filters (Fisher Scientific, Pittsburgh, PA).

Soleus muscle feed arteries (1A branches) ~160-200 μm in internal diameter (ID) and 0.5-1.0 mm in length were dissected with the aid of an Olympus dissecting microscope. Isolated vessels were cannulated at each end with glass micropipettes, secured with 11-0 nylon ligatures, and viewed through an inverted microscope (WPI, Sarasota, FL; X25). The vessels were pressurized at 66 mmHg (90 cm H_2O) by two independent fluid-filled reservoirs that were attached to the micropipettes. Changes in intraluminal pressure were achieved by raising or lowering the reservoirs, thus preventing changes in fluid flow within the vessel lumen (Figure 3.2). Vessels that failed to develop spontaneous tone during the initial equilibration period were eliminated from the study population. Endothelium-intact vessels were used for all protocols associated with the current study. Vessel diameter was assessed using an inverted microscope coupled to a video camera (CUE) and television monitor (Panasonic). A video tracking system (either from Colorado Video Calipers or from Texas A&M University) was utilized to continuously monitored vessel ID throughout a given experiment in association with Power Lab data acquisition software.

Soleus 1A feed arteries (SFAs; ~200 μm I.D.) were isolated and cannulated with glass micropipettes. Following equilibration for 1 h at 37°C, myogenic responses were assessed in SFAs following step increases and decreases in intraluminal pressure (66, 81, 96, 81, 66, 52, 37, 22, 37, 66, 96 mmHg). These pressure steps were selected based on pilot experiments and observations by Jasperse and Laughlin (Jasperse *et al.*, 1999) whereby repeatable diameter changes occurred throughout this pressure range. Vessels were given 5 min following each experimental manipulation to allow sufficient time for diameter stabilization. In a

separate series of studies, the experimental paradigm was repeated with the addition of 3.5% dextran (40 kD; Sigma) to the PSS, which contributes 34 mmHg of osmotic pressure (Kany *et al.*, 1999). Dextran experiments were performed in separate vessels from controls due to the inability to change solutions intraluminally. At the conclusion of each experiment, maximal passive vessel diameter was assessed following Ca^{2+} -free PSS (66 mmHg). Diameter measurements were expressed relative to maximal passive diameter at 66 mmHg.

3.2.9 Statistics

Minitab software (Minitab Inc., State College, PA) was used for paired-t test, unpaired t-test, and regression analyses. Each test was performed using a 95% confidence level to determine significant differences. Error bars are presented as $\pm$ standard error (SE).

3.3 Results

During each *in vivo* experiment, systemic blood pressure and arteriolar red blood cell velocity were monitored; the averaged values are given in Table 3.1. Red blood cell velocity was measured immediately before occluding the vessel. Arteriolar hydrostatic pressures (N=4) were slightly lower following the BSA/Ficoll injection (not significant, p=0.27); however, the percentage increase following occlusion was essentially identical (17.1% $\pm$ 1.8 for baseline and 17.4% $\pm$ 1.8 for BSA/Ficoll).

Baseline arteriolar tone and fluid filtration rate (J_v/S) are correlated ($p<0.001$, r^2 = 61.3%) as shown in Figure 3.3, where J_v/S is the averaged value in the initial 150

seconds of the baseline vascular occlusion. This is consistent with our hypothesis that J_v may control myogenic tone, and to further investigate this possibility, we compared the myogenic response prior to and following infusion of a BSA plus Ficoll osmotic solution (0.12 grams each) designed to decrease J_v. As shown in Figure 3.4 (panel A), the infusion successfully diminished J_v/S by approximately 50% at all time points following occlusion (N=10). The effect of decreased transvascular filtration on the myogenic response is demonstrated in Figure 3.5 (panel A). Measurement of the diameters reflected a passive stretch that lasted ~5 seconds following the step increase in pressure. This passive phase was followed by myogenic constriction. During the baseline occlusion, the vessel stretched by 2.0 ± 0.2% from the initial diameter of 25.9 ± 1.3 μm, and then actively constricted by 2.8 ± 0.4% from the passive phase maximum (D_{max}). Following a subsequent BSA/Ficoll injection and equilibration period, the same resting diameter was measured as initially (25.9 ± 1.3 μm). A second occlusion induced a passive stretch that was essentially identical to the baseline occlusion (1.9 ± 0.2%); however, myogenic constriction was only 1.4 ± 0.2%, a decrease of 47 ± 7% compared to the baseline response, closely corresponding to the 53 ± 3% decrease in filtration rate caused by the BSA/Ficoll injection.

Similar experiments were performed with BSA alone rather than a combination with Ficoll. In these experiments (N=5), a baseline occlusion and myogenic response was followed by an injection of 0.18 g BSA. As shown in Figure 3.5 (panel B), the

BSA injection was able to inhibit the myogenic response by 39 ± 7%, closely corresponding to the 50 ± 8% decrease in filtration rate (Figure 3.4, panel B).

An additional set of *in vivo* experiments was performed to investigate the potential influence of the myogenic response on the sharp initial decline in J_v/S following occlusion (see Figure 3.4). Following measurements of a baseline myogenic response, mesenteric tissue was exposed to adenosine (10^{-4} mol/L) in calcium-free buffer to reduce intracellular calcium and obtain passive behavior to attenuate a second myogenic response (Figure 3.6). This treatment slightly dilated the arterioles, with resting diameters of 24.3 ± 2.0 μm compared to a baseline of 23.9 ± 2.1 μm (N=6; $p<0.05$). Furthermore, the treatment almost completely eliminated the myogenic response. However, as shown in Figure 3.6, no change (as compared to the baseline occlusion) was observed in the resulting J_v/S values, which still dropped significantly during the time of occlusion. Illustrative raw data for isolated feed arteriole experiments are given in Table 3.2 and 3.3.

Filtration control of the myogenic response was also investigated in isolated soleus feed arterioles. Following cannulation, the vessels were pressurized to 66 mmHg, at which the internal diameters ranged from 160-200 μm. Myogenic reactivity was assessed in the absence (N=7) of, and following intraluminal addition of 3.5% 40 kD dextran (N=5) added to provide an osmotic attenuation of filtration. As shown in Figure 3.7, myogenic tone (% constriction compared to passive diameter in a Ca^{2+} -free bath) was inhibited by inclusion of intravascular dextran. The

inhibition was most pronounced (and statistically significant) at the higher pressures (81 and 96 mmHg).

Analysis of a rapid step increase from 66 to 96 mmHg (N=4 control; N=5 dextran) in isolated vessels also yielded similar results to those seen *in vivo*. As shown in Figure 3.8, the pressure step initially stretched the vessels by approximately 25% (not statistically different between control and dextran) ~10 s following the step increase. However, the degree of myogenic constriction in response to stretch in control vessels was 24.4 ± 2.4 %, compared to only 13.6 ± 2.4 % when vessels were filled with the dextran solution. This approximate 45% attenuation of myogenic constriction closely corresponds to the 35-52% reduction in the transvascular pressure gradient before and after the 30-mmHg pressure step (34 mmHg osmotic ÷66 mmHg = 52%; 34÷96=35%). Filtration rates were not measured in these isolated vessel experiments.

3.4 Discussion

A major function of the myogenic response is to control microvascular filtration during a change in pressure. For example, an increase in arterial pressure causes myogenic constriction that decreases hydrostatic pressure downstream of the arterioles, resulting in a reduction in Starling forces promoting filtration. However, we demonstrate a novel corollary in this study: that is, filtration appears capable of controlling the myogenic response.

Evidence that led us to this hypothesis was obtained from several recent studies. Two of these (Wang & Tarbell, 1995;Tada & Tarbell, 2002) included computer

simulations, which predicted that the resulting transvascular shear forces on surrounding smooth muscle cells would be of the same order of magnitude as intravascular shear on endothelial cells. This may not be immediately intuitive based on the fact that filtration rates are a small fraction of the blood flow through a vessel. However, since transvascular pathway dimensions for fluid transport are similarly a small fraction of vessel dimensions, the resulting shear forces on the surrounding smooth muscle is significant and may even exceed that present on the inner vessel wall. A second piece of evidence is that when smooth muscle cells in vitro are exposed to an increase in shear across their surface in the physiological range, the cells constrict significantly within minutes (Civelek *et al.*, 2002). Taken together, these three studies led to the hypothesis that filtration shear affects smooth muscle tone of arterioles.

The data obtained in the present study are consistent with this hypothesis. Firstly, baseline arteriolar tone is highly correlated with baseline filtration rates measured in the same arteriolar segments (Figure 3.3). Secondly, when circulating osmotic pressure was adjusted to decrease filtration rates by 40-50%, the myogenic response was similarly attenuated by almost the same percentages, both *in vivo* as well as in excised arterioles (Figures 3.5 and 3.8). It should be noted that this mechanism is not the only one determining myogenic tone, in that studies on isolated muscle cells have demonstrated contraction due to stretch (Hongo *et al.*, 1996).

To our knowledge, this is the first study to measure transvascular filtration and the myogenic response simultaneously. In the *in vivo* experiments, we used a micro-occlusion technique as a method of inducing a step change in hydrostatic pressure.

Arteriolar occlusion produced an average 17% increase in pressure upstream of the pipette (see Table 3.1), comparable to the 22.5% increase reported by Lombard and Duling in the hamster cheek pouch using the same method (Lombard, 1977). Arteriolar occlusion not only gave an increase in pressure that initiated an upstream myogenic response, but also allowed measurement of fluid filtration rate by monitoring the movement of vascular red blood cells. The equation used to measure filtration rate (equation 2.3) has a different form than reported elsewhere (Lee *et al.*, 1971;Harris, 1997), in experiments that had only a passive stretch in diameter. In fact, most studies using the Landis technique are performed in capillaries that do not have smooth muscle. In capillary occlusions, passive stretch typically lasts ~0.5 seconds (for a time course, please see reference (Harris, 1999)), and therefore only the second term on the right hand side of equation 2.3, $-(D/4x) \times (dx/dt)$, is operative. The first term, $-(1/2) \times (dD/dt)$, adjusts the value of J_v/S based on the influence of changing diameter on the movement of red blood cells. The magnitude of the mesenteric myogenic response in our study is similar to that previously reported for mesenteric vessels (Sun *et al.*, 1992), being smaller than seen in muscle microvasculature (Sun *et al.*, 1994).

The time course of the filtration rate following an occlusion shows a sharp decrease with time prior to attaining a steady state value (Figure 3.4). The mechanism underlying this phenomenon is still not clear; however, several possibilities have been considered. One is that following an occlusion, the ensuing myogenic response also constricts pathways for fluid filtration. However, our experiments with adenosine in

calcium-free buffer seem to discount this possibility: the decrease in J_v/S with time was present with or without the full myogenic response (Figure 3.6).

A second possibility is that when the relatively protein-free filtrate leaves the vessel lumen, the vascular protein concentration and associated osmotic pressure increases, thereby decreasing the effective Starling gradient promoting filtration. This phenomenon is likely to occur; however, the estimated effect is much less than the observed decrease in filtration. For example, in our experiments the vascular volume between the marker cell and occluder typically decreased by ~8% in the initial 50 seconds following an occlusion. If protein concentration increased from the usual value of ~4 g/dl (in this age of rat (Harris, 1997;Barnidge & Harris, 2000)) to a value of 4.32 (an increase of 8%), plasma oncotic pressure gradient would be expected to increase from 13.5 to 15 mmHg, using the equation derived for rat plasma proteins (Gore, 2004). Given that hydrostatic pressure is 50.6 mmHg during the occlusion (Table 3.1), the Starling gradient would only decrease by ~5% due to the increase in protein concentration (using equation 3.2): (50.6-15)/(50.6-13.5)=0.95.

A third possibility is related to the step decrease in fluid shear stress on the endothelial surface when vascular flow stops during the occlusion. Several investigators have noted an increase in endothelial hydraulic conductivity after an increase of shear (Lever *et al.*, 1992;Chang *et al.*, 2000;Williams, 1999), and thus a decrease in shear might be expected to decrease hydraulic conductivity. A related fourth possibility is that the endothelial barrier may undergo a sealing effect upon increases in hydrostatic pressure, as observed in vitro by Sill et al. (Sill *et al.*, 1995).

Many studies of the myogenic response are performed in isolated vessels that are cannulated and pressurized without flow, and therefore potentially could differ from *in vivo* responses. However, based on the similarity of our responses to those obtained in isolated microcirculatory arterioles (Zou *et al.*, 1995), these factors are unlikely to have a major influence on our interpretation of how osmotic control of filtration shear influences myogenic constriction. With respect to one difference from isolated vessels, a change in pressure *in vivo* is often accompanied by a change in shear, which in turn can regulate the concentration of vasoactive metabolites and alter nitric oxide- (NO) dependent vasodilation (de Wit *et al.*, 1998;Ungvari & Koller, 2001). However, de Wit et al. (de Wit *et al.*, 1998) have demonstrated that whereas the diameter of large arterioles are regulated by shear-induced NO release, the diameter of small arterioles are not. (It is also known that the contribution of EDHF to endothelium-dependent relaxations increases as the vessel size decreases (Tomioka *et al.*, 1999)) The reason that changes in shear forces on arteriolar endothelium would not alter NO-dependent vascular tone could be explained by the findings of Kashiwagi et al. (Kashiwagi *et al.*, 2002), who found that arterioles of the size in our study obtain their NO mainly from non-endothelial sources: little endothelial NO synthase was expressed in the smaller arterioles. Additionally, we see similar osmotic inhibition of myogenic reactivity in isolated vessels where flow influences have been eliminated. In the isolated vessel experiments, we were further able to eliminate the *in vivo* influence of signals originating in neighboring vessels of a network, signals that are known to propagate through gap junctions (Rivers, 1995;Segal & Duling, 1989).

Myogenic experiments in isolated vessels are typically performed in larger vessels with higher pressures and baseline tone compared to our *in vivo* 20-30 μm arterioles. Therefore, to determine whether our *in vivo* observations would also apply to more traditional techniques of studying the myogenic response, we repeated similar studies in isolated 1A soleus feed arterioles according to established protocols (Jasperse *et al.*, 1999;Tickerhoof *et al.*, 2003). As in the *in vivo* mesentery, attenuation of filtration decreased myogenic tone (Figure 3.7) and partially inhibited the transient myogenic response subsequent to a step increase in pressure (Figure 3.6). Inert dextran was used in these experiments to verify that our *in vivo* results were due to osmotic effects of albumin and Ficoll.

In conclusion, we have obtained evidence that transvascular fluid filtration helps control the arteriolar myogenic response. The mechanism of this response is hypothesized to be due to fluid shear forces experienced by smooth muscle cells associated with transvascular filtration flow. Continued investigation of these mechanisms may provide useful information regarding the regulation of microvascular perfusion and exchange: Future studies should be directed toward delineating the molecular pathways involved in transducing this response.

Table 3.1 Systemic blood pressure, red blood cell velocity and arteriolar pressure. Data are given as mean ± SE. N is the number of experiments, one per animal.

	BSA/Ficoll experiments			BSA experiments		
	N	Baseline	BSA /Ficoll	N	Baseline	BSA
Systemic blood pressure (mmHg)	10	97.3 ± 3.1	94.5 ± 2.3	5	99.0 ± 1.6	88.6 ± 2.2
RBC Velocity (mm/s)	10	4.0 ± 0.4	4.0 ± 0.4	5	4.0 ± 0.7	4.0 ± 0.6
Arteriolar hydrostatic pressure (mmHg)						
Preocclusion	4	43.2 ± 4.0	40.4 ± 4.1	-	-	-
Postocclusion	4	50.6 ± 4.8	47.4 ± 4.7	-	-	-

Table 3.2 Illustrative raw data of diameter in response to changes in intraluminal pressure in soleus feed arterioles. Data are given as mean ± SE. N is the number of experiments.

		Intraluminal pressure (mmHg)									
		66	81	96	81	66	52	37	22	37	66
No dextran (N=5)	active diameter (μm)	173 ±12	169 ±11	163 ±9	168 ±8	174 ±8	170 ±10	163 ±13	150 ±9	161 ±13	165 ±9
	passive diameter (μm)	234 ±6	236 ±7	241 ±10	233 ±12	230 ±12	221 ±11	208 ±9	177 ±3	211 ±5	240 ±6
Dextran (N=7)	active diameter (μm)	188 ±10	189 ±9	189 ±10	188 ±8	185 ±8	180 ±8	176 ±8	168 ±9	180 ±11	181 ±11
	passive diameter (μm)	234 ±12	235 ±12	232 ±12	231 ±12	230 ±12	220 ±13	209 ±12	184 ±11	208 ±9	232 ±9

Table 3.3 Illustrative raw data of diameter in response to step increases in pressure from 66 to 96 mmHg in soleus feed arterioles. Data are given as mean ± SE. N is the number of experiments. Where max refers to the maximally stretched state and S.S. is steady-state.

	D_{basal} (μm)	D_{max} (μm)	$D_{S.S}$ (μm)
No dextran (N=4)	163 ± 10	205 ± 5	155 ± 8
Dextran (N=5)	185 ± 12	220 ± 14	190 ± 15

Figure Legends

Figure 3.1. A schematic of micro-occlusion technique for measurements of J_v/S and hydrostatic pressure in small arterioles.

Figure 3.2. A diagram of experimental setup for myogenic reactivity of isolated soleus feed arterioles.

Figure 3.3. Percent baseline tone, $100\times(D_{max} - D_I)/D_{max}$, as a function of J_v/S. The line represents the linear regression between % tone and J_v/S (% tone = 0.96 + 260 J_v/S, $p<0.001$, r^2=61.3%).

Figure 3.4. Filtration rate vs time following arteriolar occlusion. (A) BSA/Ficoll injection (N=10 each; $p<0.05$ between paired Baseline and BSA/Ficoll data at every time point). (B) BSA injection (N=5 each; $p<0.05$ between paired Baseline and BSA data for all times ≥ 45 sec). Error bars are presented as ±SE.

Figure 3.5. Diameter (% of baseline diameter) vs time following arteriolar occlusion. (A) BSA/Ficoll injection (N=10 each; $p<0.05$ between paired Baseline and BSA/Ficoll data for all times > 30 sec). (B) BSA injection (N=5 each; $p<0.05$ between paired Baseline and BSA data for all times > 30 sec except time = 240 sec). Error bars are presented as ± SE.

Figure 3.6. Filtration rate vs time (panel A) and diameter (% of baseline diameter) vs time (panel B) following arteriolar occlusions (N=6 each) under baseline conditions and subsequent adenosine exposure. For diameter change vs time, $p<0.05$ between paired groups for all times > 30 sec. Error bars are presented as $\pm$ SE.

Figure 3.7. Effect of intravascular dextran on the pressure-myogenic tone relationship of isolated arterioles. Myogenic tone (%) is defined as (1- active/passive diameter)×100. N=5 for controls (No Dextran; mean diameter = 173 ± 12 μm at 66 mmHg) and N=7 for Dextran (mean diameter = 188 ± 9.7 μm at 66 mmHg). Results are presented as mean $\pm$ SE. * $p < 0.05$.

Figure 3.8. Myogenic reactivity of excised arterioles in response to a step increase in pressure from 66 to 96 mmHg (N=4 for No Dextran controls and N=5 for Dextran). (A) Diameters normalized to basal conditions, and (B) Myogenic constriction (%), which is defined as $100\times(D_{max} - D_{S.S.})/D_{max}$ where max refers to the maximally stretched state and S.S. is steady-state. Results are presented as means $\pm$ SE. * $p < 0.05$.

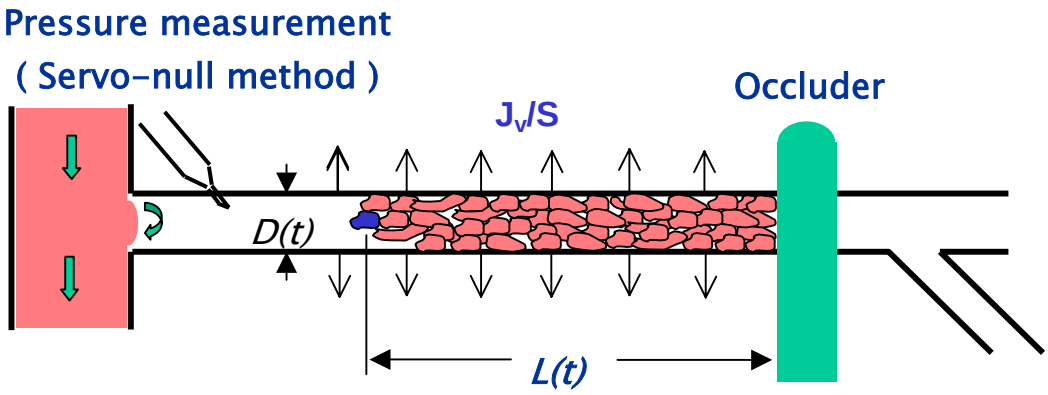

$J_v/S=-(1/2)(dD/dt)-(D/4L)(dL/dt)$

Figure 3.1

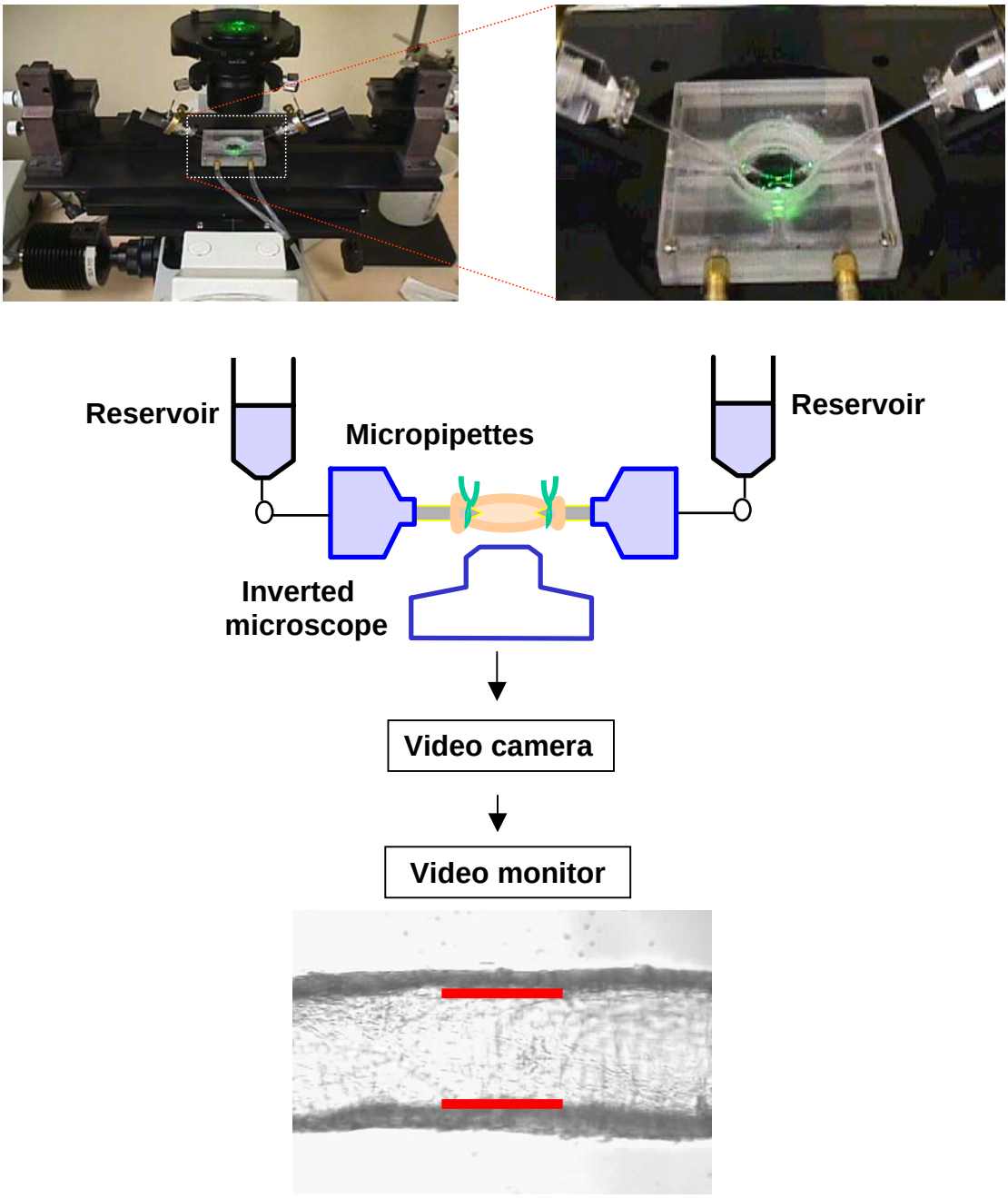
Reservoir
Micropipettes
Reservoir
Inverted
microscope
Video camera
Video monitor

Figure 3.2

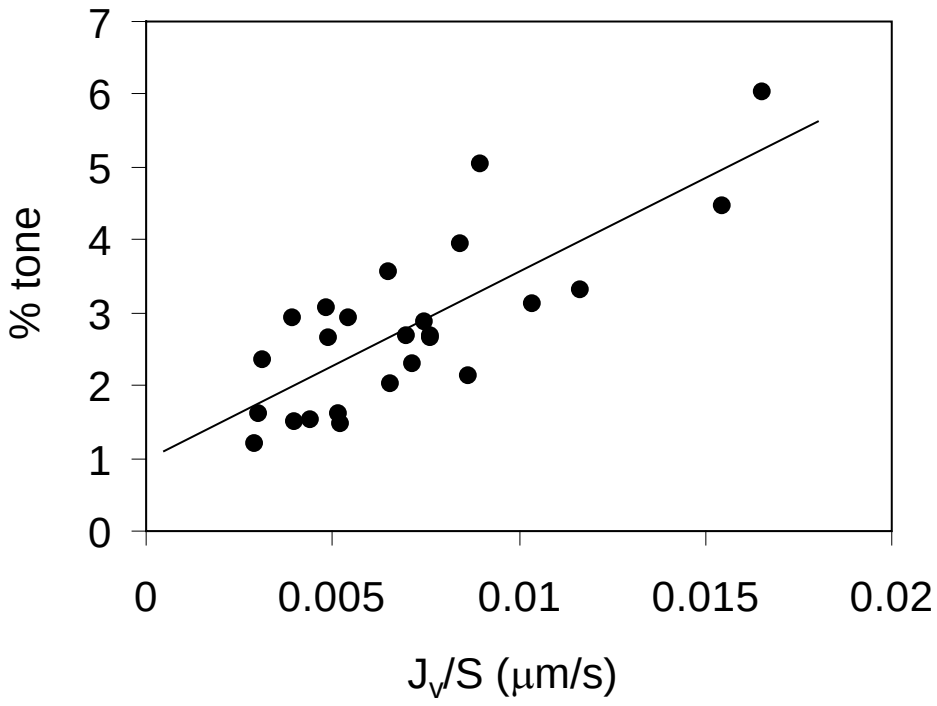

Figure 3.3

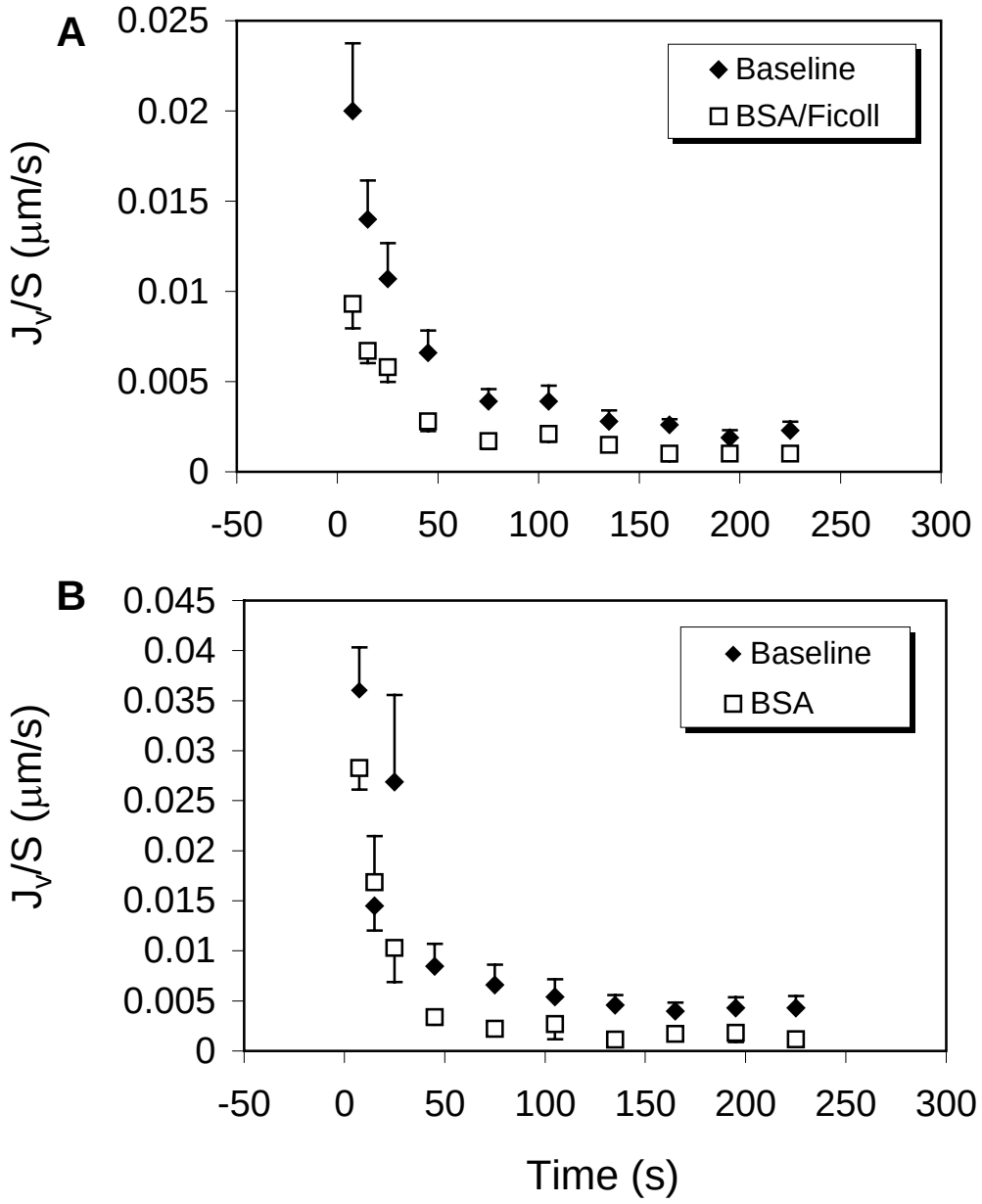
A
0.025
0.02
0.015
0.01
0.005
0
Jv/S (µm/s)
Baseline
BSA/Ficoll
-50
0
50
100
150
200
250
300
B
0.045
0.04
0.035
0.03
0.025
0.02
0.015
0.01
0.005
0
Jv/S (µm/s)
Baseline
BSA
-50
0
50
100
150
200
250
300
Time (s)

Figure 3.4

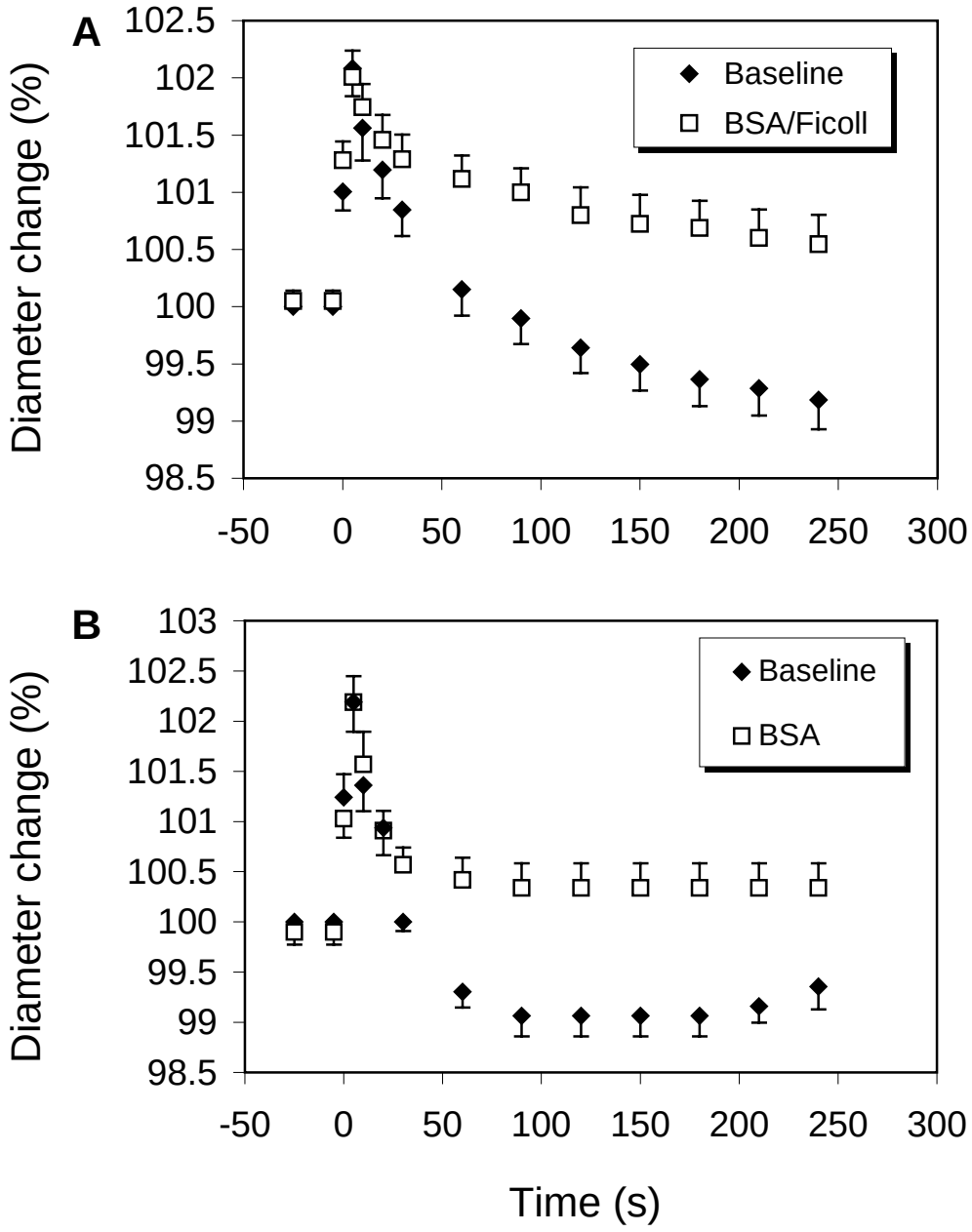
A
Diameter change (%)
102.5
102
101.5
101
100.5
100
99.5
99
98.5
-50
0
50
100
150
200
250
300
Baseline
BSA/Ficoll
B
Diameter change (%)
103
102.5
102
101.5
101
100.5
100
99.5
99
98.5
-50
0
50
100
150
200
250
300
Time (s)
Baseline
BSA

Figure 3.5

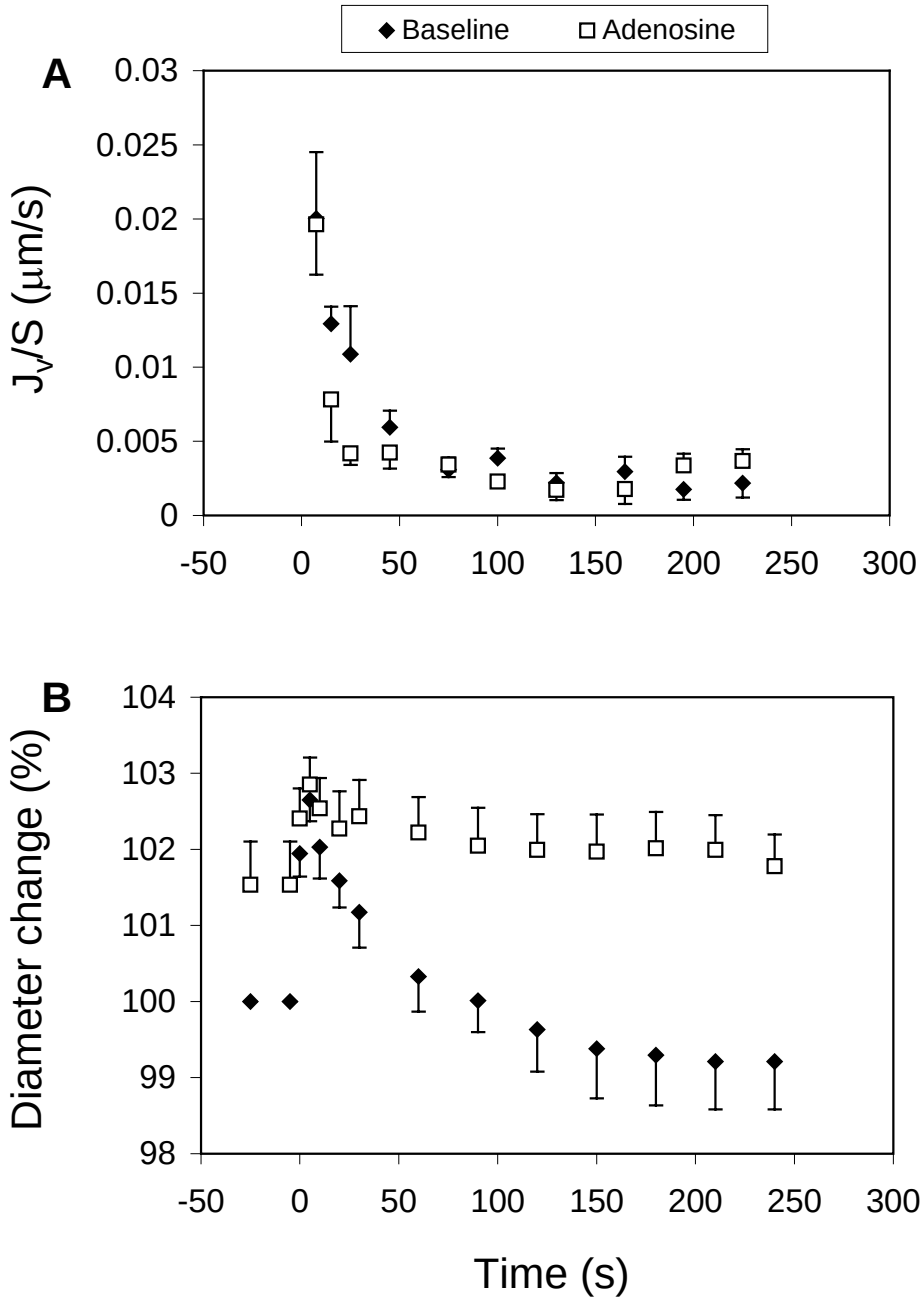
Baseline
Adenosine
A
0.03
0.025
0.02
0.015
0.01
0.005
0
J_v/S (μm/s)
-50
0
50
100
150
200
250
300
B
104
103
102
101
100
99
98
Diameter change (%)
-50
0
50
100
150
200
250
300
Time (s)

Figure 3.6

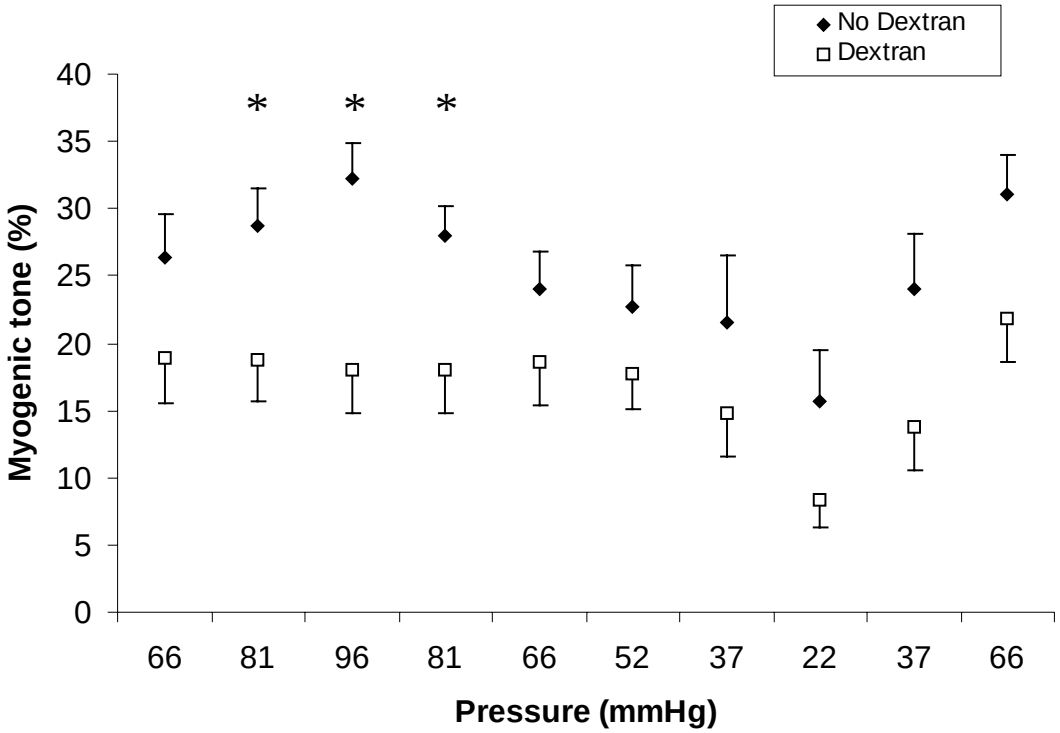
No Dextran
Dextran
Myogenic tone (%)
40
35
30
25
20
15
10
5
0
*
*
*
66
81
96
81
66
52
37
22
37
66
Pressure (mmHg)

Figure 3.7

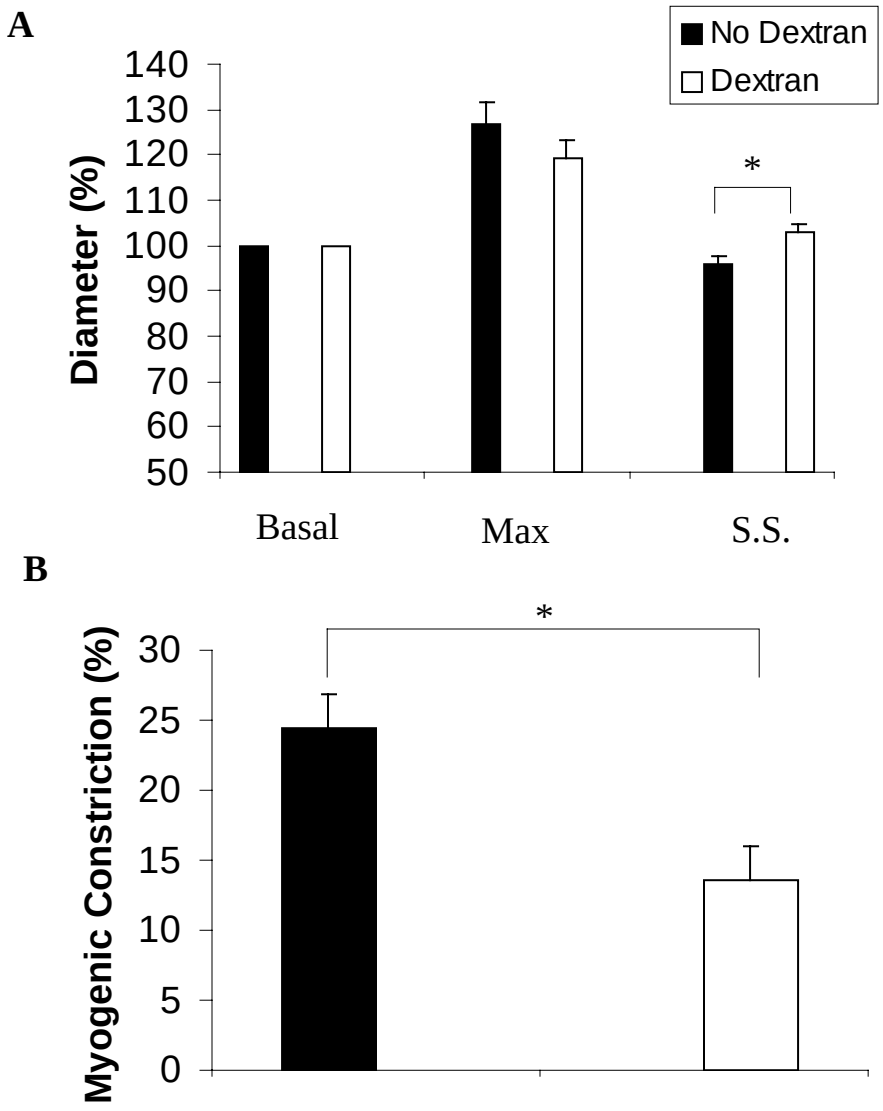
A
No Dextran
Dextran
Diameter (%)
140
130
120
110
100
90
80
70
60
50
*
Basal
Max
S.S.
B
Myogenic Constriction (%)
30
25
20
15
10
5
0
*

Figure 3.8

Chapter 4

REGULATION OF HYDRAULIC CONDUCTIVITY IN RESPONSE TO ACUTE CHANGE IN SHEAR RATE AND PRESSURE

4.1 Introduction

In 1927, Eugene Landis (Landis, 1927) published a novel technique whereby movement of red blood cells in a micropipette-occluded capillary could be used to calculate transvascular filtration rate. His technique, and modifications thereof, remain the most widely used method to investigate regulation of fluid filtration of individual microvessels in vivo (Adamson *et al.*, 2003;Glass & Bates, 2003;Victorino *et al.*, 2004;Rumbaut *et al.*, 2000b;Williams, 2003).

According to Starling's hypothesis, transvascular fluid flux through the endothelial transport barrier is regulated by either changes in pressure gradient (hydrostatic or oncotic) across the vascular wall or by permeability (oncotic reflection coefficient σ or hydraulic conductivity L_p). Application of chemical agents (e.g. histamine, thrombin) increases hydraulic conductivity and fluid filtration rate. Mechanical factors also may affect hydraulic conductivity: endothelial cells may sense and trigger mechanotransduction in response to blood flow shear stress and changes in hydrostatic pressure (Chien *et al.*, 1998;Davis, 1995).

Using the micropipette occlusion technique, Landis described how the fluid filtration rate was most rapid in the initial seconds following occlusion, becoming significantly slower in less than one minute. This was attributed at least in part by the possibility that plasma oncotic pressure could increase with time in occluded vessel,

as a result of much quicker transport of water than of protein. However, another consideration is that the vessel occlusion includes an abrupt change in flow and pressure, both of which could have a time-dependent effect on hydraulic conductivity.

As a microvessel is occluded, blood flow decreases from its basal value to essentially zero flow. Several studies have shown that transvascular exchange can be affected by a change in perfusion rate (Head *et al.*, 1996;Kajimura *et al.*, 1998;Neal & Bates, 2002;Montermini *et al.*, 2002;Yuan *et al.*, 1992;Karmakar, 2001). A small pore model has been proposed as a possible mechanism to account for flow-dependent transport of small solutes (Montermini *et al.*, 2002): moreover, there have been several recent studies of shear-induced increases in fluid filtration performed in vitro (Sill *et al.*, 1995;Chang *et al.*, 2000;Demaio *et al.*, 2001) and in vivo (Lever *et al.*, 1992;Williams, 1999;Williams, 2003). The mechanism by which shear forces could increase L_p appear to be dependent on nitric oxide (NO) (Chang *et al.*, 2000;Lakshminarayanan *et al.*, 2000;Hillsley & Tarbell, 2002). Therefore, when a capillary stops flowing, it might be expected that Lp could decline in a matter of seconds as shear-induced production of NO ceases.

Another mechanical issue associated with microvessel occlusion is the step increase in hydrostatic pressure. For example, when a capillary is occluded at its downstream end, pressure throughout the vessel increases to that of the feeding arteriole. Recent studies (Demaio *et al.*, 2004;Tarbell *et al.*, 1999) indicate that a step increase in hydrostatic pressure causes an NO-dependent decrease in L_p in what has been called a sealing effect. However, the time course of the changes in L_p in these studies were over a period of minutes to hours: it has yet to be determined whether a

pressure sealing effect would occur over a period of seconds during a microvessel occlusion experiment.

The effects of mechanical perturbations (shear stress, pressure) primarily have been examined in micropipette-cannulated vessels or in endothelial monolayers in vitro. The primary objective of the current study is to determine whether acute changes in blood flow shear and pressure might influence measurements of hydraulic conductivity in autoperfused, rather than cannulated, microvessels. Additionally, a role for NO in shear-mediated changes in Lp is investigated.

4.2 Materials and Methods

4.2.1 Animal preparation

Animal procedures were performed in accordance with institutional guidelines. Male Wistar rats weighing 250 – 300 g were anesthetized by an intraperitoneal injection of 135 mg/kg thiobutabarbital (Inactin, Sigma T-133, St. Louis). A segment of the small intestine was exteriorized through a midline abdominal incision, and the rat was placed on its right side on a Plexiglas board so that a selected section of mesentery could be draped over a glass cover slip glued on a hole centered in the board. The exposed section of the mesentery was superfused continuously with bicarbonate-buffered saline (BBS). More details about surgery and BBS preparations are given in chapter 2, section 1.

4.2.2 Video microscopy

A description of the video microscopy techniques used are described in chapter 2, section 2.

4.2.3 Measurement of transvascular filtration

Capillary and arteriolar filtration rates (J_v) were measured using a modification of the original Landis technique (Landis, 1927) during micropipette occlusion as described in chapter 2, section 2. The occluder was positioned over a selected arteriole (20-30 μm in diameter) or capillary (6-8 μm in diameter) and carefully lowered onto the vessel by micromanipulator to compress the lumen. The filtration rate was calculated from the decreasing volume (*V*) between the micropipette and red blood cells that were 250-400 μm upstream of the occluder (250–300 μm for capillaries and 300–400 μm for arterioles). More details about measurements of transvascular filtration are described in chapter 2, section 3.

4.2.4 Measurement of shear rate (SR)

Arteriolar and capillary mean RBC velocity were calculated as V_{mean} = centerline velocity / correction factor. The correction factor is expected to gradually decrease from 1.6 for arterioles to 1.0 for true capillaries (Koller & Kaley, 1991;Lipowsky & Zweifach, 1978;Davis, 1987). Assuming cylindrical geometry, wall shear rate (SR) can be obtained using the Newtonian definition, $SR = 8 \times (V_{mean}$ / diameter (D)). In some of our experiments, we induced an increase in shear rate. The normalized increase in shear rate in the same vessel can be expressed as

$$SR_{shear} / SR_{baseline} = (V_{shear} / V_{baseline}) \times (D_{baseline} / D_{shear}) \quad (4.1)$$

4.2.5 Starling forces regulating fluid filtration

Starling's equation is described in chapter 2, section 2.

4.2.6 Method of increasing shear rate and hydraulic conductivity measurements in capillary

An increase in blood flow velocity through a capillary was induced by occluding a feeding arteriole downstream of the capillary branch point. As shown in Figure 4.1, the occlusion of a third-order (A_3) arteriole can result in an increase in capillary shear rate. However, occlusion of the upstream arteriole also induces an increase in pressure upstream of the occluder and can lead to an increase in capillary pressure. In our previous measurements of A_3 arteriolar pressure (Table 3.1), the mean value was 43 mmHg and the pressure increase due to occlusion was 7 mmHg. Therefore, it is expected that the pressure increase in the capillary due to arteriolar occlusion will be approximately 7 mmHg when increasing shear. During the measurement of J_v/S using the modified Landis technique, capillary pressure will be equilibrated to the arteriolar pressure (P_a) due to capillary occlusion. In all the J_v/S measurements from capillaries, RBC movement due to filtration was measured within 50 - 100 μm from the arteriolar branch. Baseline J_v/S can be expressed as (using equation 2.5):

$$(J_v/S)_{baseline}=(L_p)_{baseline}\,[P_a-\sigma_{baseline}\,\pi_c] \qquad (4.2)$$

At the higher shear rate, capillary pressure will be increased to $P_a + \Delta P_a$ during the measurement of J_v/S and thus J_v/S at the high shear state can be expressed as

$$(J_v/S)_{shear} = (L_p)_{shear}\,[P_a+\Delta P_a - \sigma_{shear}\ \pi_c] \qquad (4.3)$$

where $\sigma_{baseline}$ and σ_{shear} refer to osmotic reflection coefficients at baseline and increased shear, respectively.

Dividing equation (4.3) by equation (4.2) and rearranging yields

$$\frac{(L_p)_{shear}}{(L_p)_{baseline}} = \frac{[P_a - \sigma_{baseline}\pi_c]}{[P_a + \Delta P_a - \sigma_{shear}\pi_c]}\ \frac{(J_v/S)_{shear}}{(J_v/S)_{baseline}} \qquad (4.4)$$

where P_a=43 mmHg, ΔP_a =7.4 mmHg (average values, from Table 3.1), $\sigma_{baseline}$=0.9 and π_c =15 mmHg (from ref.(Harris, 1997)) . The reflection coefficient at increased shear, $\sigma_{shear,}$ was assumed to be 0.9 in the estimation of normalized L_p based on assumption that the increase in shear rate would not alter σ. However, we do not rule out the possibility that there will be a change in σ with the change in shear rate and this is addressed in the data analysis.

4.2.7 Experimental protocols

After measuring baseline J_v/S for 50 s using a modified Landis technique, the micropipette occluder was released to resume blood flow in the capillary. After 10 min, the capillary was exposed to increased flow velocity for 60 s by occluding the feeding A_3 arteriole, and then J_v/S was measured for 50 s from the same capillary. The same experimental protocol was used for arteriolar J_v/S measurements, in which J_v/S was measured from fourth-order (A_4) arterioles and the feeding A_3 arteriole was occluded to induce an acute increase in shear rate through the A_4 arteriole. To further investigate whether the shear-induced change in J_v/S was associated with NO, the

nitric oxide synthase (NOS) inhibitor L-NAME (50 μM; Sigma) was superfused following the baseline J_v/S measurements. After 10 min superfusion of L-NAME, the capillary was exposed to higher shear rate for 60 s and J_v/S was measured a second time. To assess the contribution of pressure to the J_v/S response, a capillary occlusion was made to create zero shear and then after 30 s, a step increase in capillary hydrostatic pressure was induced by occluding the feeding A_3 arteriole downstream of the capillary branch, during which time J_v/S was measured for 50 s continuously.

4.2.8 Statistics

Paired-t tests or unpaired t-tests were used when two sets of data were compared using Minitab software (Minitab Inc., State College, PA). Data among groups were compared with the Bonferroni test. Error bars are presented as ± standard error (SE). Statistical significance was set at $P<0.05$.

4.3 Results

An illustrative raw data of shear rate in capillaries and small arterioles were given in Table 4.1. Increases in shear rate were almost identical for both capillaries and small arterioles.

Figure 4.2 illustrates the time-dependence of J_v/S and the change in J_v/S and estimated L_p in response to an acute increase in shear rate (N=15, SR_{shear} / $SR_{baseline}$ =2.02) in capillaries of rat mesentery. In the baseline measurement of J_v/S, there was a transient decline in which J_v/S at 50 sec of occlusion is only 55 ± 8% of the value obtained at 5 sec (Figure 4.2A). The increase in shear rate is accompanied by an

increase in pressure of 17% (Table 3.1). With an increase in shear (102%) and pressure (17%), J_v/S increased by 91% in the initial 5 sec of measurement compared to baseline, but only by 25% by 50 sec (Figure 4.2B). Assuming a 17% increase in hydrostatic pressure (from 43 to 50 mmHg), Starling's equation estimates a 24% increase in J_v/S with no change in L_p or σ (assumed to be 0.9). The time course of L_p (normalized to baseline) shows an initial increase followed by transient return to basal values in response to the increase in shear rate (Figure.4.2C). During the initial 5 s, L_p increased by 53 ±4 % from the baseline value ($P < 0.05$), and then returned to the baseline L_p after 25 - 30 s.

A positive correlation was observed between the normalized L_p and the percentage change in shear rate in the initial 10 s of measurement ($P < 0.001$, $r^2 = 71.2\%$), but there was a lack of correlation from time >= 20 sec ($P > 0.05$) as shown in Figure 4.3. In this result, normalized L_p was obtained based on the assumption that there would be a minimal pressure effect irrespective of change in shear rate. However, we can not rule out the possibility that the higher change in shear rate might be accompanied by a larger magnitude of increase in pressure, thereby resulting in larger increase in J_v/S compared to the case with smaller change in shear rate. To address this issue, the dependency of the relationship between increase in shear rate (%) and normalized L_p (t=5s) on the uncertainty in the magnitude of pressure increase (ΔP_a) was tested (Table 4.2). Considering a standard deviation of pressure measurements, the magnitude of step increases in pressure induced by arteriolar occlusion was varied from 5.4 to 9.4 mmHg (averaged value is 7.4 mmHg,

see table 3.1). When different values of ΔP_a were used depending on the percentage change in shear rate (case B), the slope of the regression plot between percentage change in shear rate and normalized L_p was diminished compared to the case A, but still positively correlated ($P<0.01$).

To further investigate the effect of NOS inhibition on the shear-induced change in J_v/S, L-NAME was administered prior to and during the increase in shear rate (Figure 4.4). The superfusion of 50μM L-NAME eliminated the shear-induced increase in L_p during the initial 10 seconds following occlusion.

Similar experiments were performed in small arterioles to investigate the potential influence of the change in shear rate on arteriolar L_p (Figure 4.5). The acute increase in shear rate in small arterioles was almost identical to that of true capillary ($106 \pm 6\%$ increase in arterioles vs 102 ± 8 % increase in capillaries). As shown in Figure 4.5 (panel A), the time course of L_p in small arterioles also showed an initial increase from its baseline value (statistically different from baseline, $P<0.05$) for 10-15 s followed by a return to baseline by 20 s following the occlusion. However, the increase in L_p during the initial 5 s in small arterioles was only 23 ± 4 %, compared to 53 ± 4 % increases in capillaries (Figure 4.5B).

An additional set of experiments was performed from capillaries to investigate the potential contribution of a pressure sealing effect following occlusion (Figure 4.6). During the initial 30 s of a baseline J_v/S measurement, a transient decrease in J_v/S is observed throught the next 25 s. After a subsequent step increase in pressure while maintaining zero shear rate via arteriolar occlusion, a similar transient J_v/S

response was observed (Figure 4.6A). There was a 38 % reduction in estimated L_p at 25 s compared to the baseline value at 5 s, and a 15 % reduction at 80 s compared to the value at 35 s (Figure 4.6B).

In these calculations of normalized L_p, we assumed a constant value of arteriolar pressure and reflection coefficient (σ). To assess the potential contribution of altered pressure and σ on the estimation of L_p, the calculations were repeated with various values of pressure and σ. Figure 4.7 demonstrates the sensitivity of the calculation when changing the baseline value of pressure in the range of 35-51 mmHg, the magnitude of pressure change in the range of 5 to 9 mmHg, and allowing σ to change in the range of 0.6-0.9 following the increase in shear. Assuming an extreme change of pressure and σ (P_a=35 mmHg, ΔP_a=9 mmHg, σ=0.6) following the increase in shear, normalized L_p was estimated to decrease from 1.53 ± 0.04 (when P_a=43 mmHg, ΔP_a=7.4 mmHg, σ=0.9) to 1.11 ± 0.03, but still significantly larger than 1 ($P<0.05$).

4.4 Discussion

The major finding of the present study is that changes in hydraulic conductivity were positively correlated with acute changes in shear rate in autoperfused microvessels in rat mesenteric tissue. Using a modified Landis technique, micropipette occlusion of microvessels allowed a measure of fluid filtration rate (J_v/S). In capillaries of the rat mesentery, we observed a transient decline in which J_v/S at 50 sec of occlusion was only 55±8 % of the value obtained at 5 sec (Figure 4.2A). This transient nature of L_p was also observed in a frog mesentery model

(Williams, 1999). There are several possible explanations for this phenomenon. One possibility is that this decline in J_v/S is due to the step reduction in shear rate (to zero) following occlusion, i.e., hydraulic conductivity (L_p) could be dependent on shear rate, and therefore decreases during occlusion. A second possibility is that the step increase in capillary pressure during the occlusion induces a pressure "sealing effect" that decreases L_p. A third possibility is that when the relatively protein-free filtrate leaves the vessel lumen, the vascular protein concentration and associated osmotic pressure increases, thereby decreasing the effective Starling gradient. However, the contribution of this effect is much less than the observed decrease in filtration as we discussed in chapter 3 for arterioles. For example, in our experiments the vascular volume between the marker cell and occluder typically decreased by ~9% in the initial 50 seconds following an occlusion. If protein concentration increased from the usual value of ~4 g/dl (in this age of rat (Harris, 1997;Barnidge & Harris, 2000)) to a value of 4.36 (an increase of 9%), plasma oncotic pressure would be expected to increase from 15 to 16.65 mmHg, using the equation derived for rat plasma proteins (Gore, 2004). Given that the hydrostatic pressure of the capillary is equal to arteriolar pressure (43 mmHg) during the occlusion (Table 3.1), the Starling gradient would only decrease by ~5% due to the increase in protein concentration (using equation 2.5): $(43-0.9\times16.65)/(43-0.9\times15)=0.95$.

In 15 rats, baseline J_v/S was measured, then prior to a second capillary occlusion, we increased baseline capillary shear rate by 102 ± 8% by occluding the feeding arteriole just downstream of the capillary branch. This technique also increases arteriolar pressure by 17 ± 2% (Table 3.1). With this increase in shear and

pressure, J_v/S increased by 91 ± 6% in the initial 5 s of measurement compared to baseline, but only by 25 ± 4% by 50 s (Figure 4.2B). With shear rates equal to zero during capillary occlusion, the 25% difference at 50 sec appears to correspond to the sustained pressure difference due to downstream arteriolar occlusion. We hypothesize that the larger change in shear may be a more important factor than the smaller change in pressure in influencing the initial decline in J_v/S following occlusion.

In this study, an arteriolar occlusion was used to elicit an increase in blood flow velocity in a non-occluded capillary branch in vivo. After measuring baseline J_v/S, the capillary was exposed to increased flow velocity for 60 seconds, and then J_v/S was measured using a modified Landis technique. The limitation of this technique in finding the effect of shear on L_p is that the capillary is in a state of zero shear rate when making measurements. Thus, this makes the interpretation of results complicated. However, we hypothesized that the increased shear effect would appear at least during the initial periods of measurements. A similar phenomenon was observed in experiments of shear-dependent vasodilation using same technique of arteriolar occlusion (Koller & Kaley, 1990;Koller & Kaley, 1991), where an increase in shear rate was followed (with a delay of 6-15 s) by an increase in diameter and further dilation occurred for 10 to 20 s after release of the occlusion.

The response curve of normalized L_p plotted as a function of percentage change in shear rate (Figure 4.3) also supported the hypothesis, in which the lack of correlation was observed after 20 s while showing a positive correlation during the initial 10 s. Another question that remains unanswered is how quickly endothelial cells can respond to change in shear. In general, it is known that inflammatory

mediators regulate microvascular permeability over a few minutes. However, Montermini et al. (Montermini *et al.*, 2002) observed a more rapid changes in permeability of small solutes within few seconds of change in perfusion rate. This finding supports our hypothesis that a step reduction in shear may account for the observed transient decrease in J_v/S to some extent.

Inflammatory mediators can change microvascular permeability by activating various signaling pathways, which leads to loose or opened intercellular junctions by dissociation of junctional proteins and their connection to the cytoskeleton (Yuan, 2000). It is well established that NO plays an important role in the regulation of microvascular permeability. In acute inflammation, a calcium-activated, NO-cGMP-dependent pathway is believed to be a common pathway to increase microvascular permeability(He *et al.*, 2000). Regarding the role of shear stress in microvascular permeability, NO release by endothelial cells has been suggested to be an important mechanism (Chang *et al.*, 2000). Investigations performed on individually perfused microvessels indicated that hydraulic conductivity is decreased by nitric oxide synthase (NOS) inhibition (He *et al.*, 1997;Rumbaut *et al.*, 1995;Rumbaut *et al.*, 2000b). However, it should be also noted that the application of NOS inhibitors can induce an increase in leukocyte adhesion to endothelial cells and a subsequent increase in hydraulic conductivity in autoperfused vessels when L-NAME is treated for longer periods of time (20 min) (Harris, 1997). These findings have suggested that the effect of NOS inhibition on hydraulic conductivity is dependent on the presence of neutrophils, with the effect reversed with anti-neutrophil serum or an antibody against the CD18 leukocyte adhesion molecule. Therefore, in the present study, the

measurements with L-NAME treatment was done within 5 to 15 min to attenuate the possible role of leukocyte adhesion in J_v/S measurements. Our in vivo observations of an attenuation in the L_p response with L-NAME in the presence of increased shear also supports the previous in vitro findings (Chang *et al.*, 2000;Sill *et al.*, 1995) that a change in fluid shear stress may regulate hydraulic conductivity by releasing NO.

Another interesting observation in the present study is that there was a differential sensitivity of hydraulic conductivity to shear rate between true capillaries and arterioles. It would appear that a capillary endothelium is more sensitive to a change in shear stress compared to arteriolar endothelium. The mechanisms responsible for this differential response in L_p remain unclear. However, based on the observation that NOS inhibition attenuated shear-induced change in L_p in capillaries, one possible explanation for this result is that there is a differential expression of eNOS in the rat mesenteric microcirculation. Kashiwagi et al. (Kashiwagi *et al.*, 2002) have observed abundant expression of eNOS in capillaries and venules in rat mesenteric tissue in vivo in contrast to little expression of eNOS in small arterioles.

One drawback of the current method for increasing shear rate using parallel arteriolar occlusion is that the hydrostatic pressure of the capillary also is altered at the same time. Recent studies (Tarbell *et al.*, 1999;Demaio *et al.*, 2004) have shown a time-dependent decrease in L_p on application of a hydrostatic pressure gradient, termed a “sealing effect”. Mechanical and biological mechanisms are known to be involved in this phenomenon. DeMaio et al. (Demaio *et al.*, 2004) have suggested that the sealing effect reduces the size of the small pore pathway for water transport mechanically on pressure application during the initial periods of time in bovine

aortic endothelial cell (BAEC) monolayer experiments. They also observed a significant increase in tight junction protein zonula occludins-1 (ZO-1) after longer periods of pressure application suggesting the role of a biological mechanism in this phenomenon. In the present study, we have tested the relative contribution of pressure "sealing effect" in our J_v/S measurements. To remove the possible interaction of shear effect, a step increase in pressure was applied and J_v/S was measured after maintaining zero shear rate for 30 s. We hypothesized that the occlusion of capillaries for 30 sec before the pressure increase would remove the possible shear effect in our measurements based on the observation in Figure 4.3. According to our data, it is likely that pressure-induced sealing effect might contribute to our L_p measurements. It appears that both shear and pressure sealing effects may account for the 38% reduction in L_p at 25 s compared to the baseline response (value at 5 s), however, the 15% decrease in L_p at 80 s from the value at 35 s can be attributed to the pressure sealing effect. However, for more quantitative estimation of pressure sealing effect on hydraulic conductivity, further detailed investigation is required.

In conclusion, the results of this study indicate the possible contributions of shear and pressure sealing effects in regulating fluid filtration through endothelium following vascular occlusion in vivo. We have obtained evidence that an acute change in shear rate may regulate L_p of arteriolar and capillary endothelium. It appears that an acute change in shear regulates L_p in mesenteric capillaries by a NO-dependent mechanism. The differential response of L_p between arterioles and capillaries may indicate heterogeneity in endothelium sensitivity to a mechanical stimulus within microvascular network. Furthermore, our results indicate that an

adaptive sealing effect induced by a step change in pressure also partially contributes to regulate endothelial barrier function. These findings support the idea that endothelial transport barrier responds actively to changes in hemodynamic forces in microcirculation and regulate transport pathway for water through biological as well as mechanical mechanisms.

Potential source of errors in estimating normalized L_p

In estimating a normalized value of L_p using equation 4.4, the ratio of the pressure gradient is an important factor. In the current experiments, arteriolar pressure was measured separately for few selected cases (Table 3.1) and an averaged value was used in determining normalized L_p. Considering a standard deviation of pressure measurements, baseline hydrostatic pressure of small arterioles were varied from 35 to 51 mmHg. In addition, the magnitude of step increases in pressure induced by arteriolar occlusion was varied from 5.4 to 9.4 mmHg based on a standard deviation of 2 mmHg in actual pressure measurements of the pressure change. Therefore, these uncertainties in pressure measurements can result in a potential error in determining L_p. Furthermore, in the present study, assumed values of osmotic reflection coefficients were used to estimate normalized L_p ($\sigma_{baseline}=\sigma_{shear}=0.9$). An alteration of osmotic reflection coefficient as well as L_p has been reported in the presence of inflammatory mediators. Thus, we cannot rule out the possibility that our observed L_p at increased shear was overestimated due to the overestimation of σ_{shear}.

To address this issue, we performed a sensitivity analysis by changing arteriolar pressure before and after arteriolar occlusion and osmotic reflection coefficient. The

sensitivity of the normalized L_p to each variable can be seen in Figure 4.7. For all cases, normalized L_p was significantly different from 1. This result indicates that uncertainties of pressure measurement and osmotic reflection coefficient might not be critical to our interpretations. Therefore, it is likely that a change in L_p is a major contributor to change in J_v/S. However, it should be noted that L_p was increased by only 10% when we assumed an extreme change of pressure increase (26% increase in pressure) and osmotic reflection coefficient (decrease in σ_{shear} from 0.9 to 0.6) in response to increase in shear rate (Figure 4.7B).

Table 4.1 Illustrative raw data of shear rate for capillaries and small arterioles.

	Shear Rate (s^{-1})	
	Capillaries (N=15)	Arterioles (N=11)
Baseline	1725 ± 192	815 ± 128
Shear	3415 ± 370	1657 ± 257

Table 4.2 Dependency of the relationship between increase in shear rate (%) and normalized L_p (t=5s) on the uncertainty in the magnitude of the pressure increase (ΔP_a). Case A is the same as the result shown in Figure 4.2A, in which same values of arteriolar pressure (P_a) and ΔP_a were used irrespective of changes in the shear rate (ΔSR). In case B, the same values of P_a were used irrespective of ΔSR but different values of ΔP_a were used depending on ΔSR.

Increase in Shear Rate (ΔSR, %)	Case A	Case B
$\Delta SR < 80\%$	$P_a = 43$ mmHg $\Delta P_a = 7.4$ mmHg	$P_a = 43$ mmHg $\Delta P_a = 5.4$ mmHg
$80\% < \Delta SR < 120\%$	$P_a = 43$ mmHg $\Delta P_a = 7.4$ mmHg	$P_a = 43$ mmHg $\Delta P_a = 7.4$ mmHg
$\Delta SR > 120\%$	$P_a = 43$ mmHg $\Delta P_a = 7.4$ mmHg	$P_a = 43$ mmHg $\Delta P_a = 9.4$ mmHg
Regression	$L_{p\ baseline} / L_{p\ shear}$ $= 0.00364\ \Delta SR(\%) + 1.11$	$L_{p\ baseline} / L_{p\ shear}$ $= 0.00172\ \Delta SR(\%) + 1.32$
P	$P < 0.001$	$P = 0.009$
R^2 (%)	71.2 %	40.4 %

Figure Legends

Figure 4.1. Method of increasing capillary shear rate. After the baseline J_v/S measurement, capillary shear rate was increased for 1 minute by occluding the feeding arteriole just downstream of the capillary branch. (A) Baseline capillary shear rate ($SR_{baseline}$) and pressure (P_c) before capillary occlusion. (B) Baseline capillary occlusion for J_v/S measurements; during occlusion pressure increases to that in the feeding arteriole (P_a). (C) Increased shear rate (SR_{shear}) through capillary by arteriolar occlusion that also increases arteriolar pressure (ΔP_a). (D) J_v/S measurement at increased shear rate and pressure ($P_a+\Delta P_a$). White and black arrows indicate blood flow through arteriole and capillary respectively.

Figure 4.2. Effects of acute change in shear rate on capillary J_v/S and L_p (N=15, SR_{shear} / $SR_{baseline}$ =2.02±0.08). (A) Baseline measurements of J_v/S. (B) % change in J_v/S in response to acute increase in shear rate at time = 5 and 50 s following capillary occlusion. The increase in shear rate is accompanied by an increase in pressure of 17% which in itself would be expected to increase J_v/S by 24% according to Starling's equation. (C) Time course of normalized L_p (=$L_{p\ shear}$ / $L_{p\ baseline}$) in response to the increase in shear rate. Error bars are presented as ±SE. * : $P<0.05$, +: significantly different from 1.

Figure 4.3. Response of L_p for true capillaries. (A) Normalized L_p as a function of percentage change in shear rate (N=14). The line represents the linear regression between normalized L_p and percentage change in shear rate (where $L_{p\ baseline} / L_{p\ shear} = 0.00364\ \Delta SR(\%)+1.11$). (B) Slope of the linear regression relation between normalized L_p and percentage change in shear rate at different times following capillary occlusion.

Figure 4.4. Effects of L-NAME on L_p for capillaries to acute increase in shear rate. (A) Time course of normalized L_p with and without L-NAME (50 μM) in response to increase in shear rate (N=5, $SR_{shear} / SR_{baseline} = 1.92\pm0.15$ for shear only and $SR_{shear} / SR_{baseline} = 1.91\pm0.13$ for shear with L-NAME). (B) % increase in L_p at time=5 and 50 s. Error bars are presented as ±SE. * $P<0.05$ between shear only and shear with L-NAME data.

Figure 4.5. Normalized L_p to increase in shear rate for small arterioles and capillaries. (A) Time course of normalized L_p for small arterioles (N=11, $SR_{shear} / SR_{baseline} = 2.06\pm0.06$). (B) Comparison of percentage change in L_p at time=5 and 50 s between arterioles (N=11) and true capillaries (N=15, $SR_{shear} / SR_{baseline} = 2.02\pm0.08$). Error bars are presented as ± SE. * Significantly different from 1 ($P<0.05$), + $P<0.05$.

Figure 4.6. Effects of step change in pressure on the time course of J_v/S (N=7, where J_v/S at 100% = 0.027±0.00641 μm/s) in capillaries. (A) A selected true capillary was occluded for baseline measurements of J_v/S, which results in zero shear rates (The hydrostatic pressure of capillary can be assumed to be equal to arteriolar pressure P_a). After 30 sec, down stream of feeding arteriole was occluded to initiate increase in pressure through capillary while maintaining zero shear rates (The hydrostatic pressure of capillary will increase from P_a to $P_a+\Delta Pa$). A small transient decrease in J_v/S was observed following the step increase in pressure. (B) Percentage change in L_p at 25 s and 80 s normalized from the value at 5s and 35s, respectively. Error bars are presented as ±SE. * $P<0.05$.

Figure 4.7. Sensitivity of the normalized L_p (t=5s) with respect to uncertainties in the baseline arteriolar pressure (P_a), magnitude of pressure increase (ΔP_a), and osmotic reflection coefficients (N=15).

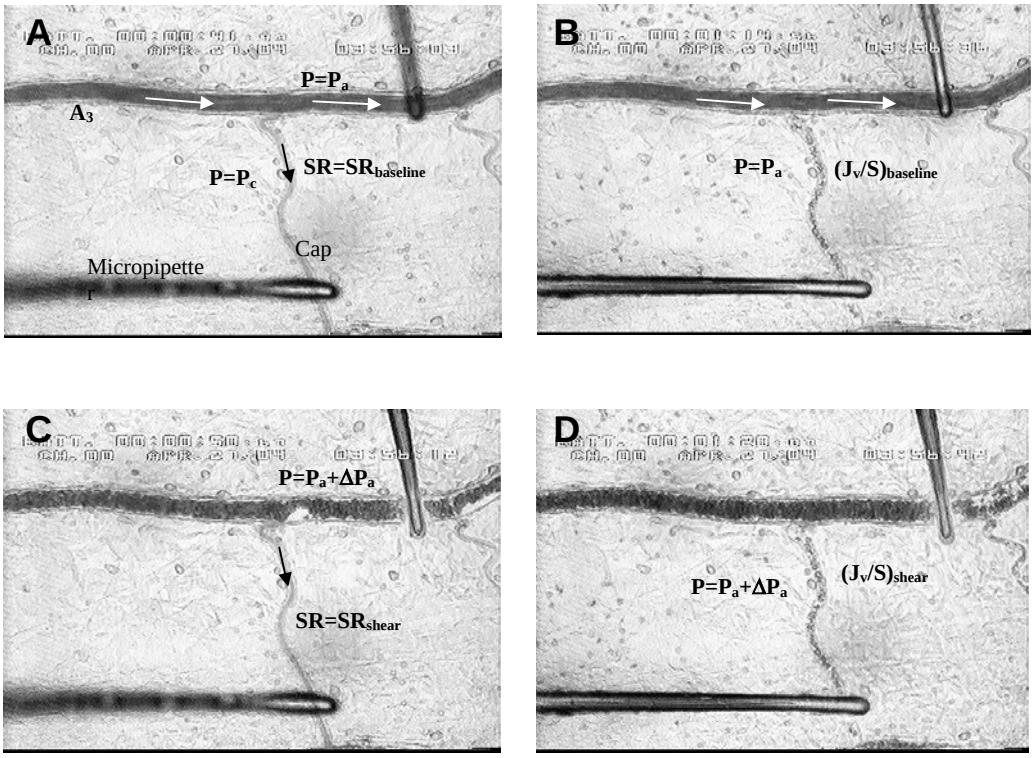
A
P=P$_a$
A$_3$
P=P$_c$
SR=SR$_{baseline}$
Cap
Micropipette
B
P=P$_a$
(J$_v$/S)$_{baseline}$
C
P=P$_a$+ΔP$_a$
SR=SR$_{shear}$
D
P=P$_a$+ΔP$_a$
(J$_v$/S)$_{shear}$

Figure 4.1

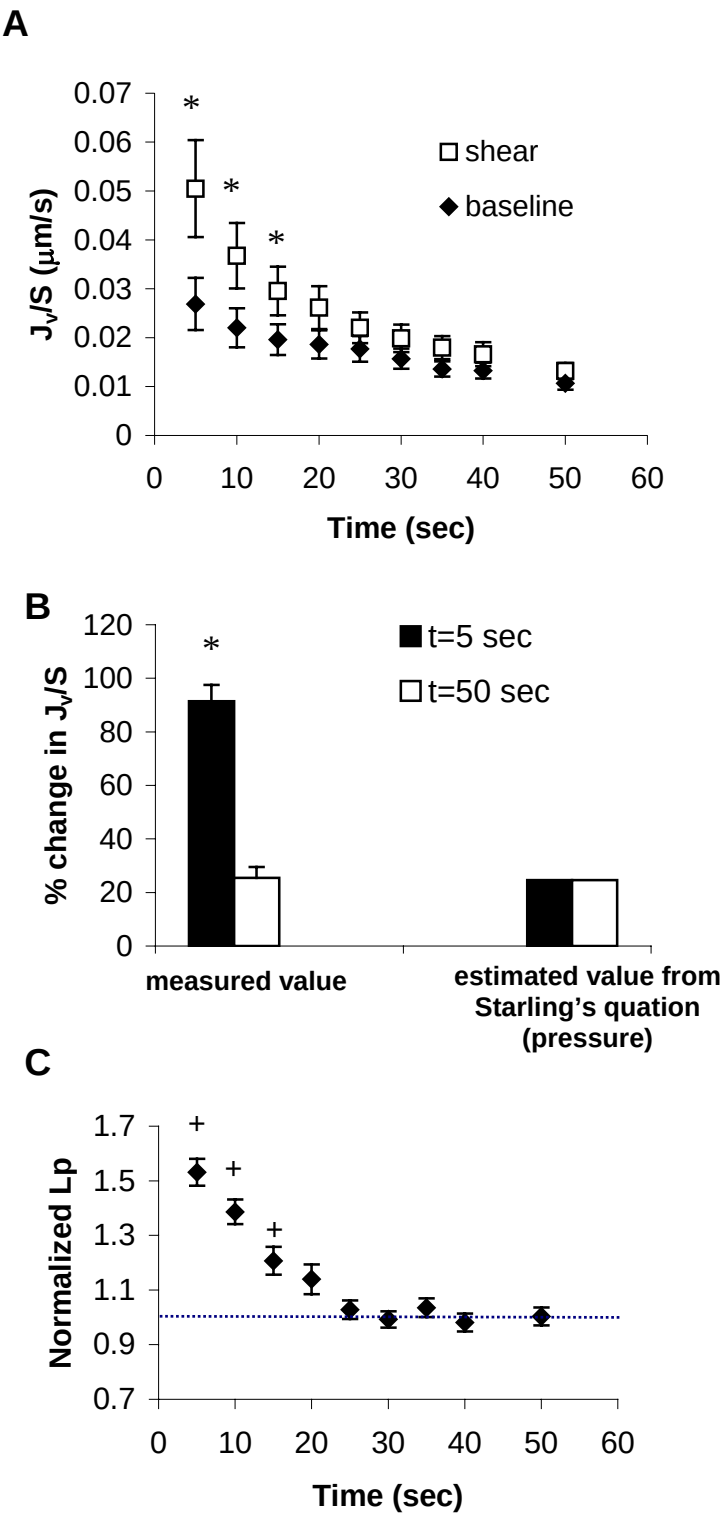
A
0.07
0.06
0.05
0.04
0.03
0.02
0.01
0
J_v/S (µm/s)
shear
baseline
0
10
20
30
40
50
60
Time (sec)
B
120
100
80
60
40
20
0
% change in J_v/S
t=5 sec
t=50 sec
measured value
estimated value from Starling's quation (pressure)
C
1.7
1.5
1.3
1.1
0.9
0.7
Normalized Lp
0
10
20
30
40
50
60
Time (sec)

Figure 4.2

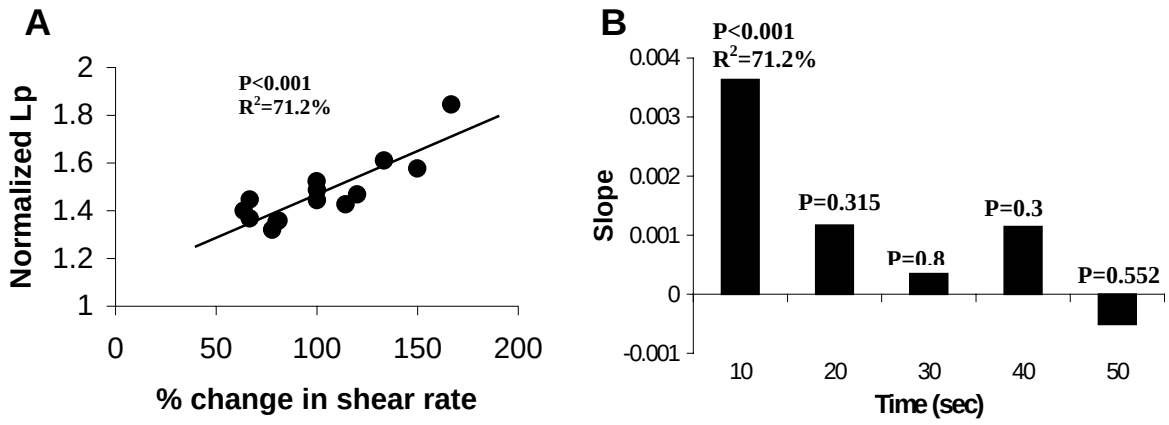
A
Normalized Lp
2
1.8
1.6
1.4
1.2
1
P<0.001
R2=71.2%
0
50
100
150
200
% change in shear rate
B
Slope
0.004
0.003
0.002
0.001
0
-0.001
P<0.001
R2=71.2%
P=0.315
P=0.3
P=0.552
10
20
30
40
50
Time (sec)

Figure 4.3

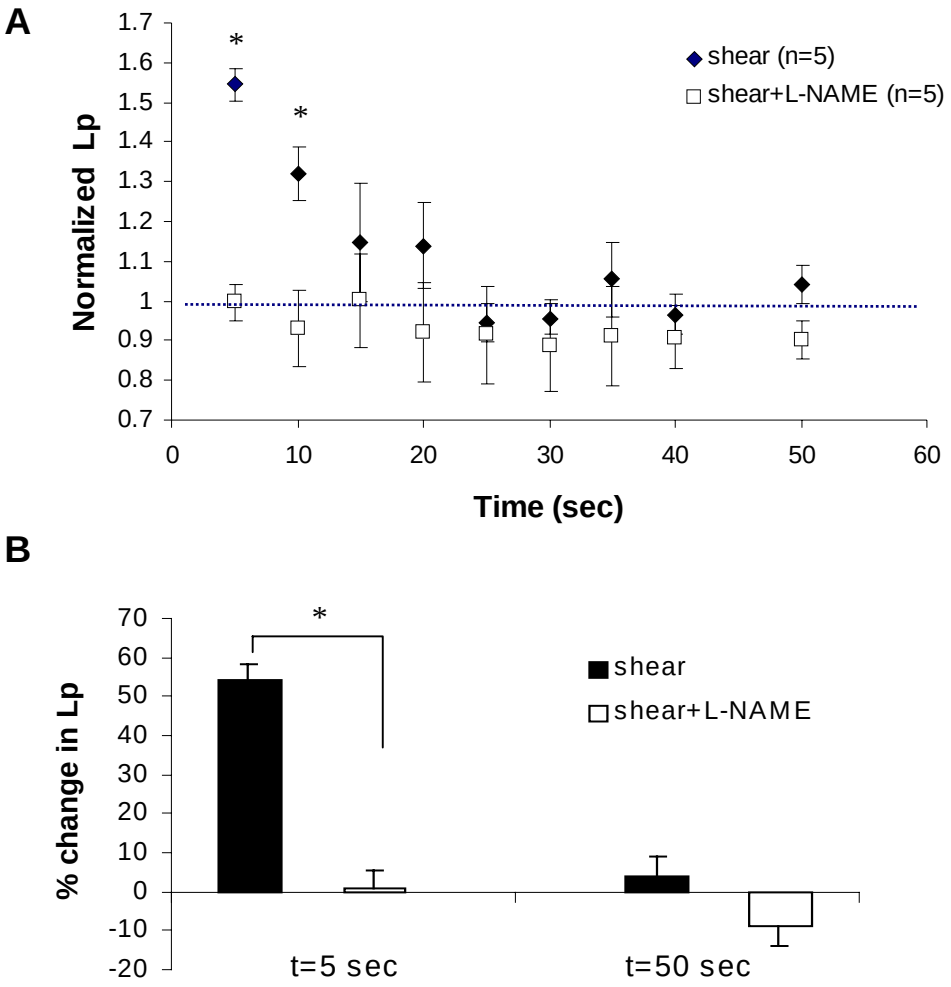
A
Normalized Lp
1.7
1.6
1.5
1.4
1.3
1.2
1.1
1
0.9
0.8
0.7
*
*
shear (n=5)
shear+L-NAME (n=5)
0
10
20
30
40
50
60
Time (sec)
B
% change in Lp
70
60
50
40
30
20
10
0
-10
-20
*
shear
shear+L-NAME
t=5 sec
t=50 sec

Figure 4.4

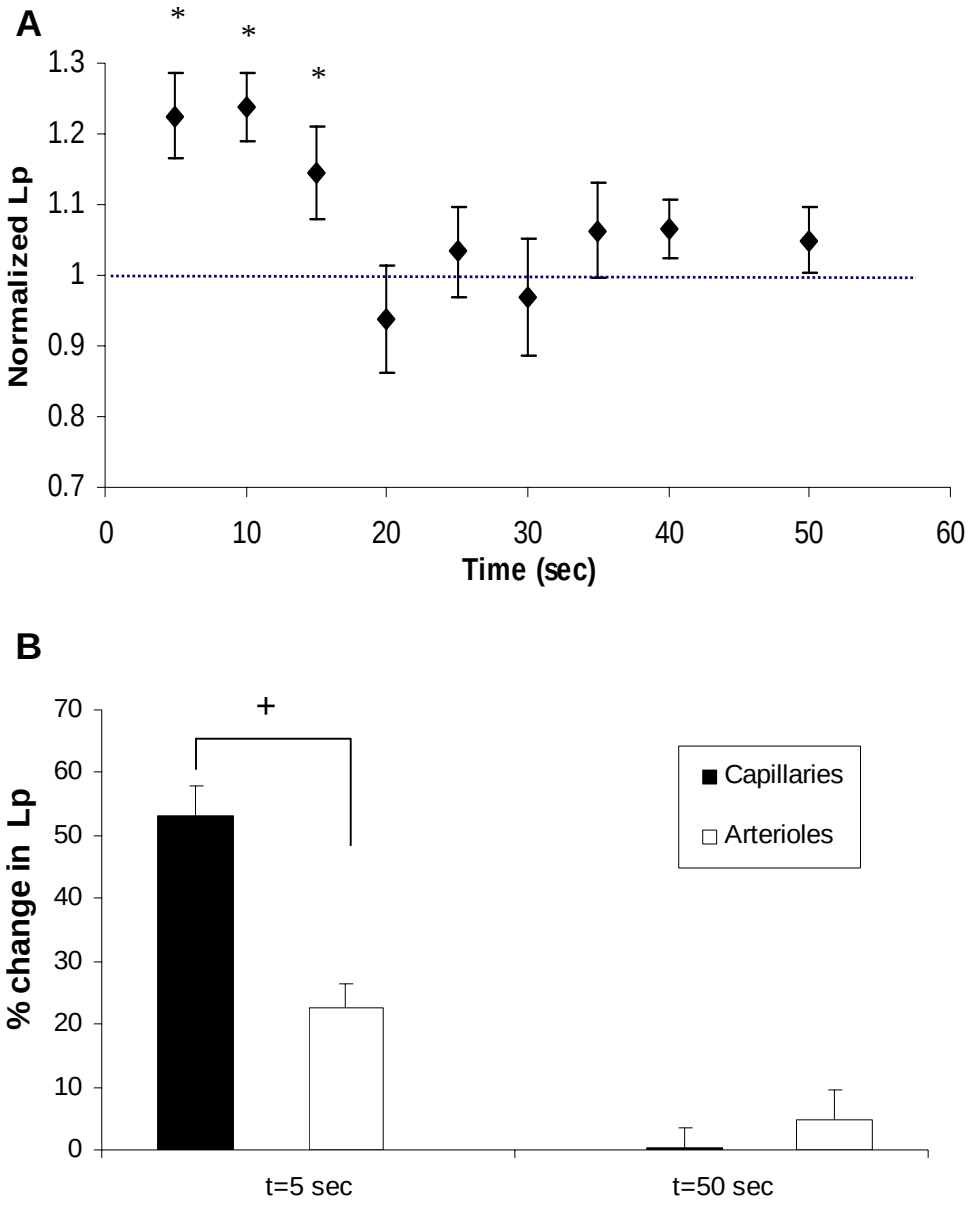
A
*
*
*
1.3
1.2
1.1
1
0.9
0.8
0.7
Normalized Lp
0
10
20
30
40
50
60
Time (sec)
B
+
70
60
50
40
30
20
10
0
% change in Lp
Capillaries
Arterioles
t=5 sec
t=50 sec

Figure 4.5

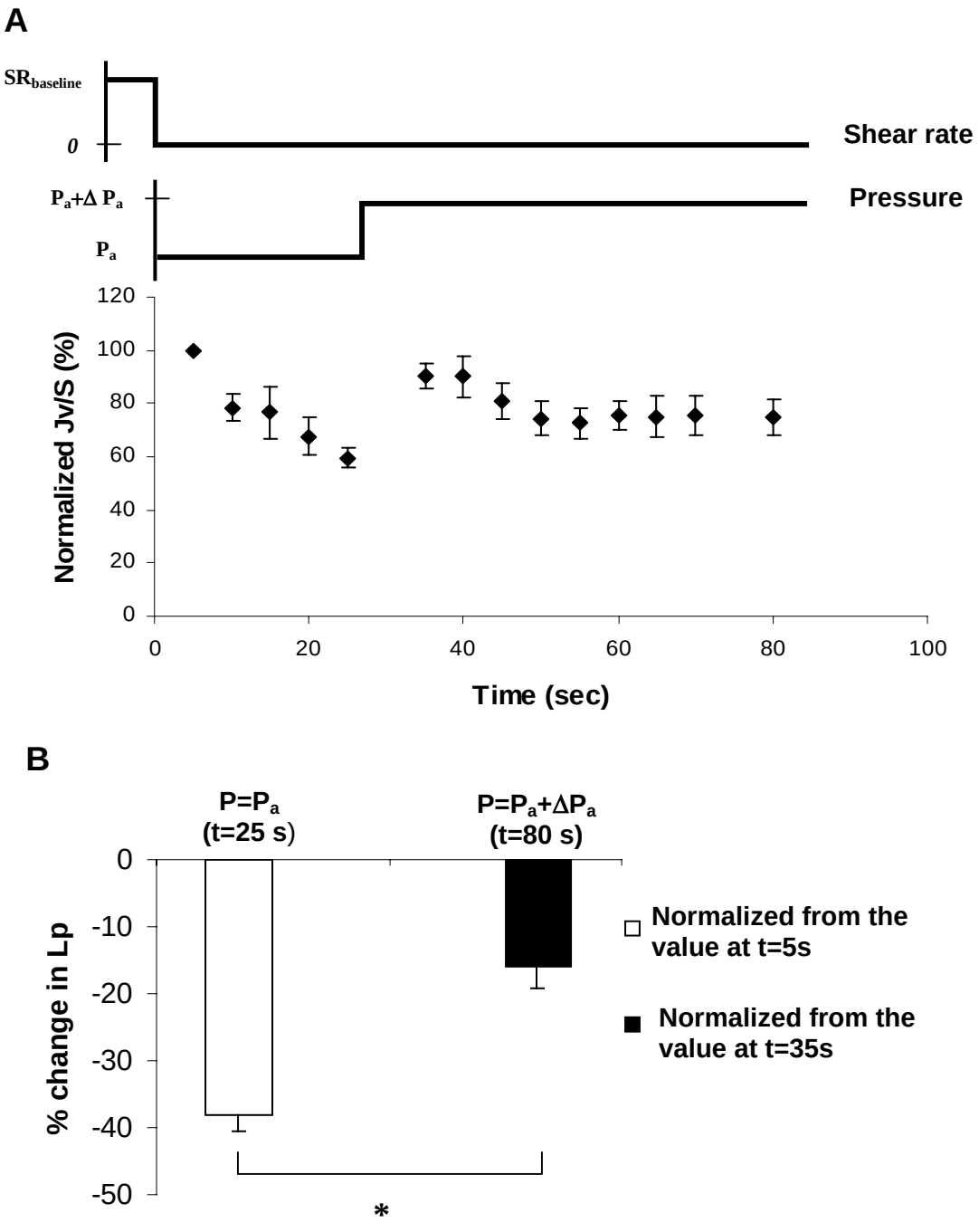
A
SR baseline
0
Shear rate
Pa+Δ Pa
Pa
Pressure
Normalized Jv/S (%)
120
100
80
60
40
20
0
0
20
40
60
80
100
Time (sec)
B
P=Pa (t=25 s)
P=Pa+ΔPa (t=80 s)
% change in Lp
0
-10
-20
-30
-40
-50
*
Normalized from the value at t=5s
Normalized from the value at t=35s

Figure 4.6

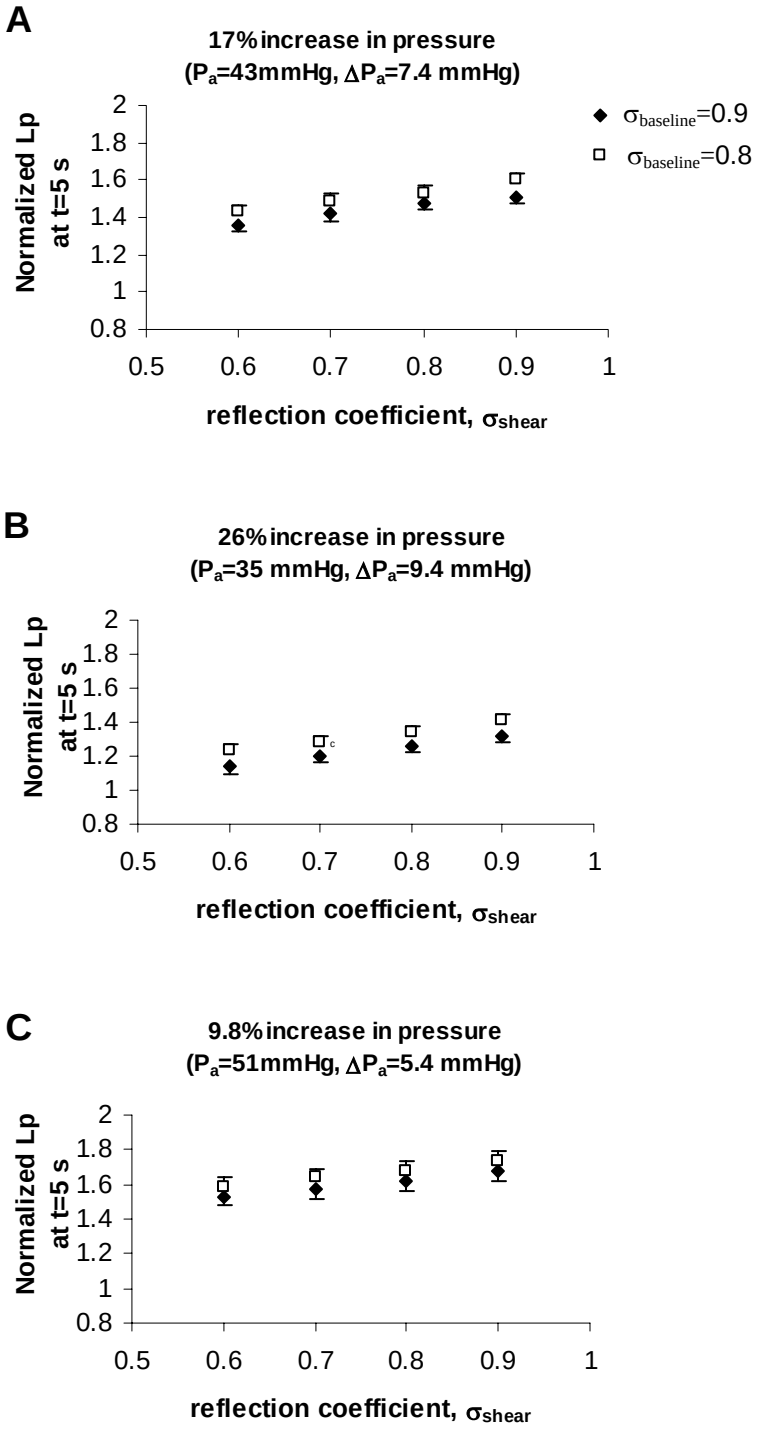
A
17% increase in pressure
(Pa=43mmHg, ΔPa=7.4 mmHg)
Normalized Lp at t=5 s
2
1.8
1.6
1.4
1.2
1
0.8
0.5
0.6
0.7
0.8
0.9
1
reflection coefficient, σshear
σbaseline=0.9
σbaseline=0.8
B
26% increase in pressure
(Pa=35 mmHg, ΔPa=9.4 mmHg)
Normalized Lp at t=5 s
reflection coefficient, σshear
C
9.8% increase in pressure
(Pa=51mmHg, ΔPa=5.4 mmHg)
Normalized Lp at t=5 s
reflection coefficient, σshear

Figure 4.7

Chapter 5

REGULATION OF HYDRAULIC CONDUCTIVITY IN RESPONSE TO SUSTAINED CHANGES IN PRESSURE

5.1 Introduction

According to Starling's hypothesis, transvascular fluid flux through the endothelial transport barrier is regulated by either a change in pressure gradient (hydrostatic or oncotic) across the vascular wall or by permeability (oncotic reflection coefficient σ or hydraulic conductivity L_p). It is generally believed that L_p does not change with an acute change in pressure and this principle has been used in measuring L_p in micropipette-perfused capillary beds, where the slope of the linear regression plot between J_v/S and pressure is considered to be L_p. This linear relationship was confirmed from various vessel preparations (He *et al.*, 1997;Neal & Bates, 2001;Neal & Bates, 2002;Rumbaut *et al.*, 1995;Rumbaut *et al.*, 2000b;Williams, 1999). However, most of those results were obtained for time periods typically less than 1 min. Despite extensive studies regarding this issue, relatively little attention has been drawn for the issue of a change in pressure over an extended time period which might give us insight into characteristic tissue fluid volume shifts in microgravity conditions and pulmonary edema associated with pulmonary hypertension. Interestingly, from in vitro studies of cultured endothelial cell models, a time-dependent change in L_p was observed when endothelial cell was exposed to step increases in pressure over extended periods of time (Tarbell *et al.*, 1999).

To our knowledge, there have been few studies to address this issue using an in vivo model. Therefore, the primary objective of the current study was to determine whether sustained changes in microvascular pressure might influence hydraulic conductivity measured from cannulated microvessels *in situ*. Additionally, a role for NO in pressure-mediated changes in L_p was investigated.

5.2 Materials and Methods

5.2.1 Animal preparation

Animal procedures were performed in accordance with institutional guidelines. Male Wistar rats weighing 250 – 300 g were anesthetized by an intraperitoneal injection of 135 mg/kg thiobutabarbital (Inactin, Sigma T-133, St. Louis). A segment of the small intestine was exteriorized through a midline abdominal incision, and the rat was placed on its right side on a Plexiglas board so that a selected section of mesentery could be draped over a glass cover slip glued on a hole centered in the board. The exposed section of the mesentery was superfused continuously with bicarbonate-buffered saline (BBS). More details about surgery and BBS preparations are given in chapter 2, section 1.

5.2.2 Video microscopy

A description of the video microscopy techniques used are described in chapter 2, section 2.

5.2.3 Microperfusin technique and measurement of transvascular filtration

In this experiment, unbranched (500–1000 μm from branch to branch point) third-order arterioles ($A_{3,}$ 25 – 35 μm in diameter) and small venules (30 – 45 μm in diameter) with minimal leukocyte rolling and adherence were selected and cannulated in situ using a beveled glass micropipette filled with BBS solution containing 1% bovine serum albumin (BSA, Sigma) and blue-dyed microspheres (1 μm diameter, Polysciences, Inc) which acted as filtration markers during occlusion. The micropipette was connected to micropressure system (Micropressure System 900A, World Precision Instruments, Sarasota, FL) to control pressure changes. To measure J_v/S, selected arterioles or venules were occluded with a glass micropipette occluder at a position downstream from the cannulation site (Figure 5.1). The occluder was positioned over the selected arteriole or venule and carefully lowered onto the vessel by micromanipulator to compress the lumen. The filtration rate was calculated using equation 2.3 from the decreasing volume between the micropipette occluder and a flow marker that was 250-350 μm upstream of the occluder. More details about measurements of transvasular filtration are described in chapter 2, section 3.

5.2.4 Measurement of hydraulic conductivity for cannulated vessels

Using the simplified Starling's equation from equation 2.5 in chapter 2, section 2,

$$J_v/S = L_p(P_p-\sigma\pi_p) \quad (5.1)$$

Thus, hydraulic conductivity can be expressed as

$$L_p=(J_v/S)/(P_p-\sigma\pi_p) \quad (5.2)$$

Since the protein concentration (1% BSA) in perfusate and the associated π_p are negligible for a cannulated arteriole (π_p of 1% BSA equals 1.8 mmHg), the expression for L_p can be reduced as

$$L_p=(J_v/S)/P_p \quad (5.3)$$

Assuming σ=0.9 and π_p=1.8 mmHg for a cannulated venule, the equation can be assumed as

$$L_p=(J_v/S)/(P_p-1.6) \quad (5.4)$$

5.2.5 Experimental protocols

Using the technique of micropipette perfusion, then measuring fluid filtration rate, the effects of sustained changes in transvascular pressure on water transport were assessed. In this experiment, a third-order arteriole (A_3) in the microcirculatory bed of rat mesentery was cannulated and BBS with BSA and blue-dyed microspheres were perfused. After cannulation, baseline pressure was set at 50 and 20 mmHg for arterioles and venules, respectively, and baseline J_v/S was measured for 30 min without changing perfusion pressure.

To investigate the effect of a pressure change on J_v/S, perfusion pressure was changed from 50 to 100 mmHg for arterioles and from 20 to 40 mmHg for venules by the controlling micropressure system (Micropressure System 900A, World Precision Instruments, Sarasota, FL). After baseline measurement of J_v/S at 30 min, pressure change was induced at no flow condition during the vascular occlusion, and then, J_v/S was measured immediately after pressure increase (at 31 min). The transvascular filtration was measured for 90-150 min following pressure application by observing

the movement of microspheres. During the entire experiment, J_v/S was measured occasionally every 10 minute to minimize the damage of the microvessels due to micropipette occlusion. During each occlusion, the velocity of the flow marker was measured 10 s after onset of the vascular occlusion to minimize the potential influence of shear effect in our J_v/S measurements based on our previous observations (see Figure 4.3). After J_v/S measurement at each time point, the micropipette occluder was released to resume flow, vessel was flowing 9.5 min of every 10 min, with 20-30 s of occlusion. Hydraulic conductivity was calculated using equation 5.3 or 5.4.

To investigate the effect of NOS inhibition on pressure-induced changes in hydraulic conductivity, arterioles and venules were superfused with the NOS inhibitor L-NAME (100 μM). This concentration of L-NAME has been used widely in testing effect of NOS inhibition on microvascular permeability from various microvessels using micro-perfusion (Rumbaut *et al.*, 2000b;Rumbaut *et al.*, 2000a). For arterioles, J_v/S was measured in the presence of L-NAME during the entire experiment, in which baseline J_v/S was measured for 30 min at 50 mmHg, and then pressure was increased to 100 mmHg and J_v/S was measured for 60 min. For venules, after the baseline measurement of J_v/S for 30 min at 20 mmHg of perfusion pressure, pressure was increased to 40 mmHg. J_v/S was then measured for an additional 90 min at higher pressure. At the end of this period, L-NAME was superfused for 30 min during which J_v/S was measured.

5.2.6 Statistics

Paired-t tests or unpaired t-tests were used when two set of data were compared using Minitab software (Minitab Inc., State College, PA). Data among groups were compared with the Bonferroni test. Error bars are presented as ± standard error (SE). Statistical significance was set at $P<0.05$.

5.3 Results

Experiments to measure transvascular filtration in response to change in pressure were performed from small arterioles and venules of the rat mesentery. All data were obtained using a micro-perfusion technique, in which baseline perfusion pressure was set at 50 mmHg for arterioles and 20 mmHg for venules after cannulation.

Figure 5.2A illustrates time course of J_v/S in small arterioles when a step increase in pressure (from 50 to 100 mmHg) was applied at 30 min. At each time point, vascular occlusion was made for 20 s. As shown in Figure 5.2B, each measurement has a transient nature in the time course of J_v/S. This transient response is similar to those observed in auto-perfused vessels (see chapter 4). Because this transient response during the initial 10 s might be expected due to the interaction of shear and pressure following vascular occlusion (see Figure 4.2), at each time point, J_v/S was obtained by taking an average of the values between 10 and 20 s following occlusion.

Figure 5.3 compares the results for small arterioles experiencing a step increase in pressure from 50 to 100 mmHg at 30 min (illustrative raw data are given in Table

5.1) and control data at 50 mmHg without change in pressure. There was a transient decrease in J_v/S during the initial 30 min and then moderate increase ($P<0.05$, 14% increase compared to the value baseline at 30 min) but still below the initial value at time 0 when perfusion pressure was maintained at 50 mmHg. The initial decrease in J_v/S is expected to be a pressure-induced sealing phenomenon. When the pressure was increased to 100 mmHg at 30 min, J_v/S increased by 104 ± 4.5% immediately followed by a reduction in J_v/S for 20 ~ 30 min and then there was a sustained increase, in which the value at 90 min was significantly higher than the value at 31 min (immediately after pressure increase). The immediate increase of J_v/S in response to the pressure increase corresponds to the two-fold increase in perfusion pressure (from 50 to 100 mmHg) and thus resulted in no significant change in L_p immediately after the pressure change. At 90 min, there was a significant change in L_p compared to the value at 31 min when pressure was increased to 100 mmHg, whereas no significant change in L_p for control experiments.

A **s**imilar transient response in J_v/S was observed for venules in response to an increase in pressure from 20 to 40 mmHg as shown in Figure 5.4 (illustrative raw data are given in Table 5.1). A step increase in pressure resulted in a substantial increase in J_v/S after 90 min. As expected, the value of L_p at 31 min (immediately after pressure increase) was not significantly different from the value at 30 min (immediately before pressure increase). However, L_p increased by 48 ± 13% at 120 min compared to the baseline value at 30 min and this was significantly different from the values at 31 min and 60 min. A pressure-induced sealing response also was observed for the initial 20~30 min following pressure increase.

To investigate the effect of NOS inhibition on the increase in L_p following a pressure change, L-NAME was superfused and J_v/S and L_p were measured from arterioles and venules. Figure 5.5 illustrates the response of small arterioles to a step change in pressure from 50 to 100 mmHg in the presence and absence of L-NAME. Normalized J_v/S and L_p were compared between two data groups. There was a significant attenuation in J_v/S at 90 min for L-NAME experiments. At 90 min, the increases in L_p following the pressure increase in control experiments was 36 ± 7%, compared to only an 8±11% increase in the presence of L-NAME. There was no statistically significant difference at 31 and 60 min between two groups: the sealing phenomenon also was observed in the presence of L-NAME.

NOS inhibition also was performed for venules. Figure 5.6 shows normalized J_v/S and L_p for venules, in which L-NAME was administered at the end of the control experiments. Before the superfusion of L-NAME, there was a transient increase in J_v/S following 20-30 min of a sealing period after the pressure change. However, the response was reversed significantly after 30 min of L-NAME treatment. There was a reduction of L_p by 19 ± 3% compared to the baseline value after L-NAME treatment in contrast to a 42 ± 11% increase at 120 min before L-NAME treatment.

5.4 Discussion

The present study addresses the effect of a sustained change in pressure on microvascular permeability assessed by hydraulic conductivity measurements from microvessels of the rat mesentery. Using a micro-perfusion technique, transvascular

filtration was measured from small arterioles and venules. The baseline value of venular L_p reported in this study (baseline $L_p = 2.35 \times 10^{-7}$ cm s^{-1} cm H_2O^{-1}) is similar to that reported by Rumbaut et al. (mean $L_p = 2.3 \times 10^{-7}$ cm s^{-1} cm H_2O^{-1}) using a similar model (Rumbaut *et al.*, 2000b). The baseline value of arteriolar L_p (baseline $L_p = 0.26 \times 10^{-7}$ cm s^{-1} cm H_2O^{-1}) was approximately 11% of venular L_p. This result corresponds to the previous observations obtained from frog mesentery, in which arteriolar L_p was only 6 % of venular L_p (Williams, 1999).

The main finding of this study is that step changes in microvascular pressure led to time-dependent alterations of L_p. Immediately after a step increase in pressure, the increased J_v/S was linearly proportional to the pressure change, thus resulting in no significant change in L_p when pressure was increased acutely at a no flow condition. This result is consistent with previous findings from various microvessel preparations using micro-perfusion techniques (Neal & Bates, 2001;Rumbaut *et al.*, 2000b;Williams, 1999) and indicates that the response is purely mechanical, induced only by the increase in hydrostatic pressure gradient and not involving any alteration of permeability coefficients. However, when J_v/S was measured for longer periods of time, there was a transient change of J_v/S even though pressure was maintained at a constant increased value, indicating an alteration of hydraulic permeability. Similar transient responses were observed for both small arterioles and venules. In cannulated venules, after a step increase in pressure from 20 to 40 mmHg, there was a substantial increase in L_p after 30-40 min. In arterioles, a step increase in pressure from 50 to 100 mmHg also resulted in a significant increase in L_p after 60 min. However, when pressure was maintained for 90 min with 50 mmHg, there was no significant change

in L_p. This finding indicates that the pressure change may be an important factor that leads to a substantial increase in L_p.

The mechanisms responsible for these changes in L_p by a sustained change in pressure are not yet clearly understood. One possibility is that endothelium might be ruptured by an increase in pressure after longer periods of time, thereby resulting in high transvascular filtration. However, this seems unlikely because the transient increases in L_p were reversed by the addition of DBcAMP for arterioles (data not shown) or L-NAME for venules and this may suggest that microvascular endothelium was intact during the pressure increase. Another possible mechanism is the activation of a biochemical response induced by the mechanical stimulus. However, regarding the mechanism of mechanical stimulus, it is not still clear whether the response of long-term increases in L_p is due to a direct effect of pressure or indirect effects such as pressure-induced cell stretch or pressure-induced increase in transmural flow. In a previous in vitro study, Tarbell et al.(Tarbell *et al.*, 1999) suggested that elevated endothelial cleft shear stress induced by increased transmural flow might be a more important factor in influencing the substantial increase in L_p than a direct effect of pressure or stretch of endothelial cells, based on the reasoning that the increase in L_p was regulated by a similar downstream signaling pathway as shear-induced changes in hydraulic conductivity, that is, a NO-cAMP dependent mechanism. Our results of NOS inhibition with L-NAME also support this hypothesis. However, it should be noted that opening of new transcellular pathways or stretch-induced separation of endothelial junctions also contribute to increase in L_p at much higher pressure, enough to rupture endothelium (Neal & Michel, 1996;Parker & Ivey, 1997).

There is a technical consideration in using the microperfusion technique to change pressure in this study, in which a step increase in pressure also can result in an increase in shear rate along the luminal surface of microvessels. Flow-induced shear stress is known to regulate microvascular permeability in a NO-dependent mechanism in vivo (Yuan *et al.*, 1992) or in vitro (Chang *et al.*, 2000;Sill *et al.*, 1995). Therefore, we cannot rule out the possibility that the increase in shear stress accompanying the pressure change might trigger NO release from endothelium of microvessels and thereby lead to an increase in L_p. To minimize the potential interaction of pressure and shear in our measurements of J_v/S, at each time point of increased pressure, data were collected after 10s following the onset of occlusion based on our previous study of a shear effect on L_p, in which a positive correlation between the increase in shear rate and hydraulic conductivity was no longer found after 10s of vascular occlusion (see Figure 4.3). It has been generally known that shear-induced changes in microvascular permeability occur very rapidly, within seconds of a change in shear rate (Montermini *et al.*, 2002). However, our results of J_v/S measurements demonstrated that the increase in L_p occurred after longer periods of time rather than occurring rapidly following pressure application, suggesting that shear might not be an important factor in influencing our J_v/S measurements.

Another important finding was that there was a characteristic time-dependent decrease in J_v/S for the initial 30 min following the pressure increase. This result is consistent with previous measurements of endothelial monolayers in vitro, in which a step increase in pressure gradient (from 10 to 20 cmH_2O) led to a significant reduction in transvascular filtration during the initial 30 min. However, it should be

noted that there was a slight difference in magnitude between in vivo and in vitro findings even though a similar transient decrease in L_p was observed for both in vivo and in vitro models. Despite a higher step increase in pressure in our in vivo experiments (50 mmHg increase for arterioles and 20 mmHg increase for venules), the degree of reduction in L_p during the initial 30 min was only approximately 20%, compared to 50% decrease for in vitro experiments. The mechanism responsible for the characteristic time-dependent decrease in L_p in response to increase in pressure, the sealing effect, was revealed recently in an in vitro model of endothelial monolayers (Demaio *et al.*, 2004). Mechanical and biological mechanisms were hypothesized to be involved in this phenomenon. It was suggested that pressure application might seal a small pore pathway for water transport passively during the initial periods; on the other hand, biological mechanisms regulate tight junction protein zonula occludins-1 (ZO-1) after longer periods of time (Demaio *et al.*, 2004).

Potential errors in measurements of J_v/S and L_p

One potential source of errors in measuring L_p is the pressure drop through the tapered micropipette tip. In our experimental system, the micropressure controller sets perfusion pressure at the entrance of micropipette. Therefore, perfusion pressure in cannulated vessels can be less than the input pressures due to the pressure drop along the narrowing tip of micropipette. However, the estimated value of pressure drop was negligible based on our simple calculations using the Hagen-Poiseuille equation (see APPENDIX for detailed calculations). In our measurements of flow velocity from cannulated arterioles for a few selected cases, values ranged from 1 to 5 mm/s. Within

this range of flow velocity, calculated values of pressure drop were less than 3 mmHg.

To measure J_v/S using modified Landis technique, three microspheres were chosen and the movement was observed during the vascular occlusion. During the vascular occlusion, some microspheres moved downward to the endothelium and did not continue to move forward (possibly due to the gravity effect). Therefore, choosing those microspheres could underestimate J_v/S. To reduce the potential error resulted from choosing a microsphere, three different microspheres were chosen to observe movements and J_v/S was measured by taking an average. However, if the measured value from one selected microsphere was significantly lower than the other two values, this measurement was excluded from the average.

During the entire experiment, each vessel was occluded at least 10 times for J_v/S measurements. Because the micropipette occluder may damage the vessel at occlusion site, successive measurement obtained by occluding the same damaged site could over-estimate J_v/S. Therefore, each successive occlusion was made approximately 5 μm upstream of the previous site, so that any damage incurred by one occlusion would not affect the filtration measurement of the following occlusion.

Table 5.1 Illustrative raw data of J_v/S for small arteriole and venules in response to increases in pressure. Data are given as mean ± SE. N is the number of experiments, one per animal.

Time (min)	Arteriole (N=7)		Venule (N=7)	
	Pressure (mmHg)	J_v/S (μm/s)	Pressure (mmHg)	J_v/S (μm/s)
0	50	0.033 ± 0.009	20	0.076 ± 0.009
10	50	0.027 ± 0.008	20	0.071 ± 0.009
20	50	0.024 ± 0.006	20	0.063 ± 0.008
30	50	0.027 ± 0.008	20	0.062 ± 0.009
31	100	0.055 ± 0.016	40	0.114 ± 0.017
40	100	0.052 ± 0.015	40	0.103 ± 0.016
50	100	0.050 ± 0.017	40	0.093 ± 0.014
60	100	0.047 ± 0.014	40	0.096 ± 0.014
70	100	0.051 ± 0.011	40	0.101 ± 0.015
80	100	0.060 ± 0.014	40	0.109 ± 0.016
90	100	0.068 ± 0.015	40	0.122 ± 0.019
100	100	-	40	0.138 ± 0.017
110	100	-	40	0.159 ± 0.017
120	100	-	40	0.178 ± 0.019

Figure Legends

Figure 5.1 Micro-perfusion techniques used in small arterioles and venules. (A) Schematic illustration showing microperfusion technique for pressure change and J_v/S measurements. (B) Microscopic image showing cannulation site. (C) Microscopic image showing microspheres used for flow markers downstream of cannulation site.

Figure 5.2 Time course of J_v/S for small arterioles (N=5). (A) J_v/S (μm/s) vs time (min) with step change in pressure. Pressure was increased from 50 to 100 mmHg at 30 min. Each value was obtained by taking an average for the values between 10 and 20 s following vascular occlusion. (B) Transient response of J_v/S at each time point.

Figure 5.3 J_v/S and percentage change in L_p as a function of time for small arterioles. (A) Percentage change in J_v/S normalized to baseline at 30 min for control experiments with no step change in perfusion pressure (50 mmHg, N=3) and experiments with step change in pressure from 50 to 100 mmHg (N=7). (B) Percentage change in L_p normalized to baseline at 30 min. Error bars are presented as ± SE. * : $P<0.05$

Figure 5.4 J_v/S and percentage change in L_p as a function of time for small venules (N=8). (A) Percentage change in J_v/S normalized to baseline at 30 min with step change in pressure from 20 to 40 mmHg. (B) Percentage change in L_p normalized to baseline at 30 min. Error bars are presented as ± SE. * : $P<0.05$

Figure 5.5 Effects of L-NAME (100 μM) on J_v/S and percentage change in L_p for small arterioles. (A) Percentage change in J_v/S normalized to baseline at 30 min with step change in pressure from 50 to 100 mmHg without L-NAME (N=7) and with L-NAME (N=4). (B) Comparison of percentage change in L_p normalized to baseline at 30 min between results without L-NAME and with L-NAME. Error bars are presented as ± SE. * : $P<0.05$

Figure 5.6 Effects of L-NAME (100 μM) on J_v/S and percentage change in L_p for small venules (N=4). (A) Percentage change in J_v/S normalized to baseline at 30 min with step change in pressure from 20 to 100 mmHg, in which L-NAME was superfused after 120 min. (B) Percentage change in L_p normalized to baseline at 30 min between results without L-NAME and with L-NAME. Error bars are presented as ± SE. * : $P<0.05$

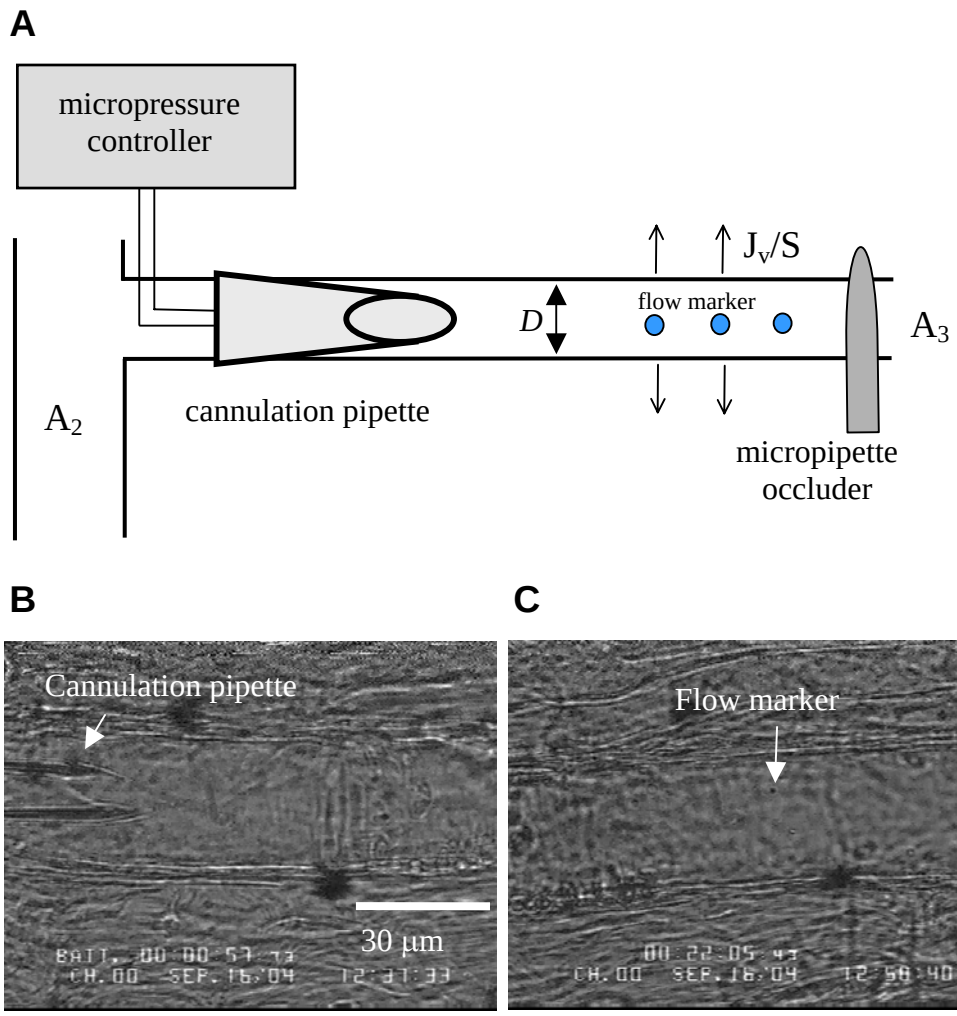
A
micropressure controller
J_v/S
flow marker
D
A_3
A_2
cannulation pipette
micropipette occluder
B
C
Cannulation pipette
30 μm
Flow marker

Figure 5.1

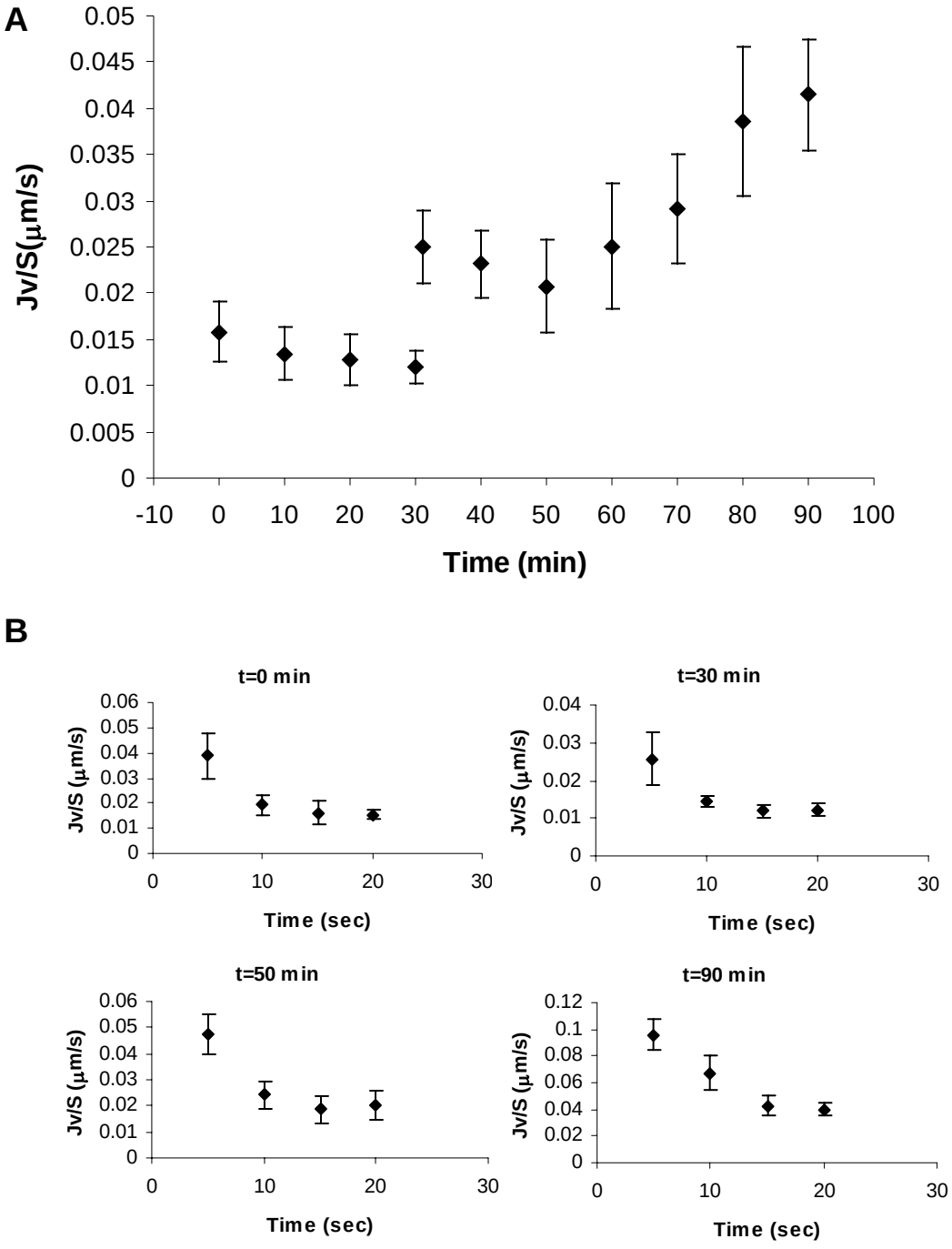
A
Jv/S(µm/s)
0.05
0.045
0.04
0.035
0.03
0.025
0.02
0.015
0.01
0.005
0
-10
0
10
20
30
40
50
60
70
80
90
100
Time (min)
B
t=0 min
t=30 min
t=50 min
t=90 min
Jv/S (µm/s)
Time (sec)

Figure 5.2

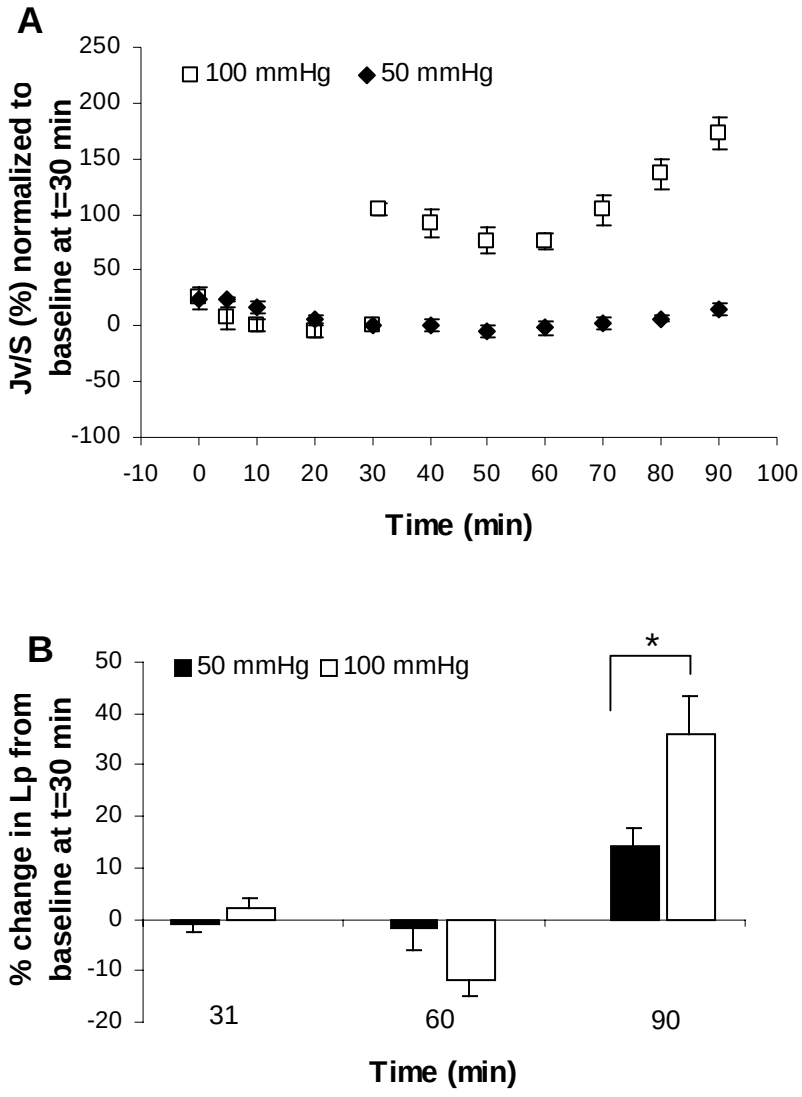
A
Jv/S (%) normalized to baseline at t=30 min
100 mmHg
50 mmHg
250
200
150
100
50
0
-50
-100
-10
0
10
20
30
40
50
60
70
80
90
100
Time (min)
B
% change in Lp from baseline at t=30 min
50 mmHg
100 mmHg
*
50
40
30
20
10
0
-10
-20
31
60
90
Time (min)

Figure 5.3

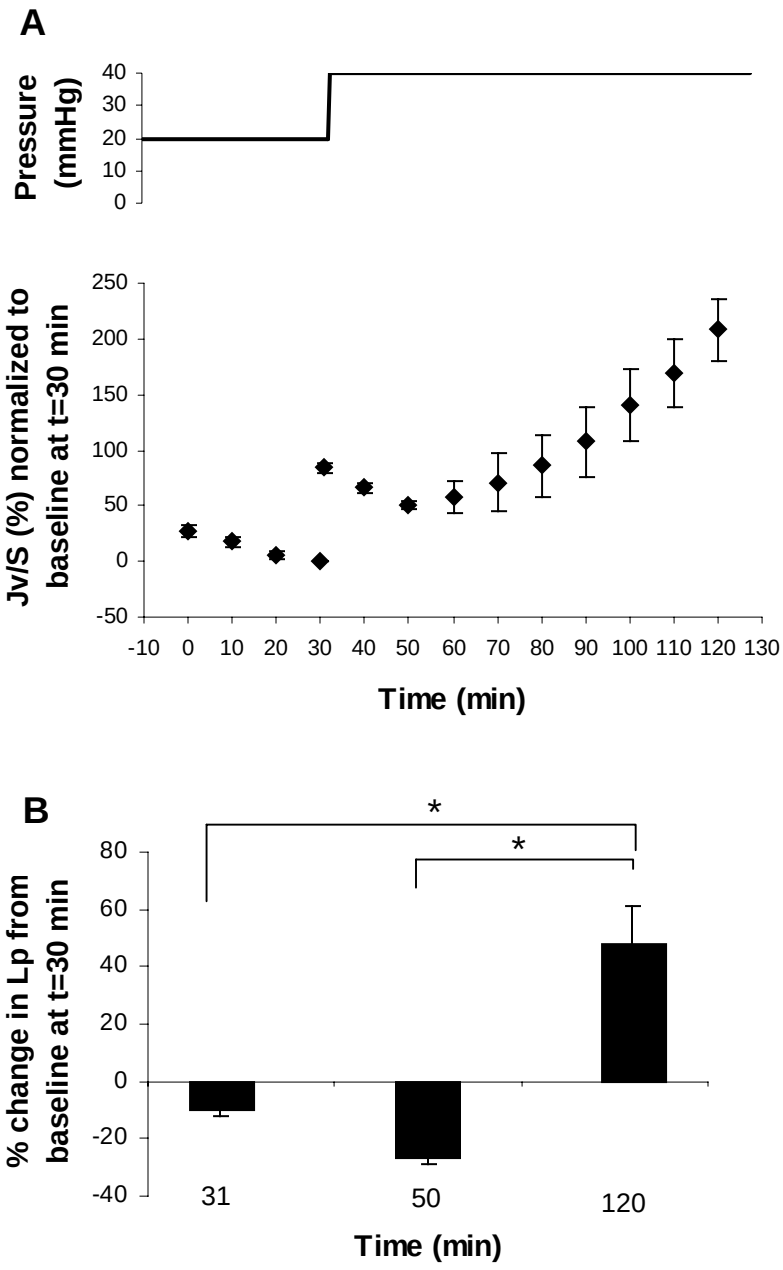
A
Pressure (mmHg)
40
30
20
10
0
Jv/S (%) normalized to baseline at t=30 min
250
200
150
100
50
0
-50
-10 0 10 20 30 40 50 60 70 80 90 100 110 120 130
Time (min)
B
% change in Lp from baseline at t=30 min
80
60
40
20
0
-20
-40
*
*
31
50
120
Time (min)

Figure 5.4

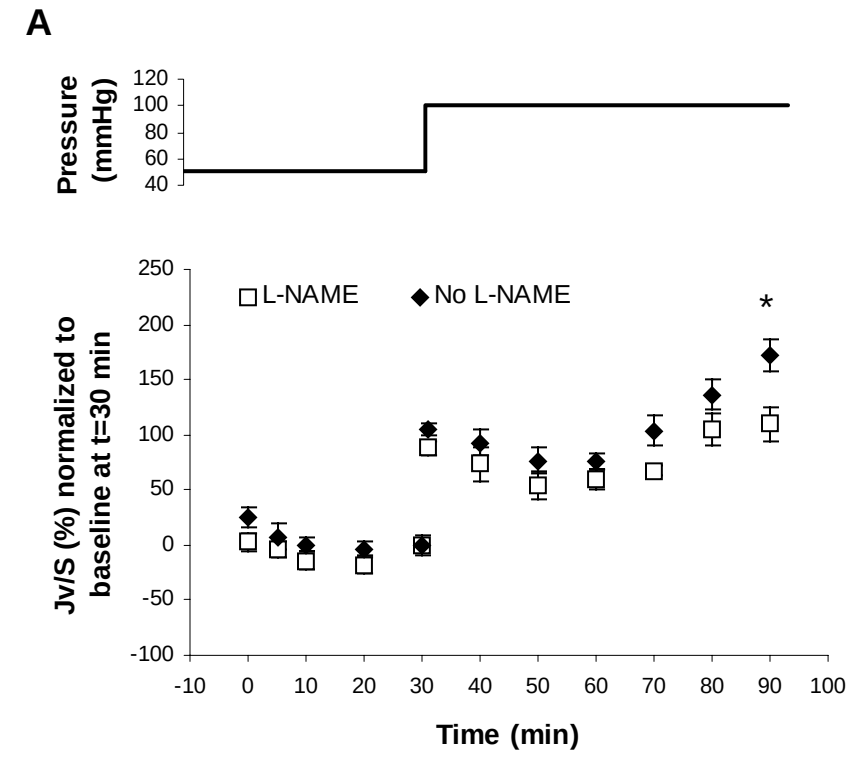
A
Pressure (mmHg)
120
100
80
60
40
Jv/S (%) normalized to baseline at t=30 min
L-NAME
No L-NAME
*
250
200
150
100
50
0
-50
-100
-10
0
10
20
30
40
50
60
70
80
90
100
Time (min)

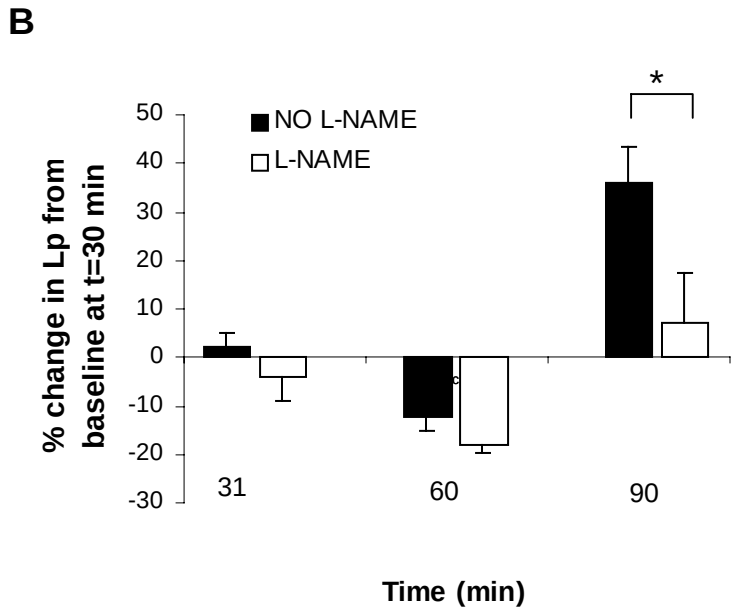
B
% change in Lp from baseline at t=30 min
NO L-NAME
L-NAME
*
50
40
30
20
10
0
-10
-20
-30
31
60
90
Time (min)

Figure 5.5

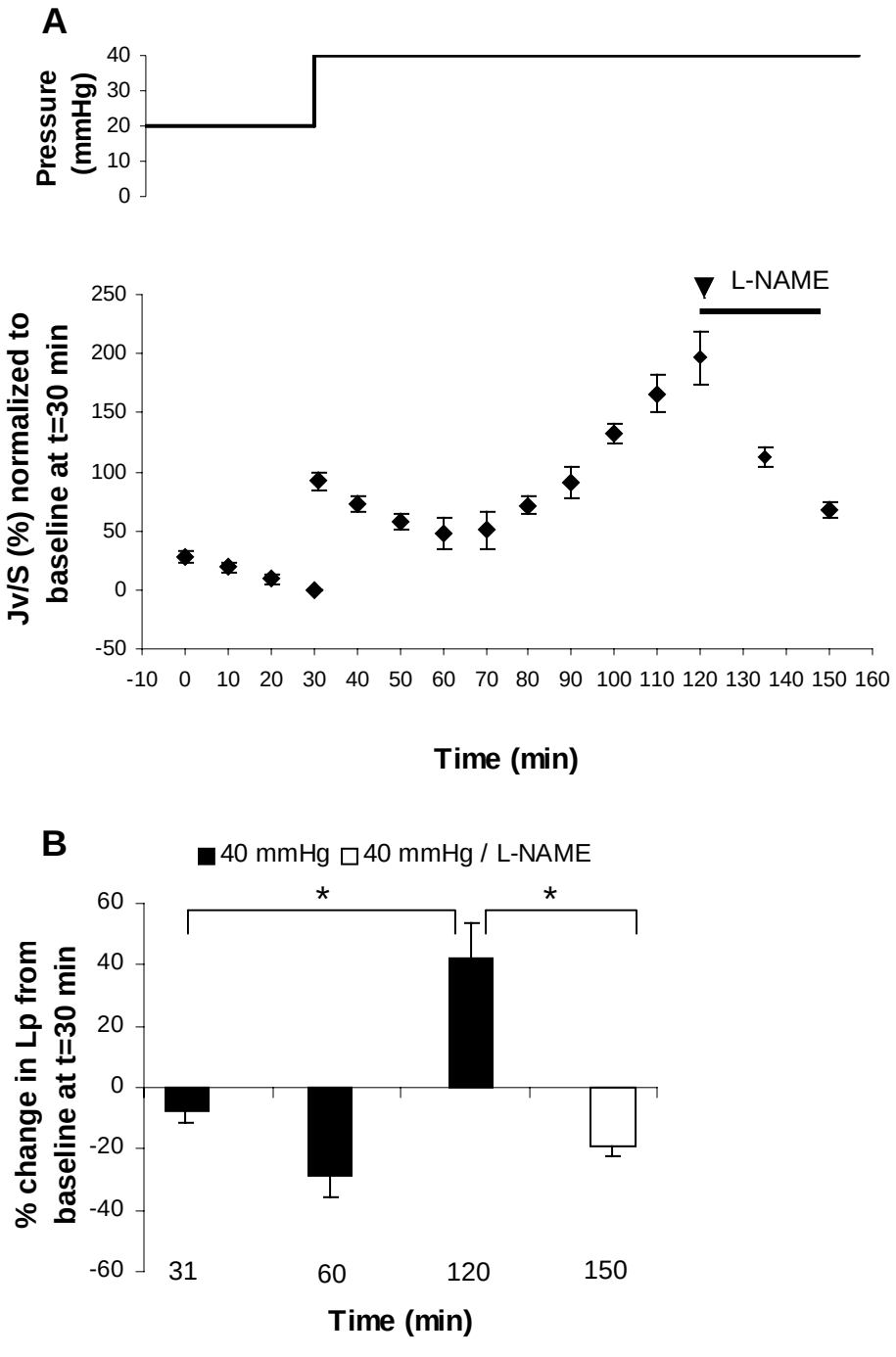
A
Pressure (mmHg)
40
30
20
10
0
L-NAME
Jv/S (%) normalized to baseline at t=30 min
250
200
150
100
50
0
-50
-10 0 10 20 30 40 50 60 70 80 90 100 110 120 130 140 150 160
Time (min)
B
40 mmHg
40 mmHg / L-NAME
*
*
% change in Lp from baseline at t=30 min
60
40
20
0
-20
-40
-60
31
60
120
150
Time (min)

Figure 5.6

Chapter 6

SUMMARY AND FUTURE STUDY

6.1 Summary

One main hypothesis of the current study is that transvascular filtration-induced shear stress might play an important role in endothelial barrier function and SMC contractions. To address this hypothesis, we investigated the effect of pressure-induced transvascular fluid flux on SMC contraction in vivo. We also investigated the effects of pressure and shear on endothelial barrier function for water transport.

In the current study performed *in vivo* and in excised arterioles, interstitial flow-induced shear stress through vascular wall driven by transvascular filtration was hypothesized to be a third mechanical factor that can play a role in the myogenic response in addition to other factors such as wall tension and pressure-induced vascular stretch. To address this hypothesis, we investigated the relationship between filtration rate (J_v) and the myogenic response by modifying plasma osmotic pressure to attenuate J_v during a step increase in hydrostatic pressure. Consistent with our hypothesis, we found a statistically significant correlation *in vivo* between basal myogenic tone and J_v. The mechanism of this response was hypothesized to be due to fluid shear forces experienced by smooth muscle cells associated with transvascular filtration flow.

To understand the role of hemodynamic forces in regulating microvascular permeability, we have investigated effects of acute changes in shear and pressure on endothelial barrier function for water transport. The effect of sustained changes in

pressure on hydraulic conductivity was also investigated. In the study performed in the microvessels of the mesentery, we have obtained evidence that hydraulic conductivity might be regulated via a NO-dependent mechanism in response to acute changes in shear rate. Additionally, the effect of sustained changes in pressure on hydraulic conductivity was also investigated using a micro-perfusion technique. A substantial increase in hydraulic conductivity was observed following pressure increase in both small arterioles and venules. It is likely that a pressure-induced mechanical stimulus activates a biochemical response that can lead to an increase in hydraulic conductivity in response to pressure change. Furthermore, our results suggested that an adaptive sealing effect induced by a step change in pressure also partially contributes to regulate endothelial barrier function. These findings support the idea that endothelial transport barrier responds actively to changes in hemodynamic forces in microcirculation and regulates the transport pathway for water through biological as well as mechanical mechanisms.

6.2 Recommendations for Future Study

Although current results have provided evidence that changes in hemodynamic forces play important roles in controlling microvascular perfusion and transvascular exchange, it is obvious that many questions still remain unanswered.

6.2.1 Role of transvacular filtration in regulating myogenic response

We have suggested evidence that transvascular filtration-induced shear stress helps control the arteriolar myogenic response. However, much is unknown about the

mechanism by which vascular SMC sense changes in shear stresses and converts them into cell contraction. There are two main directions for future study in association with this issue.

One is to identify a specific sensing site on which interstitial flow induced-shear stress acts. There has been recent interest in the role of integrins, a class of heterodimeric transmembrane glycoproteins, in a tension-sensing mechanism of the vascular myogenic response. Integrins are known to interact with matrix proteins and cytoskeletal proteins via a recognition site that contains the tripeptide RGD (Arg-Gly-Asp), thereby providing a structural molecular link for the transmission of mechanical forces between extra cellular matrix (ECM) and vascular smooth muscle cytoskeleton (Davis *et al.*, 2001;Osol, 1995). A growing body of evidence suggests that integrins can transduce mechanical force across the plasma membrane and initiate intracellular signaling (Katsumi *et al.*, 2004;Davis *et al.*, 2001;Osol, 1995). Several recent studies have suggested a role for integrins in the myogenic response by showing inhibition of myogenic tone by integrin-specific peptides or by showing regulation of the calcium entry pathway that is required for myogenic tone by integrins [reviewed in (Davis *et al.*, 2001)]. Although most of those studies are focused on the role of pressure-induced stretch or tension in triggering integrin signaling, we cannot rule out the possibility that the integrin signaling may be activated by interstitial flow-induced shear stress acting on ECM and SMCs, and thereby regulate vascular tone. Another possible specific sensing site in triggering mechano-transduction of SMCs is the glycosaminoglycan (GAG) component of the surface glycocalyx layer. Recent in vitro studies have shown that glycocalyx participates in mechanosensing that

mediates NO production in endothelial cells (Florian *et al.*, 2003) and regulates contraction in vascular SMCs (Ainslie *et al.*, 2004) in response to a change in shear stress.

Another important issue is to unveil the signaling pathway regulating SMC contraction induced by shear stress. It is well established that calcium entry and calcium sensitization processes in vascular SMCs are important mechanisms in initiating and sustaining the myogenic response, respectively. It is not clear whether shear stress regulates the myogenic response via a calcium-dependent or calcium sensitization pathway. A recent in vitro study (Civelek *et al.*, 2002) provided evidence that flow-induced shear stress might mediate SMC contraction via calcium-independent, Rho-kinase and protein kinase C pathways. With this in vitro evidence, further experiments performed from isolated and cannulated arteioles would help to characterize signaling mechanism regulated by shear stress.

6.2.2 Role of hemodynamic forces in regulating hydraulic permeability

We have provided evidence that an acute change in shear stress might regulate hydraulic conductivity in a NO-dependent mechanism. We also have shown that NO is involved in pressure-induced changes in L_p. It was hypothesized that pressure-induced endothelial cleft shear stress might play an important role in regulating L_p. However, more in vivo evidence is required to confirm this hypothesis. In addition, information related to upstream and downstream mechanisms of the NO pathway is not still clearly understood. Future study using various inhibitors will help us to

nderstand NO-associated signaling pathways in response to changes in shear stress and pressure.

Reference List

Adamson, R. H. (1993). Microvascular Endothelial-Cell Shape and Size In-Situ. ***Microvascular Research*** **46, 77-88.**

Adamson, R. H., Michel, C. C., Parker, K. H., Phillips, C. G., & Wang, W. (1993). Pathways Through the Intercellular Clefts of Frog Mesenteric Capillaries. ***Journal of Physiology-London*** **466, 303-327.**

Adamson, R., Zeng, M., Adamson, G., Lenz JF, & Curry FE (2003). PAF-and bradykinin-induced hyperpermeability of rat venules is independent of actin-myosin contraction. ***American Journal of Physiology-Heart and Circulatory Physiology*** **285, H406-H417.**

Ainslie, K., Garanich, J., Dull, R., & Tarbell, J. (2004). Vascular smooth muscle cell glycocalyx influences shear stress-mediated contractile response. ***Journal of Applied Physiology*** **In press.**

Alshihabi, S. N., Chang, Y. S., Frangos, J. A., & Tarbell, J. M. (1996). Shear stress-induced release of PGE(2) and PGI(2) by vascular smooth muscle cells. ***Biochemical and Biophysical Research Communications*** **224, 808-814.**

Barakat, A. I., Uhthoff, P. A. F., & Colton, C. K. (1992). Topographical Mapping of Sites of Enhanced Hrp Permeability in the Normal Rabbit Aorta. ***Journal of Biomechanical Engineering-Transactions of the Asme*** **114, 283-292.**

Barnidge, J. & Harris, N. R. (2000). Requirement of arteriovenular pairing for increased capillary filtration during acute inflammation. ***Microcirculation*** **7, 259-268.**

Butler, P. J., Tsou, T. C., Li, J. Y., Usami, S., & Chien, S. (2002). Rate sensitivity of shear-induced changes in the lateral diffusion of endothelial cell membrane lipids: a role for membrane perturbation in shear-induced MAPK activation. ***FASEB J*** **16, 216-218.**

Butler, P. J., Weinbaum, S., Chien, S., & Lemons, D. E. (2000). Endothelium-dependent, shear-induced vasodilation is rate-sensitive. *Microcirculation* 7, 53-65.

Chang, Y. S., Yaccino, J. A., Lakshminarayanan, S., Frangos, J. A., & Tarbell, J. M. (2000). Shear-induced increase in hydraulic conductivity in endothelial cells is mediated by a nitric oxide-dependent mechanism. *Arteriosclerosis Thrombosis and Vascular Biology* 20, 35-42.

Chien, S., Li, S., & Shyy, J. (1998). Effects of mechanical forces on signal transduction and gene expression in endothelial cells. *Hypertension* 31 [part 2], 162-169.

Civelek, M., Ainslie, K., Garanich, J. S., & Tarbell, J. M. (2002). Smooth muscle cells contract in response to fluid flow via a Ca2+-independent signaling mechanism. *Journal of Applied Physiology* 93, 1907-1917.

D'Angelo, G., Davis, M. J., & Meininger, G. A. (1997). Calcium and mechanotransduction of the myogenic response. *American Journal of Physiology-Heart and Circulatory Physiology* 42, H175-H182.

Davis, M. J. (1987). Determination of volumetric flow in capillary tubes using an optical Doppler velocimeter. *Microvascular Research* 34, 223-230.

Davis, M. J. & Hill, M. A. (1999). Signaling mechanisms underlying the vascular myogenic response. *Physiological Reviews* 79, 387-423.

Davis, M. J., Xu, X., Nurkiewicz, T. R., Kawasaki, J., Davis, G. E., Hill, M. A., & Meininger, G. A. (2001). Integrins and mechanotransduction of the vascular myogenic response. *American Journal of Physiology-Heart and Circulatory Physiology* 280, H1427-H1433.

Davis, P. (1995). Flow-mediated endothelial mechanotransduction. *Physiological Reviews* 75, 519-560.

de Wit, C., Jahrbeck, B., Schafer, C., Bolz, S. S., & Pohl, U. (1998). Nitric oxide opposes myogenic pressure responses predominantly in large arterioles in vivo. *Hypertension* 31, 787-794.

Demaio, L., Chang, Y. S., Gardner, T. W., Tarbell, J. M., & Antonetti, D. A. (2001). Shear stress regulates occludin content and phosphorylation. ***American Journal of Physiology-Heart and Circulatory Physiology*** **281, H105-H113.**

Demaio, L., Tarbell, J. M., Scaduto, R. C., Gardner, T. W., & Antonetti, D. A. (2004). A transmural pressure gradient induces mechanical and biological adaptive responses in endothelial cells. ***American Journal of Physiology-Heart and Circulatory Physiology*** **286, H731-H741.**

Falcone, J. C., Davis, M. J., & Meininger, G. A. (1991). Endothelial independence of myogenic response in isolated skeletal muscle arterioles. ***American Journal of Physiology*** **260, H130-H135.**

Figueroa, X. F., Martinez, A. D., Gonzalez, D. R., Jara, P. I., Ayala, S., & Boric.M.P. (2001). In vivo assessment of microvascular nitric oxide production and its relation with blood flow. ***American Journal of Physiology-Heart and Circulatory Physiology*** **280, H1222-H1231.**

Florian, J., Kosky, J., Ainslie, K., Dull, R., & Tarbell, J. (2003). Heparan Sulfate Proteoglycan Is a Mechanosensor on Endothelial Cells. ***Circulation Research*** **93, e136-142.**

Frank, J. S. a. F. A. M. (1989). Ultrastructure of the intima in WHHL and cholesterol-fed rabbit aortas prepared by ultra-rapid freezing and freezing-etching. ***Journal of Lipid Research*** **30, 967-978.**

Glass, C. & Bates, D. (2003). Role of endothelial Ca2+ stores in the regulation of hydraulic conductivity of Rana microvessels in vivo. ***American Journal of Physiology-Heart and Circulatory Physiology*** **284, H1468-H1478.**

Gore, R. W. (2004). Fluid exchange across single capillaries in rat intestinal muscle. ***American Journal of Physiology*** **242, H268-H287.**

Harris, N. R. (1997). Opposing effects of L-NAME on capillary filtration rate in the presence or absence of neutrophils. ***American Journal of Physiology*** **273, G1320-G1325.**

Harris, N. R. (1999). Reperfusion-induced changes in capillary perfusion and filtration: effects of hypercholesterolemia. ***American Journal of Physiology*** **277, H669-H675.**

He, P., Liu, B., & Curry, F. E. (1997). Effect of nitric oxide synthase inhibitors on endothelial [Ca2+](i) and microvessel permeability. ***American Journal of Physiology-Heart and Circulatory Physiology*** **41, H176-H185.**

He, P., Zeng, M., & Curry, F. E. (2000). Dominant role of cAMP in regulation of microvessel permeability. ***American Journal of Physiology-Heart and Circulatory Physiology*** **278, H1124-H1133.**

Head, S. D., Kajimura, M., & Michel, C. C. (1996). Effects of flow and on pottasium and fluid permeability of single microvessels. ***International Journal of Microcirculation: Clinical and Experimental*** **16, suppl. 1, 216.**

Hill, M. A., Zou, H., Davis, M. J., Potocnik, S. J., & Price, S. (2000). Transient increases in diameter and [Ca2+](i) are not obligatory for myogenic constriction. ***American Journal of Physiology-Heart and Circulatory Physiology*** **278, H345-H352.**

Hillsley, M. & Tarbell, J. (2002). Oscillatory shear alters endothelial hydraulic conductivity of cultured bovine retinal microvascular endothelial cell monolayers. ***Biochemical and Biophysical Research Communications*** **293, 1466-1471.**

Hongo, K., White, E., Guennec, J. Y., & Orchard, C. H. (1996). Changes in [Ca2+]i, [Na+]i and Ca2+ current in isolated rat ventricular myocytes following an increase in cell length. ***Journal of Physiology*** **491 (Pt.3), 609-619.**

Huang, Y., Jan, K. M., Rumschitzki, D., & Weinbaum, S. (1998). Structural changes in rat aortic intima due to transmural pressure. ***Journal of Biomechanical Engineering-Transactions of the Asme*** **120, 476-483.**

Huang, Y. Q., Rumschitzki, D., Chien, S., & Weinbaum, S. (1997). A fiber matrix model for the filtration through fenestral pores in a compressible arterial intima. ***American Journal of Physiology-Heart and Circulatory Physiology*** **41, H2023-H2039.**

Jarajapu, Y. P. R. & Knot, H. J. (2002). Role of phospholipase C in development of myogenic tone in rat posterior cerebral arteries. *American Journal of Physiology-Heart and Circulatory Physiology* 283, H2234-H2238.

Jasperse, J. L., Laughlin, M. H., & Maurer, G. (1999). Vasomotor response of soleus feed arteries from sedentary and exercise-trained rats. *Journal of Applied Physiology* 86, 441-449.

Kajimura, M., Head, S. D., & Michel, C. C. (1998). The effects of flow on the transport of potassium ions through the walls of single perfused frog mesenteric capillaries. *Journal of Physiology-London* 511, 707-718.

Kany, H. P., Hasse, H., & Maurer, G. (1999). Thermodynamic properties of aqueous dextran solutions from laser-light scattering, membrane osmometry, and isopiestic measurements. *J.Chem.Eng.Data* 44, 230-242.

Karmakar, N. (2001). Interaction of transmural pressure and shear stress in the transport of albumin across the rabbit aortic wall. *Atherosclerosis* 156, 321-327.

Kashiwagi, S., Kajimura, M., Yoshimura, Y., & Suematsu, M. (2002). Nonendothelial source of nitric oxide in arterioles but not in venules - Alternative source revealed in vivo by diaminofluorescein microfluorography. *Circulation Research* 91, E55-E64.

Katsumi, A., Orr, A. W., Tzima, E., & Schwartz, M. A. (2004). Integrins in mechanotransduction. *J Biol Chem* 279, 12001-12004.

Koller, A. & Kaley, G. (1990). Role of Endothelium in Reactive Dilation of Skeletal-Muscle Arterioles. *American Journal of Physiology* 259, H1313-H1316.

Koller, A. & Kaley, G. (1991). Endothelial Regulation of Wall Shear-Stress and Blood-Flow in Skeletal-Muscle Microcirculation. *American Journal of Physiology* 260, H862-H868.

Kuo, L., Chilian, W. M., & Davis, M. J. (1991). Interaction of Pressure-Induced and Flow-Induced Responses in Porcine Coronary Resistance Vessels. *American Journal of Physiology* 261, H1706-H1715.

Lakshminarayanan, S., Gardner, T. W., & Tarbell, J. M. (2000). Effect of shear stress on the hydraulic conductivity of cultured bovine retinal microvascular endothelial cell monolayers. ***Current Eye Research*** **21, 944-951.**

Landis, E. M. (1927). Micro-injection studies of capillary permeability. II. The relation between capillary pressure and the rate at which fluid passes through the walls of single capillaries. ***American Journal of Physiology*** **82, 217-238.**

Lark, M. W. Y. T. M. H. L. S. H. I. H. K. a. W. T. N. (1988). Arterial chondroitin sulfate proteoglycan : Localization with a monoclonal antibody. ***The Journal of Histochemistry and Cytochemistry*** **36, 1211-1221.**

Lee, J. S., Smaje, L. H., & Zweifach, B. W. (1971). Fluid movement in occluded single capillaries of rabbit omentum. ***Circulation Research*** **82, 358-370.**

Lever, M. J., Tarbell, J. M., & Caro, C. G. (1992). The Effect of Luminal Flow in Rabbit Carotid-Artery on Transmural Fluid Transport. ***Experimental Physiology*** **77, 553-563.**

Lipowsky, H. H. & Zweifach, B. W. (1978). Application of the "two-slit" photometric technique to measurement of microvascular volumetric flow rates. ***Microvascular Research*** **15, 93-101.**

Lombard, J. H. a. D. B. R. (1977). Relative contributions of passive and myogenic factors to diameter changes during single arteriole occlusion in the hamster chick pouch. ***Circulation Research*** **41, 365-373.**

Masuda, H., Zhuang, Y. J., Singh, T. M., Kawamura, K., Murakami, M., Zarins, C. K., & Glagov, S. (1999). Adaptive remodeling of internal elastic lamina and endothelial lining during flow-induced arterial enlargement. ***Arteriosclerosis Thrombosis and Vascular Biology*** **19, 2298-2307.**

Meininger, G. & Davis, M. (1992). Cellular mechanisms involved in the vascular myogenic response. ***American Journal of Physiology-Heart and Circulatory Physiology*** **263, H647-H659.**

Michel, C. C. & Curry, F. E. (1999). Microvascular permeability. ***Physiological Reviews*** **79, 703-761.**

Montermini, D., Winlove, C. P., & Michel, C. C. (2002). Effects of perfusion rate on permeability of frog and rat mesenteric microvessels to sodium fluorescein. *Journal of Physiology-London* 543, 959-975.

Neal, C. R. & Bates, D. O. (2001). Measurement of hydraulic conductivity by double cannulation of single capillaries and pressure equilibration between periods of controlled shear rate in the frog mesentery. *Journal of Physiology-London* 536, 3P-4P.

Neal, C. R. & Bates, D. O. (2002). Measurement of hydraulic conductivity of single perfused Rana mesenteric microvessels between periods of controlled shear stress. *Journal of Physiology-London* 543, 947-957.

Neal, C. R. & Michel, C. C. (1996). Openings in frog microvascular endothelium induced by high intravascular pressures. *Journal of Physiology-London* 492, 39-52.

Nitenberg, A., Antony, I., Aptecar, E., Arnoult, F., & Lerebours, G. (1995). Impairment of flow-dependent coronary dilation in hypertensive patients. Demonstration by cold pressor test induced flow velocity increase. *Am J Hypertens* 8(5 Pt 2), 13S-18S.

Okano, M. & Yoshida, Y. (1994). Junction Complexes of Endothelial-Cells in Atherosclerosis-Prone and Atherosclerosis-Resistant Regions on Flow Dividers of Brachiocephalic Bifurcations in the Rabbit Aorta. *Biorheology* 31, 155-161.

Osol, G. (1995). Mechanotransduction by vascular smooth muscle. *J.Vasc.Res.* 32, 275-292.

Papadaki, M., Ruef, J., Nguyen, K. T., Li, F. Z., Patterson, C., Eskin, S. G., McIntire, L. V., & Runge, M. S. (1998a). Differential regulation of protease activated receptor-1 and tissue plasminogen activator expression by shear stress in vascular smooth muscle cells. *Circulation Research* 83, 1027-1034.

Papadaki, M., Tilton, R. G., Eskin, S. G., & McIntire, L. V. (1998b). Nitric oxide production by cultured human aortic smooth muscle cells: stimulation by fluid flow. *American Journal of Physiology-Heart and Circulatory Physiology* 43, H616-H626.

Parker, J. C. & Ivey, C. L. (1997). Isoproterenol attenuates high vascular pressure-induced permeability increases in isolated rat lungs. *Journal of Applied Physiology* 83, 1962-1967.

Rivers, R. J. (1995). Remote effects of pressure changes in arterioles. *American Journal of Physiology* 268, H1379-H1382.

Rumbaut, R. E., Mckay, M. K., & Huxley, V. H. (1995). Capillary Hydraulic Conductivity Is Decreased by Nitric-Oxide Synthase Inhibition. *American Journal of Physiology-Heart and Circulatory Physiology* 37, H1856-H1861.

Rumbaut, R. E., Wang, J., & Huxley, V. H. (2000a). Differential effects of L-NAME on rat mesenteric venule permeability. *Faseb Journal* 14, A26.

Rumbaut, R. E., Wang, J. J., & Huxley, V. H. (2000b). Differential effects of L-NAME on rat venular hydraulic conductivity. *American Journal of Physiology-Heart and Circulatory Physiology* 279, H2017-H2023.

Schubert, R., Kalentchuk, V. U., & Krien, U. (2002). Rho kinase inhibition partly weakens myogenic reactivity in rat small arteries by changing calcium sensitivity. *American Journal of Physiology-Heart and Circulatory Physiology* 283, H2288-H2295.

Schubert, R. & Mulvany, M. J. (1999). The myogenic response: established facts and attractive hypotheses. *Clinical Science* 96, 313-326.

Segal, S. S. & Duling, B. R. (1989). Conduction of vasomotor responses in arterioles: role for cell-to-cell coupling? *American Journal of Physiology* 256, H838-H845.

Sill, H. W., Chang, Y. S., Artman, J. R., Frangos, J. A., Hollis, T. M., & Tarbell, J. M. (1995). Shear-Stress Increases Hydraulic Conductivity of Cultured Endothelial Monolayers. *American Journal of Physiology-Heart and Circulatory Physiology* 37, H535-H543.

Somlyo, A. P. & Somlyo, A. V. (1994). Signal-Transduction and Regulation in Smooth-Muscle. *Nature* 372, 231-236.

Sun, D., Huang, A., Koller, A., & Kaley, G. (2002). Enhanced NO-mediated dilations in skeletal muscle arterioles of chronically exercised rats. ***Microvascular Research*** **64, 491-496.**

Sun, D., Kaley, G., & Koller, A. (1994). Characteristics and Origin of Myogenic Response in Isolated Mesenteric Arterioles. ***American Journal of Physiology*** **266, H1177-H1183.**

Sun, D., Messina, E. J., Kaley, G., & Koller, A. (1992). Characteristics and Origin of Myogenic Response in Isolated Mesenteric Arterioles. ***American Journal of Physiology*** **263, H1486-H1491.**

Taba, Y., Sasaguri, T., Miyagi, M., Abumiya, T., Miwa, Y., Ikeda, T., & Mitsumata, M. (2000). Fluid shear stress induces lipocalin-type prostaglandin D(2) synthase expression in vascular endothelial cells. ***Circulation Research*** **86, 967-973.**

Tada, S. & Tarbell, J. M. (2000). Interstitial flow through the internal elastic lamina affects shear stress on arterial smooth muscle cells. ***American Journal of Physiology-Heart and Circulatory Physiology*** **278, H1589-H1597.**

Tada, S. & Tarbell, J. M. (2001). Fenestral pore size in the internal elastic lamina affects transmural flow distribution in the artery wall. ***Annals of Biomedical Engineering*** **29, 456-466.**

Tada, S. & Tarbell, J. M. (2002). Flow through internal elastic lamina affects shear stress on smooth muscle cells (3D simulations). ***American Journal of Physiology-Heart and Circulatory Physiology*** **282, H576-H584.**

Tarbell, J. M., Demaio, L., & Zaw, M. M. (1999). Effect of pressure on hydraulic conductivity of endothelial monolayers: role of endothelial cleft shear stress. ***Journal of Applied Physiology*** **87, 261-268.**

Taylor, A. E. a. G. D. N. (1984). Exchange of macromolecules across the microcirculation. In ***Handbook of Physiology, section 2, The cardiovascular system, Volume IV*** **The Microcirculation. Am. Physiol. Soc., Bethesda.**

Tickerhoof, M. M., Farrell, P. A., & Korzick, D. H. (2003). Alterations in rat coronary vasoreactivity and vascular protein kinase C isoforms in type I diabetes. *American Journal of Physiology-Heart and Circulatory Physiology*.

Tomioka, M. M., Hattori, Y., Fukao, M., Sato, A., Liu, M., Sakuma, I., Kitabatake, A., & Kanno, M. (1999). Relaxation in different-sized rat blood vessels mediated by endothelium-derived hyperpolarizing factor: importance of processes mediating precontractions. *J.Vasc.Res.* 36, 311-320.

Ungvari, Z. & Koller, A. (2001). Selected contribution: NO released to flow reduces myogenic tone of skeletal muscle arterioles by decreasing smooth muscle Ca2+ sensitivity. *Journal of Applied Physiology* 91, 522-527.

Ungvari, Z., Sun, D., Huang, A., Kaley, G., & Koller, A. (2001). Role of endothelial [Ca2+]i in activation of eNOS in pressurized arterioles by agonists and wall shear stress. *American Journal of Physiology-Heart and Circulatory Physiology* 281, H606-H612.

Victorino, G., Newton, C., & Curran, B. (2004). Modulation of microvascular hydraulic permeability by platelet-activating factor. *Journal of Trauma* 56, 379-384.

Wang, D. M. & Tarbell, J. M. (1995). Modeling Interstitial Flow in An Artery Wall Allows Estimation of Wall Shear-Stress on Smooth-Muscle Cells. *Journal of Biomechanical Engineering-Transactions of the Asme* 117, 358-363.

Wang, S. & Tarbell, J. M. (2000). Effect of fluid flow on smooth muscle cells in a 3-dimensional collagen gel model. *Arteriosclerosis Thrombosis and Vascular Biology* 20, 2220-2225.

White, R. J., Leonard, J. I., Srinivasan, R. S., & Charles, J. B. (1991). Mathematical-Modeling of Acute and Chronic Cardiovascular Changes During Extended Duration Orbiter (Edo) Flights. *Acta Astronautica* 23, 41-51.

Wight, T. N. a. H. V. C. (1983). Proteoglycans in primate arteries. III.Characterization of the proteoglycan synthesized by arterial smooth muscle cells in culture. *Journal of Cell Biology* 96, 167-176.

Williams, D. A. (1999). Network assessment of capillary hydraulic conductivity after abrupt changes in fluid shear stress. ***Microvascular Research*** **57, 107-117.**

Williams, D. A. (2003). Intact capillaries sensitive to rate, magnitude, and pattern of shear stress stimuli as assessed by hydraulic conductivity (L-P). ***Microvascular Research*** **66, 147-158.**

Yuan, Y. (2000). Signal transduction pathways in enhanced microvascular permeability. ***Microcirculation*** **7, 395-403.**

Yuan, Y., Granger, H. J., Zawieja, D. C., & Chilian, W. M. (1992). Flow Modulates Coronary Venular Permeability by A Nitric Oxide-Related Mechanism. ***Circulation*** **86, 641.**

Zou, H., Ratz, P. H., & Hill, M. A. (1995). Role of Myosin Phosphorylation and [Ca2+](I) in Myogenic Reactivity and Arteriolar Tone. ***American Journal of Physiology-Heart and Circulatory Physiology*** **38, H1590-H1596.**

APPENDIX

Estimation of pressure drop through the micropipette tip

A steady, laminar flow of incompressible fluid through a rigid-walled cylindrical tube can be modeled using the well-known Hagen-Poiseuille equation,

$$Q_o = \frac{\pi R^4}{8\mu}\frac{dP}{dz}$$

where Q_o is the volumetric flow rate, μ is the dynamic viscosity of the fluid, R is the radius of the cylindrical channel, and dP/dz is the pressure gradient along the tube. This equation can be applied to estimate a pressure drop through the tapered channel of a micropipette tip. Taking an integration of above equation for calculation of pressure drop yields

$$\Delta P = \frac{8\mu Q_o}{\pi}\int_0^L \frac{1}{R^4(z)}dz$$

where L is the length of micropipette tip, ΔP is the pressure drop along the channel length, and $R(z)$ is the radius of the micropipette at distance z from the entrance of the channel. Assuming a linearly varying radius for micropipette tip, $R(z)$ can be expressed as

$$R(z) = \frac{R_L - R_0}{L}\, z + R_0$$

where R_L and R_0 refer to radius of micropipette at $z=L$ and $z=0$, respectively. Calculations were performed for various value of Q_o. The following are parameters used in current calculations.

$\mu = 1$ cp

$R_L = 1 \times 10^{-5}$ m

$R_0 = 0.5 \times 10^{-3}$ m

$L = 1 \times 10^{-2}$ m

$Q_o = 7 \times 10^{-14} \sim 7 \times 10^{-11}\ m^3/s$

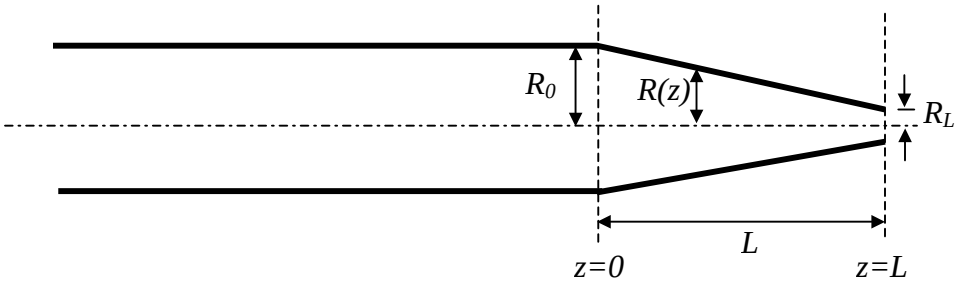

The following are the calculated values of pressure drop through the tapered micropipette tip for various assumed values of volumetric flow rates.

Flow velocity (m/s)	Volumetric flow rate Q_o (m^3/s)	Calculated pressure gradient ΔP (mmHg)
0.0001	7×10^{-14}	0.029
0.001	7×10^{-13}	0.29
0.01	7×10^{-12}	2.9
0.1	7×10^{-11}	29

VITA

Min-ho Kim

EDUCATION

2000 - present	Doctor of Philosophy in Bioengineering, Pennsylvania State University, December 2004
1994 – 1996	Master of Science in Aerospace Engineering, INHA University, South Korea
1990 - 1994	Bachelor of Aerospace Engineering INHA University, South Korea

WORK EXPERIENCE

Jul. 2004 – present	**Research Assistant**, Department of Molecular and Cellular Physiology, Louisiana State University Health Science Center
Aug. 2001 –Jun. 2004	**Research Assistant**, Department of Bioengineering, Pennsylvania State University
Jan. 2001 – Jul. 2001	**Research Assistant**, Center for Locomotion Studies, Pennsylvania State University
1998 - 2000	**Full-time lecturer**, Republic of Korea Airforce Academy, South Korea
1995-1997	**Research Assistant**, INHA University, South Korea

SELECTED PUBLICATIONS

1 **Kim M**, Harris NR and Tarbell JM , " Control of the arteriolar myogenic response by transmural fluid filtration ", *Microvascular Research*, 68, pp. 30-37, 2004.

2 **Kim M,** Harris NR and Tarbell JM. Fluid filtration rate transient following capillary occlusion. FASEB J 17(5): A247, 2004.

3 **Kim M,** Harris NR and Tarbell JM. Myogenic constriction in the absence of ascular stretch is controlled by transvascular fluid filtration. FASEB J 17(5): A127, 2003.